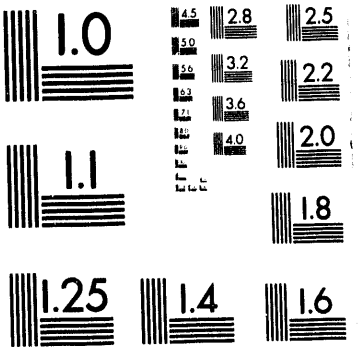
1.0
4.5
2.8
2.5
5.0
3.2
2.2
5.6
3.6
2.0
6.3
4.0
1.1
1.8
1.25
1.4
1.6

1 of 2

RECEIVED

FEB 17 1994

DEPARTMENT OF DEVELOPMENT
OHIO COAL DEV OFFICE

OCDO -- 94009366

FINAL REPORT:

FUNDAMENTAL STUDY OF AMMONIA-SULFUR DIOXIDE REACTIONS TO FORM SOLID PARTICLES

Grantee:

The Department of Civil and Environmental Engineering
University of Cincinnati
Cincinnati, Ohio 45221

Project Number CDO/R88-14
Expiritation Date: May 31, 1992

Project Manager:
Tim C. Keener, Ph.D
Telephone: 513/556-2518

This Project Was Funded in Part by The Ohio Coal Development Office
Department of Development, State of Ohio

January 18, 1994

Contributing Project Investigators:

Pratim Biswas

Hsunling Bai

MASTER

DISTRIBUTION OF THIS DOCUMENT IS UNLIMITED

TABLE OF CONTENTS

CONTENTS	Page
EXECUTIVE SUMMARY	1
NOMENCLATURE	2
LIST OF FIGURES	4
LIST OF TABLES	7
INTRODUCTION	8
TECHNOLOGY REVIEW	11
OBJECTIVES	14
TECHNICAL DISCUSSION	15
NH_3-SO_2 REACTIONS AT TRACE WATER CONDITIONS	15
NH_3-SO_2 REACTIONS IN THE PRESENCE OF INERT PARTICLES	43
NH_3-SO_2 REACTIONS AT HUMID CONDITIONS	62
APPLICABILITY TO A FULL SCALE FGD SYSTEM	84
CONCLUSIONS	93
RECOMMENDATION FOR FUTURE WORK	95
LITERATURE CITED	96
APPENDICES	101
Appendix A: List of Dimensionless Parameters in Particle Formation Model	101
Appendix B: Microscope Pictures of the NH_3-SO_2 Reactions	102
Appendix C: Sample Computer Program "SO2NH3.F"	104

EXECUTIVE SUMMARY

The reaction between NH_3 and SO_2 in the gas phase has been shown to be an effective method of controlling SO_2 emissions from flue gas. This project's objectives were to conduct fundamental studies of the NH_3-SO_2 reaction which were conducted experimentally and theoretically. One of the best ways to utilize ammonia injection is in conjection with a spray dryer system. The removal technique has the potential of achieving over 90% SO_2 removal on high sulfur coal flue gas through the careful application of a combined $Ca(OH)_2/NH_3$ based spray dryer system. Other advantages with the scheme include that it is relatively simple, can be utilized in existing power plants with minimal space requirements, and produce a dry product which can be sold as a fertilizer.

The products of the NH_3-SO_2 reaction are solid particles. The effects of reaction residence time, presence of initial seed particles and moisture content on the SO_2 removal and the product particle size distributions have been determined experimentally. A gas to particle conversion model for the NH_3-SO_2 system was developed, considering simultaneous chemical reaction, nucleation, condensation and coagulation. A thermodynamic analysis of the reaction was also carried out accounting for several reaction mechanisms to predict the SO_2 removal by NH_3 injection. Potential applications of this system of reactions were also discussed with emphasis on the application to flue gas desulfurization (FGD) processes.

The results showed that the time required for SO_2-NH_3 reactions to reach quasi-steady-state is very short, which indicated no further space requirement is necessary when applying ammonia injection as a means of sulfur dioxide removal from flue gases. Moisture content has the most pronounced effect on the removal of sulfur dioxide. Increasing the moisture content tends to shift the equilibrium of the system in favor of graeter product which would result in greater sulfur dioxide removal in FGD systems.

NOMENCLATURE

A	Total particle surface area
G	Particle growth rate by the condensation effect
I	Particle formation rate (nucleation rate)
I_s	Nucleation rate scale
K^*	Number of monomers in the critical size nucleus
k_B	Boltzmann constant
K_p	Equilibrium constant of the NH_3-SO_2 reaction
L_s	Scale integral length scale
M_k	k-th aerosol volume moment (k=0, 1, 2)
m_1	Monomer mass
n, $n(v,t)$	Particle density function
N_{av}	Avogadro's number (=6.02 X 10^{23} molecules/mole)
N_{sc}	Schmidt number
n_s	Monomer concentration at saturation, molecules/cm_3
P	Partial pressure of the gaseous reactant, atm
R	Pipe radius
R_r	Monomer formation rate from chemical reaction (= $R_r'\tau/n_s$)
S	Saturation ratio
T	Temperature
t	Dimensional time
t_r	Time required to reach chemical equilibrium
v	Particle volume
v^*	Monomer critical volume

v_1	Monomer volume
v_g	Geometric mean particle volume
r	Radial distance
x	Mole fraction of NH_3SO_2
y	Mole fraction of $(NH_3)_2SO_2$

Greek Symbols:

β	Collision frequency function
δ	Delta function
ε	Dimensionless condensation coefficient
ε_d	Rate of energy dissipation per unit mass
ζ	Dimensionless coagulation coefficient
η	Dimensionless condensation coefficient
θ	Dimensionless time
ρ_p	Particle density
σ	Surface tension
σ_g	Geometric mean standard deviation
ψ	Dimensionless coagulation coefficient
τ	Characteristic time for particle growth, $\tau=[n_s s_1(k_B T/2\pi m_1)^{1/2}]^{-1}$
τ_m	Characteristic time for mixing in a union tee

Subscripts:

N	Ammonia
S	Sulfur dioxide
H	Water vapor
e	Equilibrium state
in	Inlet condition

Superscripts:

Dimensional property

LIST OF FIGURES

Figure 1a. Schematic diagram of the experimental setup to study the NH_3-SO_2 reaction. ---------- 34

Figure 1b. Schematic diagram of three different setups to check for mixing conditions. ---------- 35

Figure 2a. SO_2 concentration (with $SO_{2,in}$ = 3000 ppm) as a function of average residence time at room temperature. Data are from glass reactor. ---------- 36

Figure 2b. SO_2 concentration (with $SO_{2,in}$ = 3000 ppm) as a function of average residence time at room temperature. Data are from stainless steel reactor. ---------- 37

Figure 3. Measured and calculated SO_2 equilibrium vapor pressure as a function of inlet NH_3 concentration. Symbols are experimental data and lines are theoretical results of the present model using different equilibrium constants for reactions (1) and (2): (— Landreth et al., 1985; ----- Scott and Lamb, 1970). ---------- 38

Figure 4. Size distribution of NH_3/SO_2 reaction products at room temperature with inlet SO_2 concentration of 3000 ppm and inlet NH_3 concentration of 6000 ppm at 0.63 seconds of reactor residence time. ---------- 39

Figure 5a. Measured and simulated results of cup mixing average total particle concentration as a function of average residence time. The inlet SO_2 and NH_3 concentrations are 3000 and 6000 ppm, respectively. ---------- 40

Figure 5b. Measured and simulated results of cup mixing average geometric mean particle diameter concentration as a function of average residence time. The inlet SO_2 and NH_3 concentrations are 3000 and 6000 ppm, respectively. ---------- 41

Figure 5c. Measured and simulated results of cup mixing average geometric standard deviation as a function of average residence time. The inlet SO_2 and NH_3 concentrations are 3000 and 6000 ppm, respectively. ---------- 42

Figure 6. Schematic diagram of the experimental setup to study the effect of initial seed on the NH_3-SO_2 reaction. ---------- 54

Figure 7a. The size distribution histograms of Run 1 measured from OPC. -------- 55

Figure 7b. The size distribution histograms of Run 2 measured from OPC. -------- 56

Figure 7c. The size distribution histograms of Run 3 measured from OPC. -------- 57

Figure 8. The effect of moisture content on the total particle number concentration without the introduction of seed particles. ---------- 58

Figure 9a. Measured and simulated results of cup-mixing average total particle number concentration as a function of average residence time with the presence of initial seed particles. ---------- 59

Figure 9b. Measured and simulated results of cup-mixing average geometric mean particle diameter as a function of average residence time with the presence of initial seed particles. ---------- 60

Figure 9c. Measured and simulated results of cup-mixing average geometric standard deviation as a function of average residence time with the presence of initial seed particles. ---------- 61

Figure 10. Schematic diagram of the NH_3-SO_2 main reactor system at humid and high temperature conditions. ---------- 75

Figure 11. Effect of relative humidity on SO_2 removal at room temperature and inlet SO_2 concentration of 3000 ppm. ---------- 76

Figure 12. The X-ray diffraction result of NH_3-SO_2 reaction products at room temperature and relative humidity of 20%. ---------- 77

Figure 13. $NH_4^+/SO_4^=$ and $SO_3^=/SO_4^=$ ratios from the wet chemical analysis as a function of reaction temperature at H_2O = 2.7% by volume. ---------- 78

Figure 14. Effect of reaction temperature on the sulfur dioxide removal under a moisture content of 2.7% by volume (0.017 lb H_2O/lb dry air). ---------- 79

Figure 15a. Effect of moisture content on the sulfur dioxide removal under a

temperature of 51°C (124°F). ---------- 80

Figure 15b. Ammonia utilization as a function of moisture content under a temperature of 51°C (124°F). ---------- 81

Figure 16a. Size distributions of NH_3-SO_2 reaction product at a reaction temperature of 51°C under different moisture content conditions. ---------- 82

Figure 16b. Size distributions of NH_3-SO_2 reaction product at a moisture content of 2.7% by volume under different reaction temperatures. ---------- 83

Figure 17. Simplified sketch of a typical power plant. ---------- 89

Figure 18. SO_2 removal as functions of moisture content and reaction temperature. ----------90

Figure 19. Bench scale and pilot scale results of SO_2 removal efficiencies as a function of temperature. Symbols are experimental data and lines are theoretical predictions from thermodynamic analysis. ---------- 91

Figure 20. Design of a power plant utilizing $NH_3/Ca(OH)_2$ injection as SO_2 removal technique. ---------- 92

LIST OF TABLES

Table 1. Experimental conditions and instruments used at trace water conditions. -- 29

Table 2. Comparison of the three different reactor setups: Numbers are SO_2 removal percentages at outlet. ---------- 30

Table 3. Equilibrium constants for the three NH_3-SO_2 reactions. ---------- 31

Table 4. Computed mole fraction of the three solid products for different water vapor concentrations. The computation is based on thermodynamic data of Landreth et al. (1985) and Scargill (1971). ---------- 32

Table 5. Experimental results of the particle properties from the optical particle counter with a lognormal size distribution fitting. ---------- 33

Table 6. Properties of the sodium chloride seed particles measured from LAS-X Optical Particle Counter. ---------- ---------- 50

Table 7. SO_2 removal efficiency and product properties of the NH_3-SO_2 reaction under different inert particle size distribution conditions. ---------- 51

Table 8. List of parameters used in the gas-to-particle conversion model ---------- 52

Table 9. Predictions of the SO_2 removal increased for Run 1 and typical fly ash conditions. ---------- 53

Table 10. Equipments used in humid experiments. ---------- 72

Table 11. Experimental conditions for the NH_3-SO_2-H_2O system. ---------- 73

Table 12. Possible NH_3-SO_2 reactions and their equilibrium constants. ---------- 74

Table 13. Approach to saturation temperatures at various operating temperatures and moisture contents. ---------- 88

INTRODUCTION

Sulfur dioxide is an important criteria pollutant and excessive levels of it in the ambient air lead to a significant increase in acute and chronic respiratory diseases. On combining with water vapor in the atmosphere it leads to formation of sulfuric acid, a major contributor to acid rain. It is also a primary pollutant which leads to formation of environmentally undesirable aerosols in the atmosphere. Sulfur dioxide is released into the air primarily through the burning of coal and fuel oils. According to EPA's estimates, two-thirds of all national sulfur dioxide emissions come from electric power plants. Other sources of sulfur dioxide include industrial plants related to oil shale, synfules, and oil and gas production (EPA, 1988). Utility plants and industry have been targeted for effective control of SO_2 emission since 1970. As a result of the 1990 Clean Air Act amendments, these plants will face a more stringent enforcement plan as proposed by the U.S. EPA (Lee, 1990).

Sulfur dioxide removal technologies are essential for the improvement of atmospheric air quality. Among the various technologies , flue gas desulfurization (FGD) is one of the more popular technologies. Major studies conducted related to FGD process are water scrubbing, metal ion solutions, catalytic oxidation, dry adsorption, wet lime or limestone scrubbing, double alkali process, ammonia scrubbing and other processes for SO_2 emission reduction (Marten, 1977).

Sulfur dioxide removal from coal fired power plants by ammonia injection is a flue gas desulfurization technique that has been studied by several researchers. Shale

(1971,1973) performed both bench scale and pilot plant tests and showed that complete removal of sulfur dioxide was feasible when ammonia was injected at a molar ratio (NH_3:SO_2) of slightly less than 2:1. In his study, NH_3 was injected into the gas stream saturated with water vapor and the stream cooled to below the sublimation temperature (60°C) of ammonium sulfite. Tock et al. (1979) presented a thermodynamic analysis of the SO_2-NH_3-H_2O system based on the equilibrium data provided by St. Clair (1937) and Scargill (1971). Stromberger (1984) conducted a bench scale study on sulfur dioxide removal by ammonia gas injection in simulated flue gases. His results indicated that SO_2 removal dropped to near zero at temperatures around 54°C. However, pilot scale studies (Davis et al., 1977; Keener and Davis, 1988) showed that sulfur dioxide removal from flue gas systems by ammonia injection was possible at higher temperatures (greater than 54°C). They reported that the sulfur dioxide removal was in excess of 95% at about 2:1 molar injection ratios of NH_3/SO_2 for temperatures below 85°C (185°F).

The products of the SO_2-NH_3-H_2O reactions are solid particles. Shale (1973) and Keener and Davis (1988) postulated the products to be ammonium sulfite, $(NH_4)_2SO_3$, and ammonium bisulfite, NH_4HSO_3. However, they did not conduct experiments to identify the actual products of reactions. Hartley and Matteson (1975) conducted room temperature experiments of NH_3 and SO_2 reactions, and found by X-ray diffraction that ammonium sulfate was the product under excess moisture conditions. Stromberger (1984) used X-ray diffraction and identified the products to be ammonium sulfate crystals for a reaction temperature range of 24 to 54°C.

Though there have been a number of studies on the removal of sulfur dioxide

from flue gases by ammonia injection, there is a disagreement on the conditions (such as temperature) where a high removal efficiency is obtained. There is also some controversy as to what products are formed. These are due to the lack of fundamental information on the gas phase reactions between NH_3, SO_2, and water vapor.

TECHNOLOGY REVIEW

The conversion process of the NH_3-SO_2 reaction to form particles is very complicated and few detailed studies have been conducted. Various products may form depending on the reactant concentrations, moisture content and the reaction temperature. Different products of the anhydrous reaction between NH_3 and SO_2 have been reported in studies dating to the nineteenth century (Divers and Ogawa, 1900 and Scott et al., 1969 - historical review). Badar-ud-Din and Aslam (1953) were the first to conclusively report that the products of the reaction were amidosulfurous acid (NH_3SO_2) and ammonium amidosulfite ($(NH_3)_2SO_2$) below a temperature of 10°C in the absence of water vapor. Scott and Lamb (1970) assumed an ideal solid solution of the amidosulfurous acid and ammonium amidosulfite and proposed equilibrium constants for these two products at temperatures ranging from -70°C to -10°C. Later Landreth et al (1974, 1985) repeated the equilibrium experiments for formation of NH_3SO_2 and $(NH_3)_2SO_2$ and obtained equilibrium relations for temperatures in the range of 5°C to 45°C.

Hartley and Matteson (1975) conducted room temperature experiments of NH_3 and SO_2, and found by X-ray diffraction that the products were most likely amidosulfurous acid and ammonium amidosulfite at water vapor concentrations approaching those of NH_3 and SO_2. Ammonium sulfate was found to be the product under excess moisture conditions. The reaction rate, from their experimental results, was dependent on the amount of water vapor present but independent of the oxygen concentration. Therefore they suspected that the solid that initially precipitates out of the gas stream may be a

precursor, which is the result of the reaction

$$NH_{3\,(g)} + SO_{2\,(g)} \rightleftharpoons NH_3 \bullet SO_{2\,(g)} \quad . \tag{1}$$

with the complete reactions

$$NH_3 \bullet SO_{2\,(g)} + NH_{3\,(g)} \rightleftharpoons (NH_3)_2 SO_{2\,(s)} \tag{2}$$

and

$$nNH_3 \bullet SO_{2\,(g)} \rightleftharpoons (NH_3 \bullet SO_2)_{n\,(s)} \, . \tag{3}$$

Further reaction with water vapor and oxygen may take place to form ammonium sulfate particles after the solids have been collected on surfaces . Vance and Peters (1976) experimentally studied the anhydrous reaction at 25°C and concluded that $(NH_3)_2SO_2$ is the favored reaction product except when large excess of SO_2 is present. They measured product particle size distribution using an impactor and a diffusion battery and reported that particle sizes ranged from 0.001 to 10 μm with a bimodal normal distribution. Carabine et al (1971) conducted anhydrous experiments at equimolar NH_3 and SO_2 concentrations and found the resulting aerosols contained typically 10^4 to 10^5 particles/cm^3, with particle sizes ranging from 0.05 to 0.25 μm. Their particle size distribution was lognormal with a mean diameter of around 0.12 μm.

St. Clair (1937) proposed four crystalline compounds in the NH_3-SO_2-H_2O system: anhydrous ammonium sulfite, $(NH_4)_2SO_3$; hydrated ammonium sulfite, $(NH_4)_2SO_3$ -H_2O; ammonium bisulfite, NH_4HSO_3; and ammonium pyrosulfite, $(NH_4)_2S_2O_5$. Of these four compounds, the pyrosulfite is the only one that decomposes directly into its gaseous components. The four compounds are related to each other and the systems are either

invariant or univariant. According to Lewis' valence theory, St. Clair (1937) gave the chemical structure of the pyrosulfite

$$NH_4:O:\overset{O}{\underset{\ddot{O}}{\ddot{S}}}:O:S:O:NH_4 \qquad (4)$$

while those of sulfite and bisulfite were written in the form

$$NH_4:O:S:\underset{\ddot{O}}{O}:NH_4, \text{ and } NH_4:O:\overset{O}{\ddot{S}}:O:H. \qquad (5)$$

He concluded that the sulfite and bisulfite would most likely combine with oxygen to form ammonium sulfate.

Scargill (1971) performed an experimental study of the NH_3-SO_2-H_2O reactions for a temperature range of 0 to 23°C. He found by wet chemical analysis that nearly pure $(NH_4)_2SO_3$ is formed when excess NH_3 and H_2O are present, while the product is nearly pure $(NH_4)_2S_2O_5$ with excess amount of SO_2 at trace water vapor concentrations (< 400 ppm). Landreth (1975) conducted similar experiments and obtained scattered data of the SO_2 versus H_2O equilibrium plot and explained that this may be due to the presence of both anhydrous ammonium sulfite and ammonium pyrosulfite compounds.

A more detailed analysis of the results of other studies may be found elsewhere (Bai, et. al., 1992).

OBJECTIVES

Flue gas desulfurization by means of NH_3 injection is complicated and many parameters affect sulfur dioxide removal. Moisture content can be an important parameter for determining the maximum system temperature for sulfur dioxide removal. The presence of fly ash particles may also serve as condensation surfaces for the primary vapor products. In addition, the methods of determining the total sulfur removal and the composition of products could also affect both the experimental results and the theoretical predictions. The purpose of this study is to conduct a fundamental study of the NH_3-SO_2 system in order to provide information on the design of a practical Flue Gas Desulfurization system utilizing ammonia injection. The effects of moisture content, initial seed (fly ash) particles and reaction residence time are studied both experimentally and theoretically.

The research described herein is undertaken with the following objectives:

1. Experimental study of the effect of residence time on the SO_2 removal.
2. Experimental study of the effect of initial seed (fly ash) particles on the SO_2 removal.
3. Experimental study of the effect of moisture content on the SO_2 removal.
4. Identify the composition of the NH_3-SO_2 reaction product.
5. Theoretical study on the SO_2 removal as well as on the gas to particle conversion process.

TECHNICAL DISCUSSION

NH_3-SO_2 REACTIONS AT TRACE WATER CONDITIONS

Introduction

Various NH_3-SO_2 reaction products have been proposed in the literature depending on the reactant concentrations, moisture content, reaction time and reaction temperature. Studies in the literature indicate that the products of the anhydrous reaction are primarily NH_3SO_2 and $(NH_3)_2SO_2$. However, Hartley and Matteson (1975) and Vance and Peters (1976a) also reported that water vapor acts as a catalyst during the initial particle formation process. Trace quantities of water vapor (< 400 ppm) can also act as a reactant (Scargill, 1971), and the most likely reaction product is ammonium pyrosulfite $(NH_4)_2S_2O_5$. This section presents an analysis of the NH_3-SO_2 reaction under trace water conditions by considering three reaction products: NH_3SO_2, $(NH_3)_2SO_2$ and $(NH_4)_2S_2O_5$. The equilibrium calculations performed at these conditions are compared to experimental data. The evolution of the aerosol size distribution is measured in a laminar flow reactor and compared to the predictions of a lognormal model accounting for simultaneous nucleation, condensation and coagulation.

Experimental Setup

The schematic diagram of the experimental system to study the NH_3-SO_2 reaction is shown in Figure 1a. The reactor consists of either a 40 mm i.d. glass tube or a 6.4 mm i.d. stainless steel tube. The glass tube is approximately 80 cm long. 1.02% SO_2 gas

in N_2 is fed through a 1.5 mm o.d. tube along the reactor centerline. The length of this feed tube can be adjusted to obtain desired reactor residence times (2-32 seconds). A mixture of 4.5% NH_3 gas (in N_2 gas) and clean air are introduced through a side port of the glass tube reactor. The stainless steel tube reactor was used for shorter residence times (< 1 second). Sulfur dioxide and ammonia gases were mixed in a union tee junction and then reacted in the stainless steel tube reactor. Concentrations of the gases are controlled by using MKS mass flow controllers. Compressed air is passed through a Balston filter to remove CO_2, hydrocarbons and oil, and then dried and cleaned by passing it through a silica gel air dryer and a 0.2 μm Gelman air filter (AcroFlow II). The water vapor content in both SO_2 and NH_3 tanks was provided by the manufacturer to be less than 5 ppm. The measured relative humidity of the dried, clean air is close to 0%, however the water vapor content was estimated from the data of Bower (1934) and Trusell and Diehl (1963) to be between 30 μg/l (42 ppm, 0.15% RH) and 70 μg/l (94 ppm, 0.3% RH). The PMS model LAS-X Optical Particle Counter was used as the particle measurement instrument and the Horiba PIR-2000 Infrared Gas Analyzer was used for measuring the SO_2 gas concentration. For a few of the experiments, the ammonia concentration was also measured.The experimental conditions are listed in Table 1.

An attempt was made to use the Condensation Nuclei Counter (CNC) to measure the total particle number density of the reaction products. No particles were detected by the CNC and it is suspected that the anhydrous reaction products evaporate in the CNC's saturation zone where the temperature is about 35°C. Similar observations were made

by Vance and Peters (1976a).

Preliminary experiments were conducted using three different setups (Figure 1b) to ensure that proper mixing is obtained in the reactor. The first setup was as described above for the glass tube reactor, with SO_2 being injected through the center and NH_3 through the side port of the reactor. The second setup was same as the first, but the two gas inlet ports were interchanged; that is, NH_3 entered through the center tube and SO_2 through the side port. The third setup used was the stainless steel tube reactor with the union tee mixing head, and provided a rapid mixing of the reactant gases. The results (Table 2) show that the first and the third setup produce the same SO_2 removal after a quasi-equilibrium state is attained, and the removal of SO_2 is higher than that from the second setup. This is because the diffusivity of NH_3 in air (=0.230 cm^2 sec^{-1}, Cussler, 1984) is about twice the diffusivity of SO_2 in air (=0.104 cm^2 sec^{-1}, Cussler, 1984). Thus on injecting NH_3 from the side port, better mixing is obtained amongst the gases as compared to injecting SO_2 from the side port. Similar observations have been made by Kodas et al. (1987) in their aerosol reactor studies.

Theory

Gas Phase Equilibria

Past studies (Hartley and Matteson, 1975, and Vance and Peters, 1976a) have assumed NH_3SO_2 and $(NH_3)_2SO_2$ to be the only products under anhydrous conditions. However, $(NH_4)_2S_2O_5$ could also be formed at low water vapor conditions (St. Clair, 1937; Scargill, 1971). In this work, the following three reactions to be simultaneously

occurring are examined:

$$NH_{3(g)} + SO_{2(g)} \rightleftharpoons NH_3SO_{2(s)} \quad . \tag{6}$$

$$2NH_{3(g)} + SO_{2(g)} \rightleftharpoons (NH_3)_2SO_{2(s)} \tag{7}$$

$$2NH_{3(g)} + 2SO_{2(g)} + H_2O \rightleftharpoons (NH_4)_2S_2O_{5(s)} \tag{8}$$

The equilibrium constants of (1) and (2) have been measured by Scott et al. (1969,1970) and Landreth et al. (1974,1985) and are listed in Table 3 with the appropriate temperature regimes. The computed values of the equilibrium constant differ from each other by several orders of magnitude ($Kp_1 = 1.9 \times 10^{-4}$ and 4.5×10^{-6} atm^2 from data of Landreth et al., 1985 and Scott and Lamb, 1970, respectively at 23°C). The equilibrium constant for reaction (3) has been computed by St. Clair (1937) and Scargill (1971) and is also listed in Table 3. Reasonable agreement is obtained in the values of the equilibrium constant computed by these two expressions.

Assuming that the three reaction products form an ideal solid solution with 'x' mole fraction of NH_3SO_2, 'y' mole fraction of $(NH_3)_2SO_2$, the following ideal equilibrium expressions can be written (Scott and Lamb, 1970)

$$K_{p1} = \frac{P_{N,e} P_{S,e}}{x} \tag{9}$$

$$K_{p2} = \frac{P_{N,e}^2 P_{S,e}}{y} \tag{10}$$

where P represents the partial pressure of the gaseous reactant, the subscripts 'N', 'S',and 'H' refer to the ammonia, sulfur dioxide and water vapor, respectively, and the

$$K_{p3} = \frac{P_{N,e}^2 P_{S,e}^2 P_{H,e}}{(1-x-y)} \tag{11}$$

subscript 'e' denotes the equilibrium state. Combining equations (1), (2) and (3), the overall reaction is,

$$(2-x)\,NH_3 + (2-x-y)\,SO_2 + (1-x-y)\,H_2O \leftrightarrow xNH_3SO_2$$

$$+y(NH_3)_2SO_2 + (1-x-y)\,(NH_4)_2S_2O_5 \tag{12}$$

Using equations (4) to (7), the equilibrium vapor pressure of each gas is:

$$P_{N,e} = \frac{y}{x}\frac{K_{p2}}{K_{p1}} = P_{N,in} - m(2-x) \tag{13}$$

$$P_{S,e} = \frac{x^2}{y}\frac{K_{p1}^2}{K_{p2}} = P_{S,in} - m(2-x-y) \tag{14}$$

$$P_{H,e} = \frac{(1-x-y)}{x^2}\frac{K_{p3}}{K_{p1}^2} = P_{H,in} - m(1-x-y) \tag{15}$$

where 'm' times the stoichiometric constant of the gas reactant in equation (7) gives the vapor pressure consumption of that gas when equilibrium is reached. Equations (8) to (10) are a set of three non-linear equations, and the three unknowns, x, y, and m, are solved using a non-linear equation solver, DNEQNJ (IMSL, 1987).

Particle formation mechanisms

The general dynamic equation for the gas to particle conversion process is (Friedlander, 1977):

$$\frac{\partial n}{\partial t}+\frac{\partial (Gn)}{\partial v}-I'(v^*)\,\delta(v-v^*)=$$

$$\frac{1}{2}\int_0^v \beta(v-\tilde{v},\tilde{v})\,n(v-\tilde{v},t)\,n(\tilde{v},t)\,d\tilde{v}-n(v,t)\int_0^\infty \beta(v,\tilde{v})\,n(\tilde{v},t)\,d\tilde{v} \qquad (16)$$

The first term on the left hand side (LHS) is the rate of change of the particle distribution function in the particle volume interval v to v+dv, the second term on the LHS accounts for the effect of condensation at rate G, and the third term on the LHS describes the formation of new particles of critical volume v^* at rate I'. The terms on the right hand side account for the effect of Brownian coagulation.

There are four condensible species in the system: $(NH_4)_2S_2O_5(v)$, $NH_3SO_2(v)$, $(NH_3)_2SO_2(v)$ and water vapor. However, since $(NH_4)_2S_2O_5$ vapor is the predominant product of reaction and only a trace amount of water vapor is present, homogeneous nucleation was assumed to be the mechanism. The nucleation rate, I', was described using classical Becker-Doering homogeneous nucleation theory with a scaling factor I_s,

$$I'=\frac{n_s}{\tau}S^2\left(\frac{2}{9\pi}\right)^{\frac{1}{3}}\left(\frac{\sigma v_1^{\frac{2}{3}}}{k_BT}\right)^{\frac{1}{2}}\exp\left(-\frac{K^*\ln S}{2}\right)I_s \qquad (17)$$

where n_s is the monomer concentration at saturation, τ is the characteristic time for particle growth, S is the saturation ratio of the system, σ is the surface tension of the condensing species, v_1 is the monomer volume, k_B is the Boltzmann constant, T is the reaction temperature, and K^* is the number of monomers in the critical size nucleus.

A monomer balance for the aerosol growth can be written in terms of the system saturation ratio, S (Friedlander, 1983):

$$\frac{dS}{dt} = \frac{R_r'}{n_s} - \frac{I'K^*}{n_s} - (S-1)\left(\frac{k_B T}{2\pi m_1}\right)^{\frac{1}{2}} A \tag{18}$$

where the first term on the right hand side accounts for the monomer formation rate by chemical reaction, the second and third terms account for the nucleation and condensation effects, respectively, m_1 is the monomer mass and A is the total particle surface area.

Assuming the entire size spectrum can be approximated by a lognormal function,

$$n(v) = \frac{1}{3\sqrt{2}\pi v \ln\sigma_g} \exp\left[-\frac{\ln^2(v/v_g)}{18\ln^2\sigma_g}\right] \tag{19}$$

where v_g is the geometric mean particle volume, and σ_g is the geometric standard deviation of the size distribution. The kth-moment formulation is employed to obtain the integral properties of the size distribution (Lee and Chen, 1984):

$$M_k(t) = \int_0^\infty v^k n(v,t)\, dv \tag{20}$$

Multiplying Equation (11) by "v" on both sides, and integrating over all particle sizes, the following equations are obtained for a laminar flow reactor (Pratsinis, 1988):

$$2(1-r^2)\frac{dS}{d\theta} = R_r - IK^* - \eta(S-1)M_0 \tag{21}$$

$$2(1-r^2)\frac{dM_0}{d\theta} = I - \zeta M_0^2 \tag{22}$$

$$2(1-r^2)\frac{dM_1}{d\theta} = IK^* + \eta(S-1)M_0 \tag{23}$$

$$2(1-r^2)\frac{dM_2}{d\theta} = IK^{*2} + 2\varepsilon(S-1)M_1 + 2\psi M_1^2 \qquad (24)$$

where M_0, M_1 and M_2 are the total particle number concentration, total particle volume and second volume moment, respectively, r is the dimensionless radial distance ($r=r^*/R$), θ is the dimensionless time ($=t/\tau$); η and ε are coefficients for the condensation rate, and ζ and ψ are coefficients for the coagulation rate. A list of these dimensionless parameters is provided in Appendix A.

The size distribution can be described by three parameters, M_0, v_g, and σ_g, which are usually obtainable from size measuring experiments. v_g and σ_g can be expressed in terms of the three moments as (Lee and Chen, 1984),

$$v_g = \frac{M_1^2}{M_0^{\frac{3}{2}} M_2^{\frac{1}{2}}} \qquad (25)$$

$$\ln^2\sigma = \frac{1}{9}\ln\left[\frac{M_0 M_2}{M_1^2}\right] \qquad (26)$$

Equations (16)-(19) form a set of four coupled ordinary differential equations which were solved using a differential equation solver, DIVPAG (IMSL,1987). The initial conditions for the above equations are : $S=S_{in}$ and $M_0=M_1=M_2=0$ for all radial positions (Bai and Biswas, 1990). The predominant solid product is $(NH_4)_2S_2O_5$ (as can be seen in Table 4), and this is expected as it is less volatile than the other two products. The saturation ratio for forming the $(NH_4)_2S_2O_5$ product can be written as

$$S_{in} = \frac{P_{N,in}^2 \, P_{S,in}^2 \, P_{H,in}}{K_{p3}} \tag{27}$$

if chemical equilibrium is attained before particle growth begins, and S_{in} is equal to unity if chemical reaction and particle growth occur simultaneously.

Results and Discussion

Figure 2a is a plot of the SO_2 removal from the glass tube reactor as a function of reactor residence time under anhydrous conditions ($H_2O \approx 50$ ppm, RH≈0%) for various NH_3 inlet concentrations. It seems that SO_2 removal is not favored under the anhydrous conditions. Although the SO_2 removal is higher if more NH_3 was injected (15%, 28%, and 42% removals, respectively for NH_3 inlet concentrations of 3000, 6000, and 9000 ppm in Figure 2a), the overall SO_2 removal is low for all three different inlet NH_3 concentrations. Figure 2b shows the results from the stainless steel tube reactor, which was used for short reactor residence time measurement to see the time required to reach gas phase equilibrium. It is seen that the reactions were completed in less than 0.4 seconds. The characteristic time for mixing in a union tee is calculated by (Simpson, 1975):

$$\tau_m = \left(\frac{5}{\pi}\right)^{2/3} (L_s^2/\varepsilon_d)^{1/3} \left[2/(3-N_{sc}^2)\right] \tag{28}$$

where L_s is the scale integral length scale, ε_d the rate of energy dissipation per unit mass and N_{sc} is the Schmidt number. The characteristic time for mixing in the experiment is about 0.25 seconds, and data (Figure 2b) for time periods less than this may be due to

mixing limitations.

The measured SO_2 gas phase concentration at the outlet of the reactor as a function of the inlet ammonia concentration is plotted in Figure 3. The residence time was varied to ensure that the reaction attained a quasi-equilibrium state. Calculations were also done at water vapor concentrations using the equilibrium expressions listed in Table 3, and the results are shown in Figure 3. The zero water vapor concentration results are the Landreth et al. (1985) and Scott and Lamb (1970) model of two reactions. Significant difference is obtained between the two predictions and this may be due to the different temperature regions in which the equilibrium constants were determined. The calculations were then done using the three reaction model proposed in this work, and using equilibrium constants for reactions (1) and (2) proposed by both Scott and Lamb (1970) and Landreth et al. (1985). When the Scott and Lamb (1970) equilibrium constants are used, not much change in the predicted equilibrium concentration is obtained at 50 ppm water vapor content. Also, as seen in Figure 3, the curve tends to move further away from the experimental data. However, there tends to be better agreement with the measured concentrations when the Landreth et al. (1985) expressions are used for a water vapor content between 200 to 400 ppm. This corresponds to a RH between 0.75 and 1.5%, which is slightly higher than the estimated water content of silica gel dried air streams (~0.2% RH) (Trusell and Diehl, 1963). The better agreement of predicted and measured concentrations when the Landreth et al. (1985) equilibrium constants are used as compared to the Scott and Lamb (1970) expressions maybe due to the temperature range of the Landreth et al. (1985) experiment being closer to that used

in this work. The equilibrium mole fractions of the different solid products at different water vapor contents are summarized in Table 4.

The size distribution of the aerosol is measured by the Optical Particle Counter and then fitted by a lognormal distribution function. Table 5 lists the experimental data of the average total number concentration, geometric mean particle diameter, dp_g, and the geometric standard deviation with respect to reaction residence time. Our experimental data indicate particle phase equilibrium has been reached within a short time, with the particle number density of around 10^5 #/cc and geometric mean sizes of around 0.1-0.15 μm, which compared well with results of Carabine et al. (1971), who also utilized a light scattering device to detect particles. The size distribution plot for a residence time of 0.63 seconds is shown in Figure 4.

Using the Scargill (1971) computed equilibrium constant, K_{p3}, the initial saturation ratio (equation 22) of $(NH_4)_2S_2O_5$ is of the order of 10^4 for inlet concentrations of NH_3, SO_2 and H_2O of 6000, 3000 and 50 ppm, respectively. This is much higher than the saturation ratios of the other two compounds, NH_3SO_2 and $(NH_3)_2SO_2$. Therefore, it is assumed that $(NH_4)_2S_2O_5$ is the primary nucleation product, with subsequent condensation of NH_3SO_2, $(NH_3)_2SO_2$ and $(NH_4)_2S_2O_5$ monomers onto those nuclei.

The integral properties of the size distribution are computed and compared to the predictions of the lognormal model described earlier and the results are shown in Figures 5a, 5b and 5c. Since $(NH_4)_2S_2O_5$ is the predominant product, we assumed it is the only product in the particle formation model. Both particle density and the surface tension are unknown for carrying out the gas-to-particle conversion calculation. Particle density

was estimated from data of $(NH_4)_2SO_4$ (ρ_p=1.77 g/cm^3) and NH_4HSO_3 (ρ_p=2.03 g/cm^3), and was varied in the range of 1.8-2.0 g/cm^3 in our model. The value for surface tension is not available and is adjusted to fit the experimental results (symbols in Figures 5a, 5b and 5c). Chemical reaction and particle growth may be occurring simultaneously. As indicated by equation (16), saturation ratio increases due to chemical reaction (till the reaction reaches equilibrium) and decreases due to nucleation and condensation of the vapors. Limited information is available in the literature regarding the chemical reaction order or the reaction rate for the formation of $(NH_4)_2S_2O_5$. Hence an average value of R_r was estimated from the experimental data. The time required to reach equilibrium, t_r, is between 0 and 0.4 seconds in the experiments. The average value of R_r' was thus calculated by $(P_{s,in}-P_{s,e})N_{av}/82t_rT$, where N_{av} is the Avogadro's number.

Three sets of model predictions are plotted in Figures 5a, 5b and 5c. All three sets are plotted by appropriate choice of parameters so that there are best fits with the number concentration, geometric mean particle diameter and geometric standard deviation. The solid lines are plotted with the results of model predictions accounting for simultaneous chemical reaction and particle growth; the dashed lines are plots for very fast reaction, or assuming that reaction equilibrium is attained before particle growth begins. On assuming very fast chemical reaction and on varying the surface tension, reasonable agreement of experimental data (number concentration, geometric mean particle size and standard deviation) with model predictions was obtained for a surface tension of 70 dyne/cm, this being close to the value of H_2SO_4 (Liu and Levi, 1980). The other dashed line was plotted by using a higher surface tension of 93 dyne/cm, this being less than the

surface tension of NH_4NO_3 reported in the literature (113 to 119 dyne/cm, Raes et al, 1990). The nucleation rate had to be scaled up by a factor of 10^9 for agreement between model predictions and experimental data. The solid line is plotted using a t_r of 0.04 seconds and reasonable agreement is obtained with the experimental data. Increasing t_r (slower reaction) does not yield good agreement with the experiments, and hence the results are not shown. The two dashed curves indicated that there is a burst of nucleation and formation of particles, which then primarily grow by condensation. This is also confirmed by the final geometric standard deviation tending to one. In the case of simultaneous reaction and particle growth, nucleation is delayed by a fraction of a second (short delay as reaction is still rapid). The final geometric standard deviation is higher, indicating growth occurs by both condensation and coagulation. Also, the computed characteristic time for particle growth (τ) is about 0.12 seconds, much larger than t_r (=0.04 seconds). On comparing the experimental data to the three sets of model predictions, it can be assumed that chemical reaction is extremely rapid and completed before particle growth begins.

Summary

The gas phase reactions between sulfur dioxide and ammonia at trace water vapor concentrations were studied theoretically and experimentally. The effect of reaction residence time on the SO_2 and the average product particle size have been determined. Results indicated that both gas phase and solid phase reach equilibrium in a very short time, less than 0.4 seconds. Quasi-equilibrium gas concentrations and particle properties

were measured experimentally and then compared to the predictions of a theoretical model. A three reaction mechanism leading to $NH_3SO_{2(s)}$, $(NH_3)_2SO_{2(s)}$ and $(NH_4)_2S_2O_{5(s)}$ as products was used to carry out the equilibrium calculations. A theoretical model of the gas-to-particle conversion process accounting for chemical reaction, nucleation, condensation and coagulation was developed, based on standard expressions summarized in Friedlander (1977). Since $(NH_4)_2S_2O_{5(s)}$ is the predominant product of the NH_3-SO_2 reaction, it was considered as the source of primary nuclei and further growth of particles by condensation and coagulation. The measured particle size appears to be lognormally distributed with a geometric mean diameter of 0.1 to 0.2 μm, geometric standard deviation of 1.1-1.2 and total particle number concentration of around 10^5 cm^{-3}.

Table 1

Experimental conditions and instruments used at trace water conditions.

EXPERIMENTAL CONDITIONS	
Temperature:	23.5 ± 1°C
Humidity:	0.15 ~ 0.3% (42 ~ 94 ppm)
SO_2 Concentration:	3000 ppm
NH_3 Concentration:	3000, 6000, 9000 ppm
Total Flow Rate:	1 lpm
Reactor Residence Time:	0.25 ~ 56 seconds
INSTRUMENTS	
SO_2 Analyzer:	Horiba PIR-2000 Infrared Gas Analyzer
Range:	0 - 5000 ppm
Precision:	± 100 ppm
NH_3 Analyzer:	Horiba PIR-2000 Infrared Gas Analyzer
Range:	0 - 3000 ppm
Precision	± 100 ppm
Particle Counter:	PMS Model LAS-X OPC
Range:	0.09 µm ~ >3 µm

Table 2

Comparison of the three different reactor setups: Numbers are SO_2 removal percentages at outlet.

$SO_{2,in}$=3000 ppm $NH_{3,in}$=6000 ppm

Reaction time	Setup 1	Setup 2	Setup 3
0.4 s	_	_	27%
0.6 s	_	_	27%
1.2 s	_	_	28%
2.2 s	28%	16%	_
4.5 s	30%	12%	_
32 s	30%	15%	-

Note: The comparison can not be made at the same reaction residence time due to the geometrical limitations of the reactors. However, it is seen that the SO_2 concentration reached quasi-equilibrium state in less than 0.4 seconds. The standard deviation of the experiment is around ± 4% of SO_2 removal.

Experiments were performed to measure the SO_2 adsorption to the glass walls, and the amount was found to be negligible.

Table 3

Equilibrium constants for the three of NH_3-SO_2 reactions.

Possible Reactions	Equilibrium Expressions	Temp. Range	Sources
$NH_3SO_{2(s)}=NH_3+SO_2$	$K_{p1}=exp(22.7-9259/T)$	5 to 45□C	1
	$K_{p1}=exp(42.7-16205/T)$	-10 to -70□C	2
$(NH_3)_2SO_{2(s)}=2NH_3+SO_2$	$K_{p2}=exp(43.8-16606/T)$	5 to 45□C	1
	$K_{p2}=exp(88.0-31306/T)$	-10 to -70□C	2
$(NH_4)_2S_2O_{5(s)}=2NH_3+2SO_2+H_2O$	$K_{p3}=exp(94.6-39144/T)$	60 to 110□C	4
	$K_{p3}=exp(96.5-40767/T)$	0 to 23□C	3

1. Landreth et al. (1985)
2. Scott and Lamb (1970)
3. Scargill (1971)
4. St. Clair (1937)

Table 4

Computed mole fraction of the three solid products for different water vapor concentrations. The computation is based on thermodynamic data of Landreth et al. (1985) and Scargill (1971).

	H_2O (ppm)	NH_3SO_2 x	$(NH_3)_2SO_2$ y	$(NH_4)_2S_2O_5$ 1-x-y
	0	-	-	-
	50	0.045	0.005	0.950
SO_2=3000 ppm	100	0.042	0.005	0.953
NH_3=3000 ppm	200	0.036	0.004	0.960
	400	0.024	0.002	0.974
	0	-	-	-
	50	0.086	0.020	0.894
SO_2=3000 ppm	100	0.081	0.019	0.900
NH_3=6000 ppm	200	0.077	0.018	0.905
	400	0.057	0.011	0.932
	0	-	-	-
	50	0.130	0.046	0.824
SO_2=3000 ppm	100	0.123	0.043	0.834
NH_3=9000 ppm	200	0.117	0.041	0.842
	400	0.088	0.029	0.883

Table 5

Experimental results of the particle properties from the Optical Particle Counter with a lognormal size distribution fitting.

Residence Time (seconds)	Total Number Concentration (particles/cm^3)	dp_g (μm)	σ_g
0.25[a]	1.3 X 10^5	0.15	1.18
0.63[a]	2.8 X 10^5	0.14	1.10
0.95[a]	2.7 X 10^5	0.14	1.12
4.5[b]	2.4 X 10^5	0.11	1.11
16.4[b]	1.8 X 10^5	0.11	1.09
32.7[b]	2.1 X 10^5	0.12	1.14

Note: [a] Measured from stainless steel tube reactor.

[b] Measured from glass tube reactor.

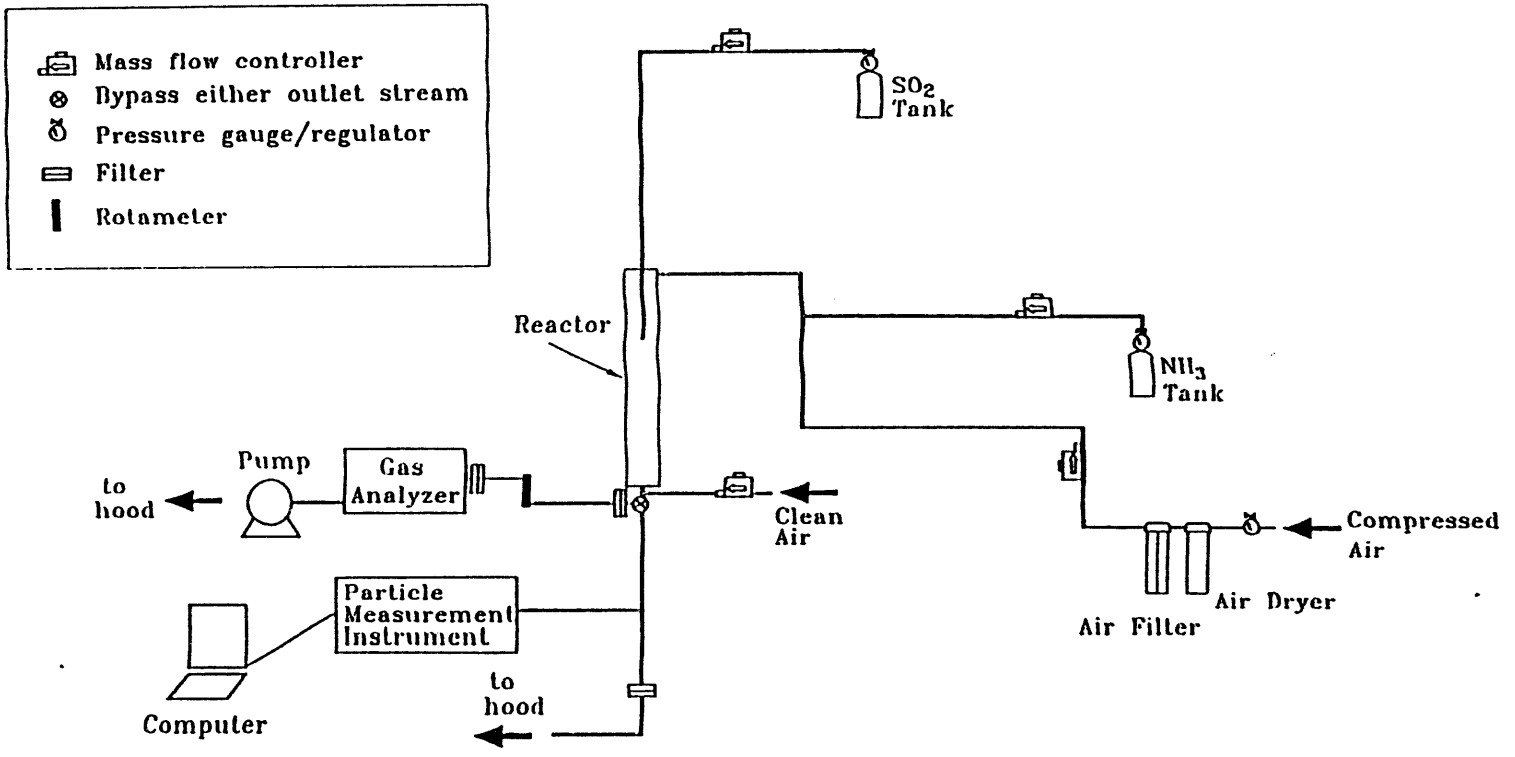

Figure 1a Schematic diagram of the experimental setup to study the NH_3-SO_2 reaction.

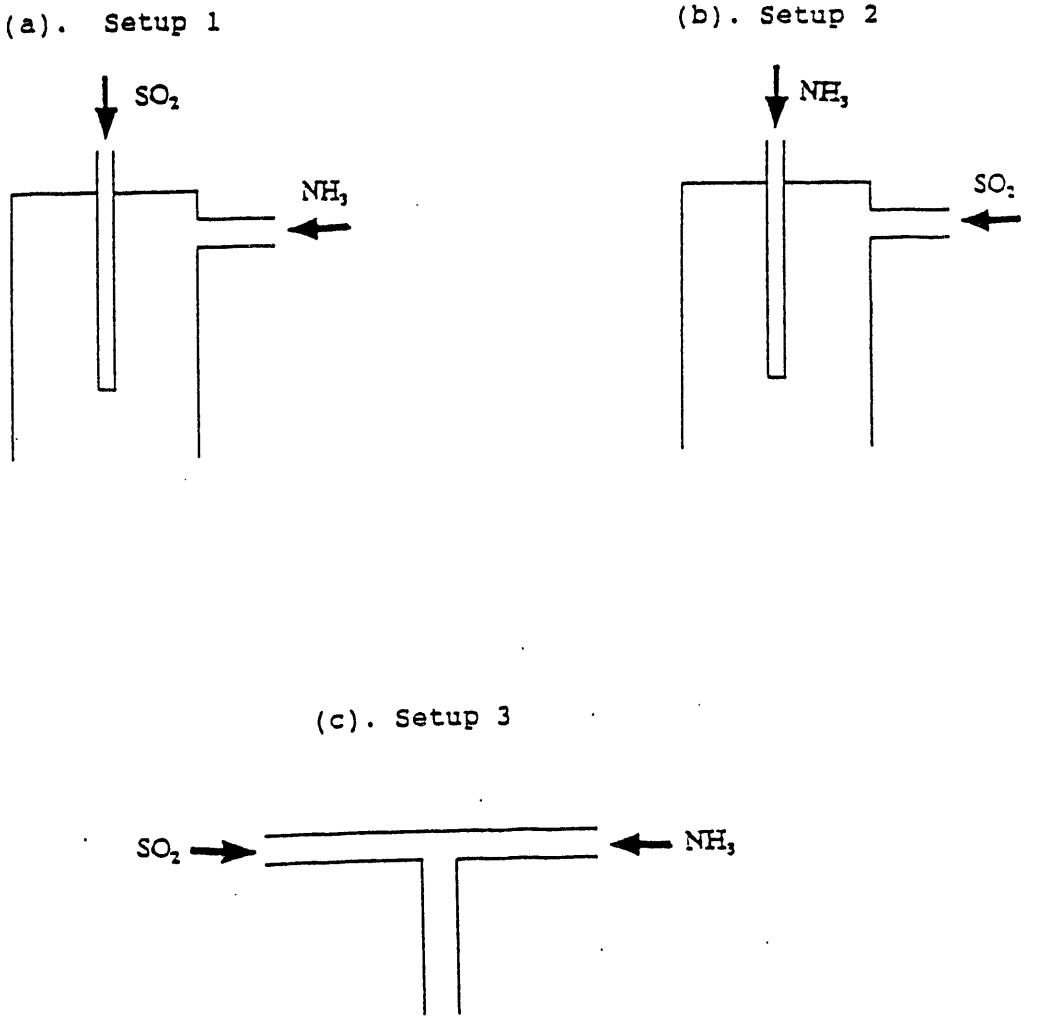

Figure 1b Schematic diagram of three different setups to check for mixing conditions.

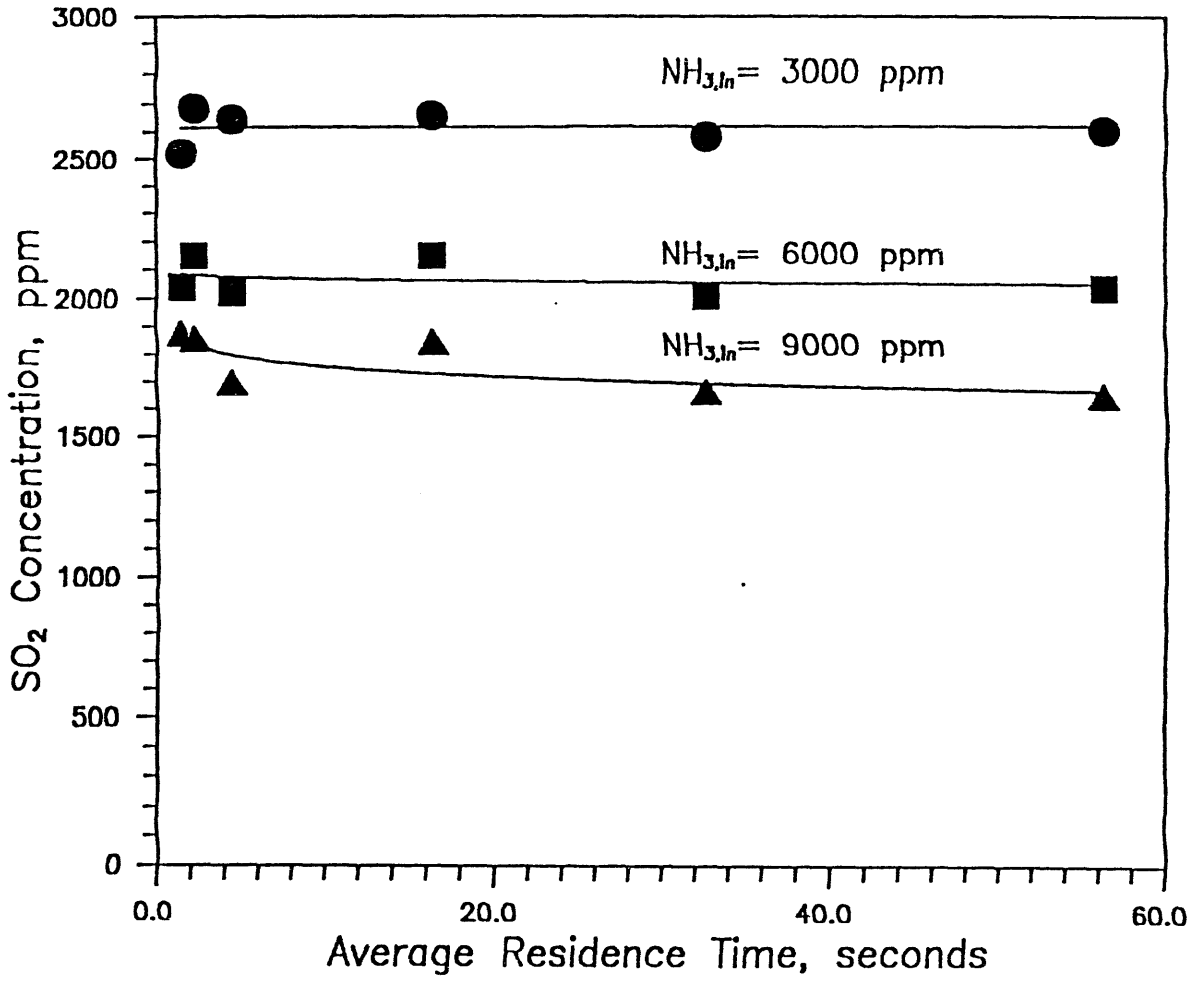

Figure 2a SO_2 concentration (with $SO_{2,in}$ = 3000 ppm) as a function of average residence time at room temperature. Data are from glass reactor.

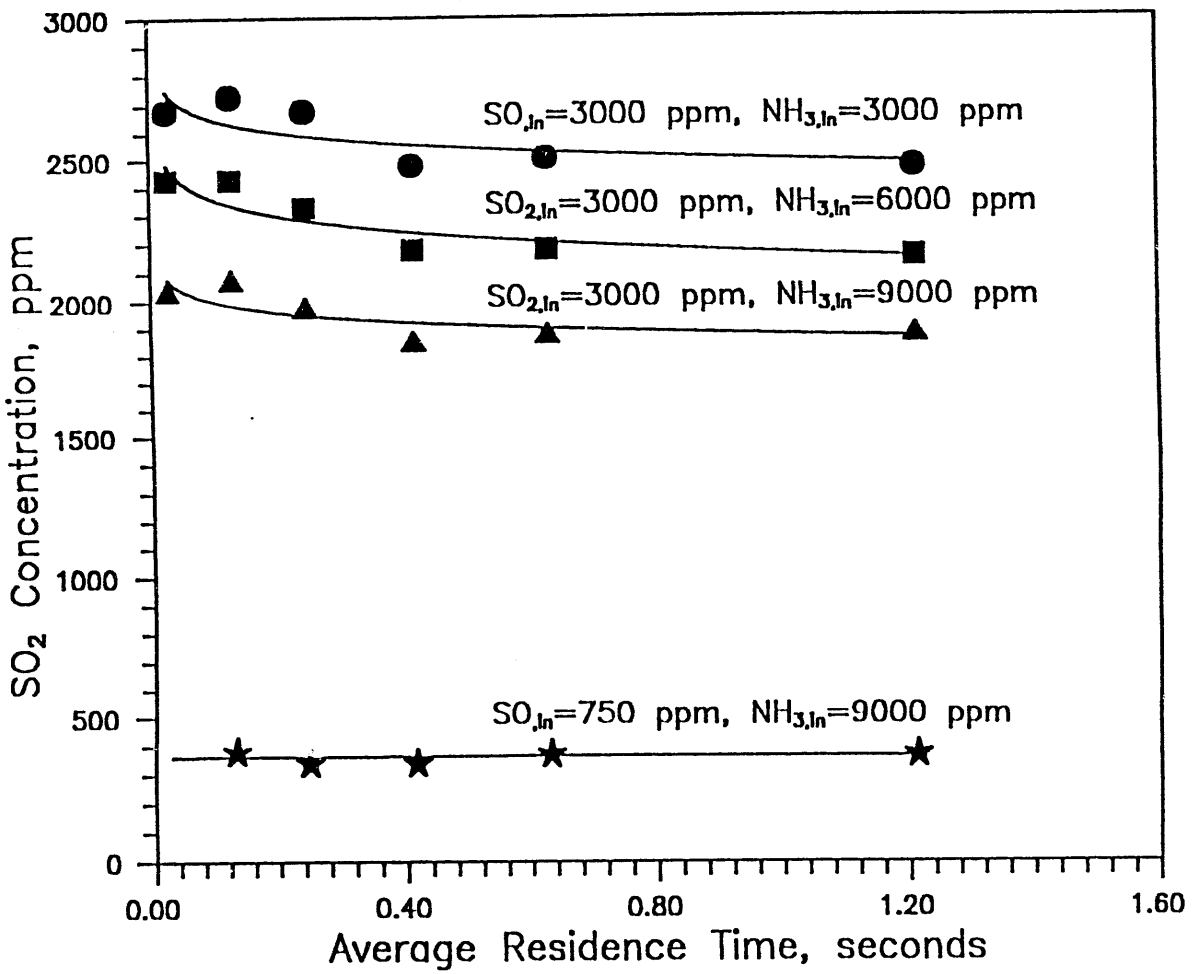

Figure 2b SO_2 concentration (with $SO_{2,in}$ = 3000 ppm) as a function of average residence time at room temperature. Data are from stainless steel reactor.

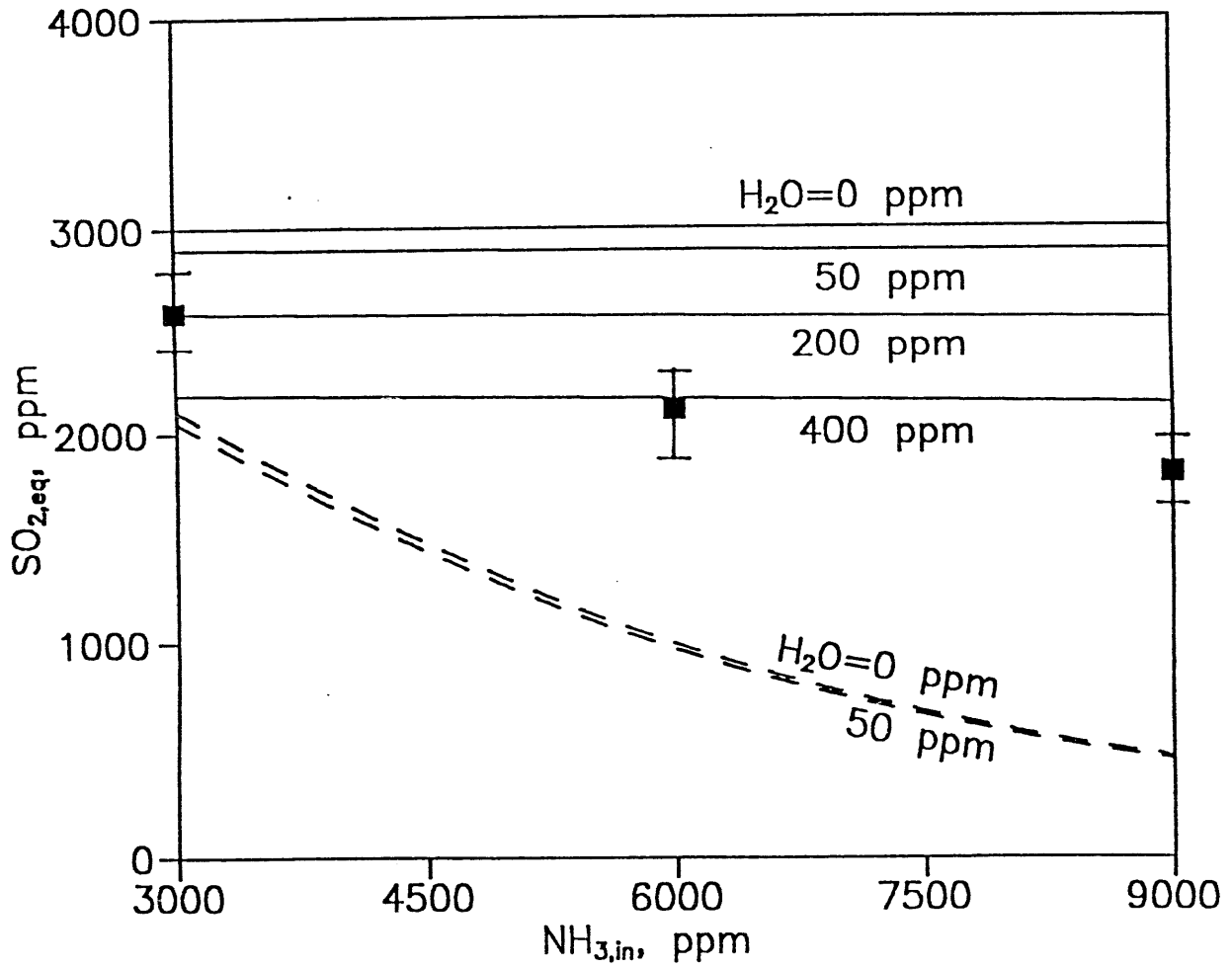

Figure 3 Measured and calculated SO_2 equilibrium vapor pressure as a function of inlet NH_3 concentration. Symbols are experimental data and lines are theoretical results of the present model using different equilibrium constants for reactions (2.1) and (2.2): (—— Landreth et al., 1985; Scott and Lamb, 1970)

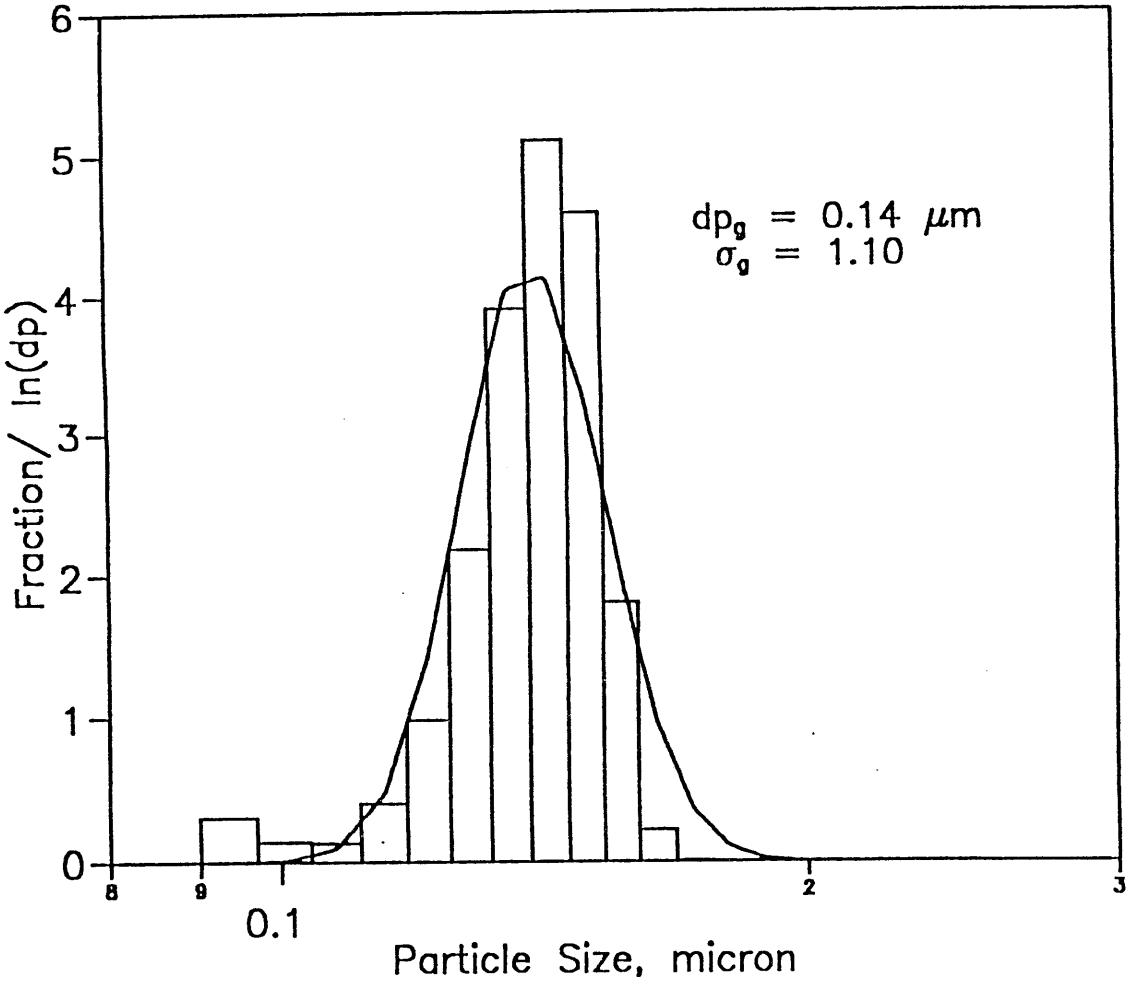

Figure 4 Size distribution of NH_3/SO_2 reaction products at room temperature with inlet SO_2 concentration of 3000 ppm and inlet NH_3 concentration of 6000 ppm at 0.63 second residence time.

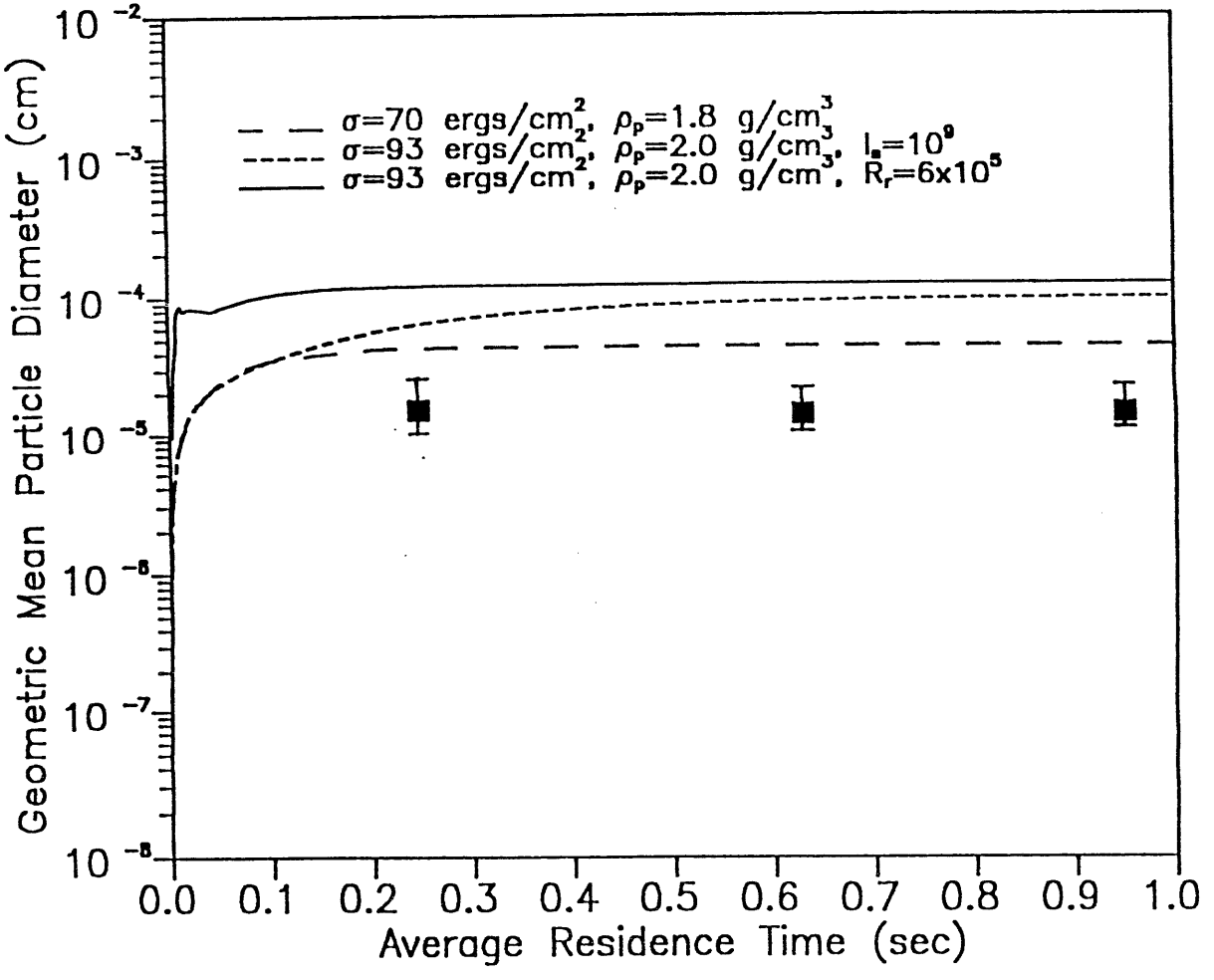

Figure 5a Measured and simulated results of cup mixing average geometric mean particle diameter concentration as a function of average residence time. The inlet SO_2 and NH_3 concentrations are 3000 and 6000 ppm, respectively.

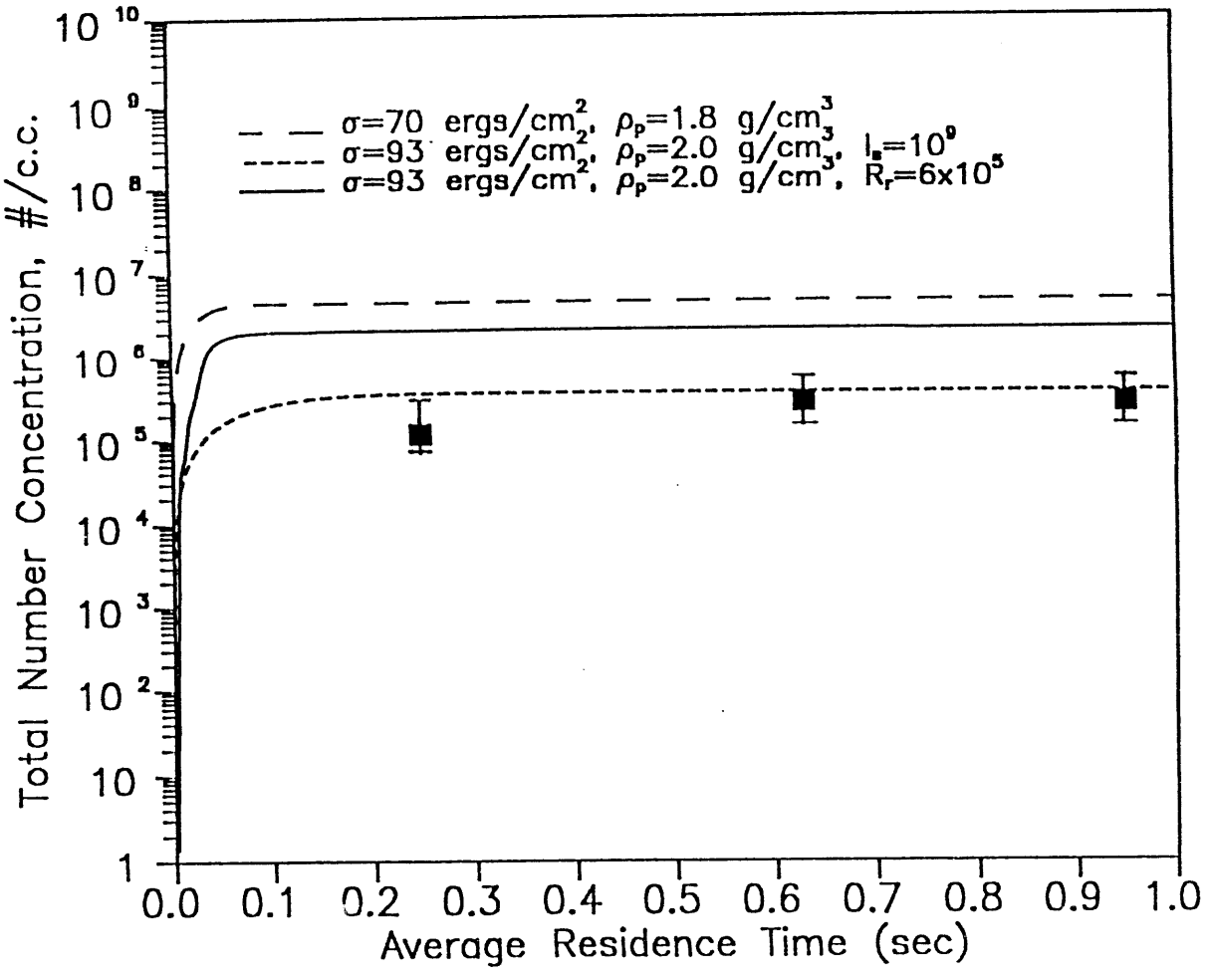

Figure 5b Measured and simulated results of cup mixing average total particle concentration as a function of average residence time. The inlet SO_2 and NH_3 concentrations are 3000 and 6000 ppm, respectively.

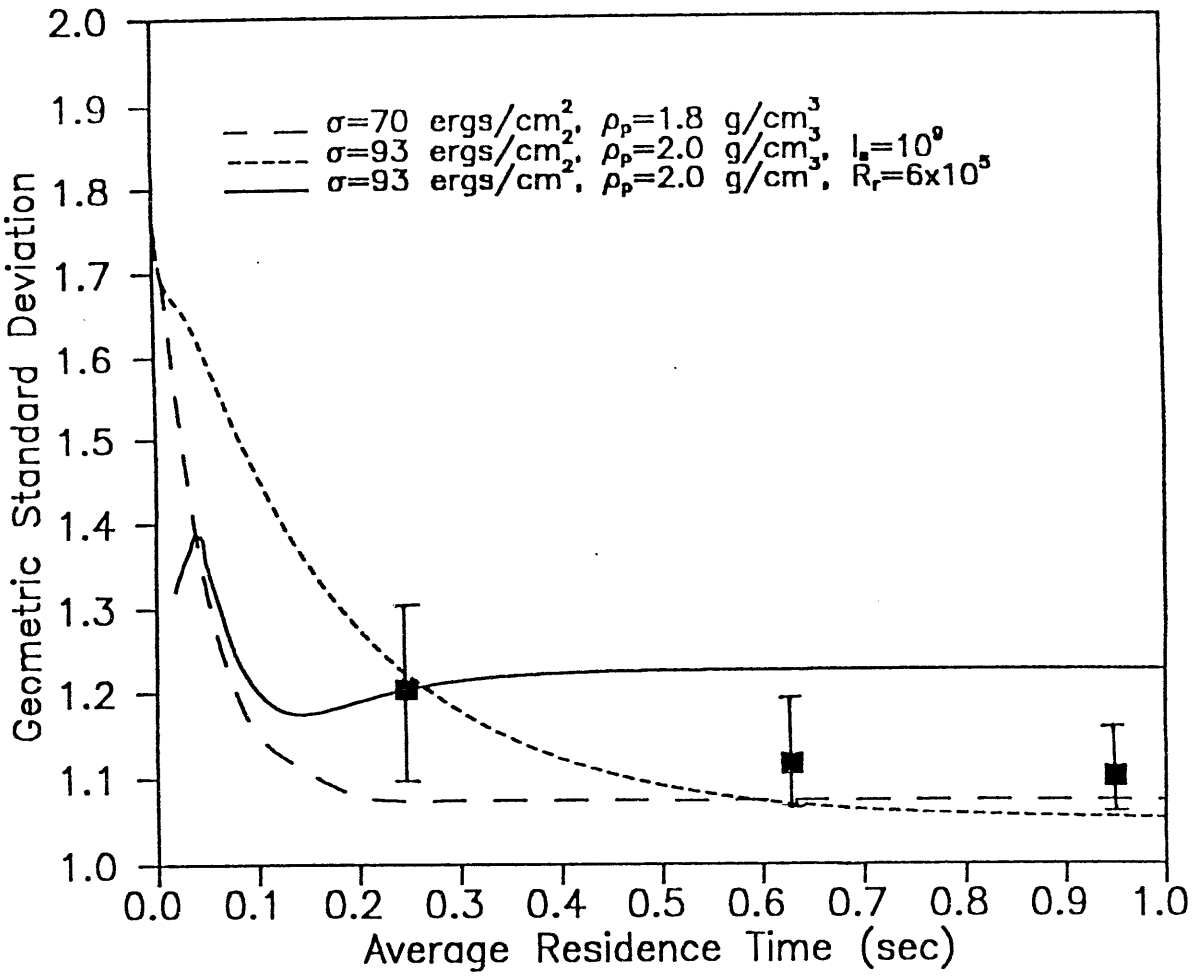

Figure 5c Measured and simulated results of cup mixing average geometric standard deviation as a function of average residence time. The inlet SO_2 and NH_3 concentrations are 3000 and 6000 ppm, respectively.

NH_3-SO_2 REACTIONS IN THE PRESENCE OF INERT PARTICLES

Introduction

Many investigators have reported enhanced SO_2 removal efficiencies in flue gas desulfurization (FGD) processes in the presence of high surface area fly ash particles. Hurst and Bielawski (1980) showed SO_2 removal efficiencies of up to 65% with a slurry containing a high alkalinity fly ash. Martinez et al. (1975) found that only 5% SO_2 removal was observed with untreated fly ash. Higher removal rates were observed when hydrated mixtures of the fly ash were used as the resultant surface area of the fly ash was greater. Reed et al. (1984) indicated that fly ash with a low alkali content did not result in significant SO_2 removal efficiencies even for high surface areas, while fly ash with a high alkali content resulted in higher SO_2 removal efficiencies for higher surface areas and longer residence times. It is therefore obvious that the SO_2 capture by fly ash depends on the physical properties as well as chemical characteristics of the fly ash particles, and the physical conditions of the flue gas stream. Though a number of such studies have indicated the role of fly ash particles in the removal of SO_2, no detailed studies have been performed toward understanding the different processes that take place. The condensation of NH_3-SO_2 reaction product vapors onto existing particles is examined in this chapter. Experiments are conducted at the conditions similar to those in the previous section. Sodium chloride particles are used as the experimental particles which are inert, and do not chemically react with the NH_3-SO_2 reaction product under dry conditions. This study therefore attempts to identify the physical processes associated

with the dependence of SO_2 removal on the characteristics of the particles. The experimental results are analyzed by the particle formation model presented previously.

Experimental Setup

Figure 6 shows the schematic diagram of the experimental setup for studying the effect of particles on the NH_3-SO_2 reaction. Clean compressed air was metered through a precalibrated rotameter before it was inlet to a TSI Model-3076 Atomizer. An aqueous solution of sodium chloride was atomized to generate the aerosol. As moisture plays a significant role in the NH_3-SO_2 reaction (this will be discussed in next section), it was essential to obtain a very dry sodium chloride aerosol, and hence the aerosol was passed through three diffusion dryers in series. The drying agents (silica gel and calcium sulfate) in the diffusion dryers were removed and dried in an oven overnight prior to each experiment. Experiments were conducted under room temperature conditions. The inlet concentrations of sulfur dioxide and ammonia gases were 3000 and 6000 ppm, respectively. The relative humidity and temperature were measured by a Vaisala HMP 36/HMI 31 sensor. It was not possible to precisely control the moisture content of the system (within 10 ppm). However, the relative humidity of the seed aerosol stream after the diffusion dryers was between 0 to 0.5% (0 to 140 ppm) for each experimental run. Three different size distributions of sodium chloride seed particles were used to examine the condensation of NH_3-SO_2 product vapors onto the particles. Table 6 lists the total surface area, the total seed number, the mode diameter and the parameters of the lognormal function describing the sodium chloride seed particle size distribution. The

aerosol in Run 1 has the highest total surface area (7.3×10^4 μm^2 cm^{-3}), which is approximately 5 and 300 times that of Runs 2 and 3, respectively. The sulfur dioxide concentration after the reaction was measured by a Horiba PIR-2000 Infrared Gas Analyzer, and the particle size distribution was measured using the LAS-X Optical Particle Counter (OPC).

Results and Discussion

The experimental conditions and parameters used in model simulation are similar to those in the previous section. Figures 7 shows the size distribution histograms of the three different runs measured using the OPC. As can be seen in Figures 7a and 7b, Runs 1 and 2 wherein higher surface area aerosols were introduced (Table 6) yield an increase in the number fraction of the larger sizes when compared to the size distribution of the inlet sodium chloride aerosol. This is possibly due to the condensation of vapors onto the sodium chloride particles. The number fraction of the smaller sizes also increases due to the formation of new particles. As the surface area of particles was low in Run 3 (Figure 7c), condensation was not dominant, with an increase in particles in the lower size ranges due to new particle formation by nucleation. The histograms of Figure 7 indicate that the size distributions of both the sodium chloride seed and the reaction products are approximately lognormal.

The sulfur dioxide removal of the three runs measured from the infrared gas analyzer is listed in Table 7. The results indicate that the amount of SO_2 removal increased by the introduction of particles is not significant. The maximum SO_2 removal

increase was only 10±6% as measured by the SO_2 Analyzer. However, it is observed that experimental runs with higher total surface areas tend to yield a slightly higher SO_2 removal.

The size distributions of the NH_3-SO_2 reaction product obtained from Optical Particle Counter (OPC) with the presence of inert particles are listed in Table 7 (Runs 1 to 3) with a lognormal approximation. It is seen that Run 1 yields a maximum total volume increase as compared to Runs 2 and 3. The result from OPC is in agreement with the SO_2 removal obtained from the gas analyzer as Run 1 has the highest surface area.

The OPC output without the presence of inert particles (Run 4) is also listed in Table 7. Although nucleation of new particles and vapor condensation were observed with the introduction of particles, experiments without sodium chloride particles yield total particle number only in the order of 100 #/cm^{-3}. This is because the amount of water vapor at near anhydrous conditions in the system is very critical for particle formation. To explain the effect of moisture content on the particle formation, the gas-to-particle conversion model was used to investigate conditions without the introduction of particles. Table 8 lists the parameters used in the model simulation. One set of values of surface tension, particle density and the nucleation rate used in Chapter 2 is used in this Chapter (σ = 93 ergs cm^{-2}, ρ_p = 2.0 g cm^{-3}, I_s = 10^9). The simulation is very sensitive to the values of surface tension and particle density used in the model. The other set of surface tension (described in previous section) and particle density (σ = 70 ergs cm^{-2}, ρ_p = 1.8 g cm^{-3}) does not yield an agreement with the experimental data in

this Chapter. Figure 8 shows the effect of moisture content on the total particle number formed without introducing inert particles. As can be seen, a slight increase of moisture content from 20 to 50 ppm results in the formation of particles increases from less than 10 cm^{-3} to more than 10^5 cm^{-3} at residence time of 1 second. It is not possible to control the moisture content for the experiments with and without inert particle conditions with this accuracy. The moisture content with the introduction of inert particles is always higher than without inert particles as the atomizer contributes some moisture even though three diffusion dryers were used. It is estimated from Table 7 and Figure 8 that the experimental moisture content without the presence of inert particles would be about 40 ppm while that with the presence of inert particles would be around 25 ppm.

The experimental data of Run 1 were simulated using the particle formation model. The size distributions of the sodium chloride particle and the NH_3-SO_2 reaction products were both assumed to be lognormal. Figures 9a, b and c show the theoretical and experimental results of the total particle number, geometric mean particle diameter and geometric standard deviation, respectively, as a function of the average residence time. Since the amount of water vapor in the reaction is unknown, simulations were done for moisture contents of 20, 40 and 50 ppm. It is seen that water vapor of 40 ppm produces a better agreement. As can be seen in Figure 9, large deviations of experimental data were observed, especially for the geometric mean diameter and standard deviation. This could be due to the difficulty in controlling the moisture content to be exactly identical for each experimental test.

Total sulfur dioxide removal can also be predicted using the particle formation

model. The computed values of total volume increase and SO_2 removal for Run 1 as a function of moisture content are listed in Table 9. It is seen by referring to Table 7 that the prediction of total particle volume increase at H_2O = 40 ppm (7.5×10^4 μm^3 cm^{-3}) fits the experimental data best. The SO_2 removal on the introduction of seed particles increases for increasing moisture content. Simulation was also carried out for a typical fly ash size distribution (McCain et al., 1975) of total particle number, geometric mean diameter and standard deviation of 6×10^7 #/cm^3, 0.06μm, and 3.0, respectively, and the results are listed in Table 9. The surface area of a typical fly ash in a coal combustion exhaust is calculated to be about 2×10^6 μm^2 cm^{-3} , which is about 30 times that of Run 1. However, as listed in Table 8, the total sulfur removal increase due to the presence of a typical fly ash is only 6 times that of Run 1 at moisture content of 20 ppm. As moisture content is increased from 20 to 200 ppm, the difference in SO_2 removal efficiencies becomes lesser (Table 8). This clearly indicates that at higher moisture contents encountered in flue gas desulfurization systems, the presence of particles will probably not play a significant role.

Summary

The gas-phase reactions between sulfur dioxide and ammonia in the presence of particles were studied theoretically and experimentally. Experiments were conducted at room temperature and under trace water conditions. Condensation of vapor products onto initially existing sodium chloride particles was examined by varying the total surface area of the aerosols. Results indicated that an increase of the total surface area yields

a slight increase in the SO_2 removal. The particle formation model presented in Chapter 2 was used to analyze the experimental data. Using the surface tension and particle density obtained from the previous section, the theoretical simulation fits the experimental data reasonably well for a moisture content of 40 ppm. Increasing the moisture content tends to increase the SO_2 removal in the presence of inert particles. The enhanced SO_2 removal due to fly ash particles was also studied theoretically. It is expected that at high moisture conditions, an increase of the total surface area does not result in a significant increase of the SO_2 removal.

Table 6 Properties of the sodium chloride particles measured using the LAS-X Optical Particle Counter.

	Run 1	Run 2	Run 3
NaCl conc. (g/c.c.)	0.010	0.007	0.005
Total surface area ($\mu m^2/cm^3$)	$7.3 \pm 1.2 \times 10^4$	$1.5 \pm 1.0 \times 10^4$	$2.3 \pm 0.8 \times 10^3$
Total seed number (#/c.c.)	$1.4 \pm 0.2 \times 10^4$	$4.9 \pm 0.6 \times 10^3$	$6.7 \pm 0.8 \times 10^3$
Mode diameter (μm)	1.13	0.57	0.23
Geometric mean diameter (μm)	0.84±0.06	0.52±0.05	0.28±0.02
Geometric standard deviation	2.51±0.04	1.56±0.03	1.53±0.04

Table 7 SO_2 removal efficiency and product properties of the NH_3-SO_2 reaction under different inert particle size distribution conditions [a].

	Run 1	Run 2	Run 3	Run 4[b]
SO_2 removal	18±6%	12±3%	10±3%	8±3%
Total particle volume increase ($\mu m^3/cm^3$)	7.6×10^4	2×10^3	6×10^2	_
Total particle number (#/c.c.)	$3.3 \pm 1.7 \times 10^4$	$1.4 \pm 0.2 \times 10^4$	$1.2 \pm 0.1 \times 10^4$	310±120
Geometric mean diameter (μm)	0.83±0.44	0.56±0.26	0.23±0.05	NA
Geometric standard deviation	2.68±0.66	1.61±0.02	1.57±0.05	NA

Note: [a] At average residence time of 0.16 seconds.
[b] Without the presence of inert particles.

Table 8 List of parameters used in the gas-to-particle formation model.

Parameter	Value
T	298.5°K
MW (Mol. Weight)	180 g/gmole
σ	93 ergs/cm^2
ρ_p	2.0 g/cm^3
I_s	10^9
NH_3	6000 ppm
SO_2	3000 ppm
$H_2O_{(v)}$	20, 40, 50 ppm

Table 9 Predictions of the SO_2 removal increased for Run 1 and typical fly ash conditions.

		Run 1	Typical fly ash
Total surface area (μm^2 cm^{-3})		7.3×10^4	2.0×10^6 [a]
Total volume increase (μm^3 cm^{-3})	H_2O = 20 ppm	3.3×10^4	2.0×10^5
	40	7.5×10^4	2.5×10^5
	50	1.6×10^5	3.0×10^5
	100	4.0×10^5	4.8×10^5
	200	7.8×10^5	[b]
Total[c] SO_2 removal increase	H_2O = 20 ppm	0.3%	1.7%
	40	0.6%	2.1%
	50	1.4%	2.6%
	100	3.4%	4.1%
	200	6.6%	—

[a] McCain et al., 1975

[b] The model diverged at larger moisture content.

[c] Based on particle density of 2.0 g cm^{-3} and molecular weight of $(NH_4)_2S_2O_5$.

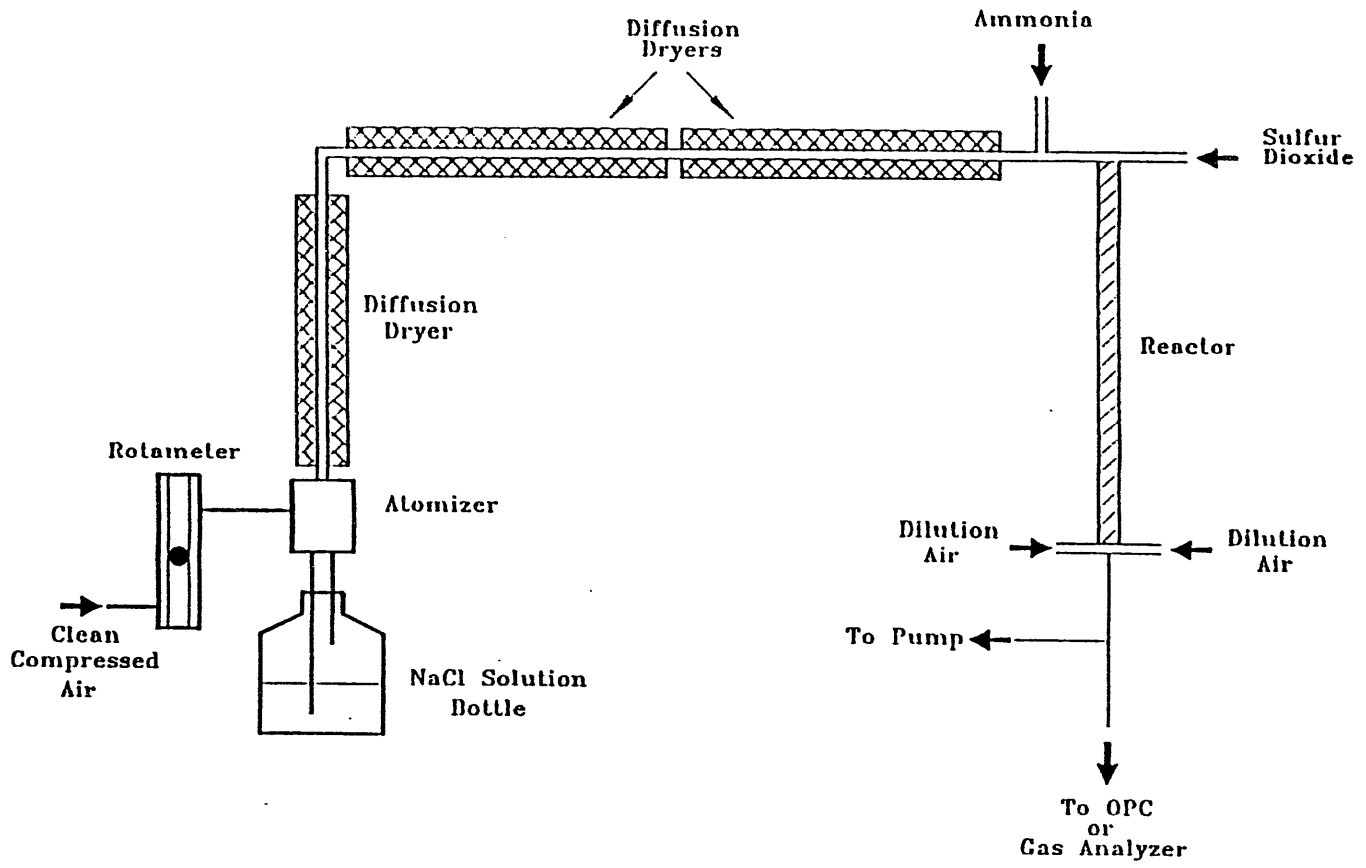

Figure 6 Schematic diagram of the experimental setup to study the effect of initial seed on the NH_3-SO_2 reaction.

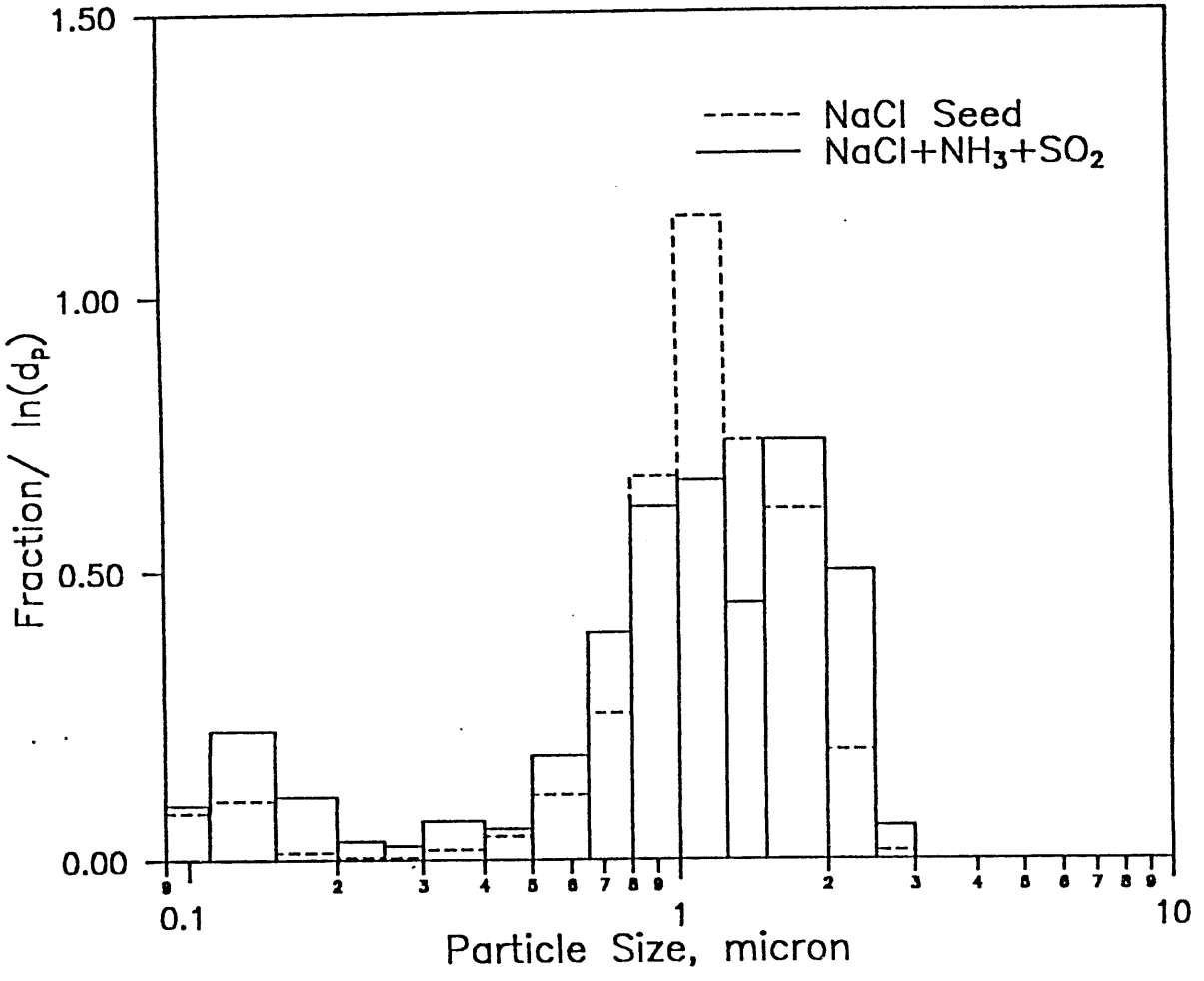

Figure 7a The size distribution histograms of Run 1 measured from OPC.

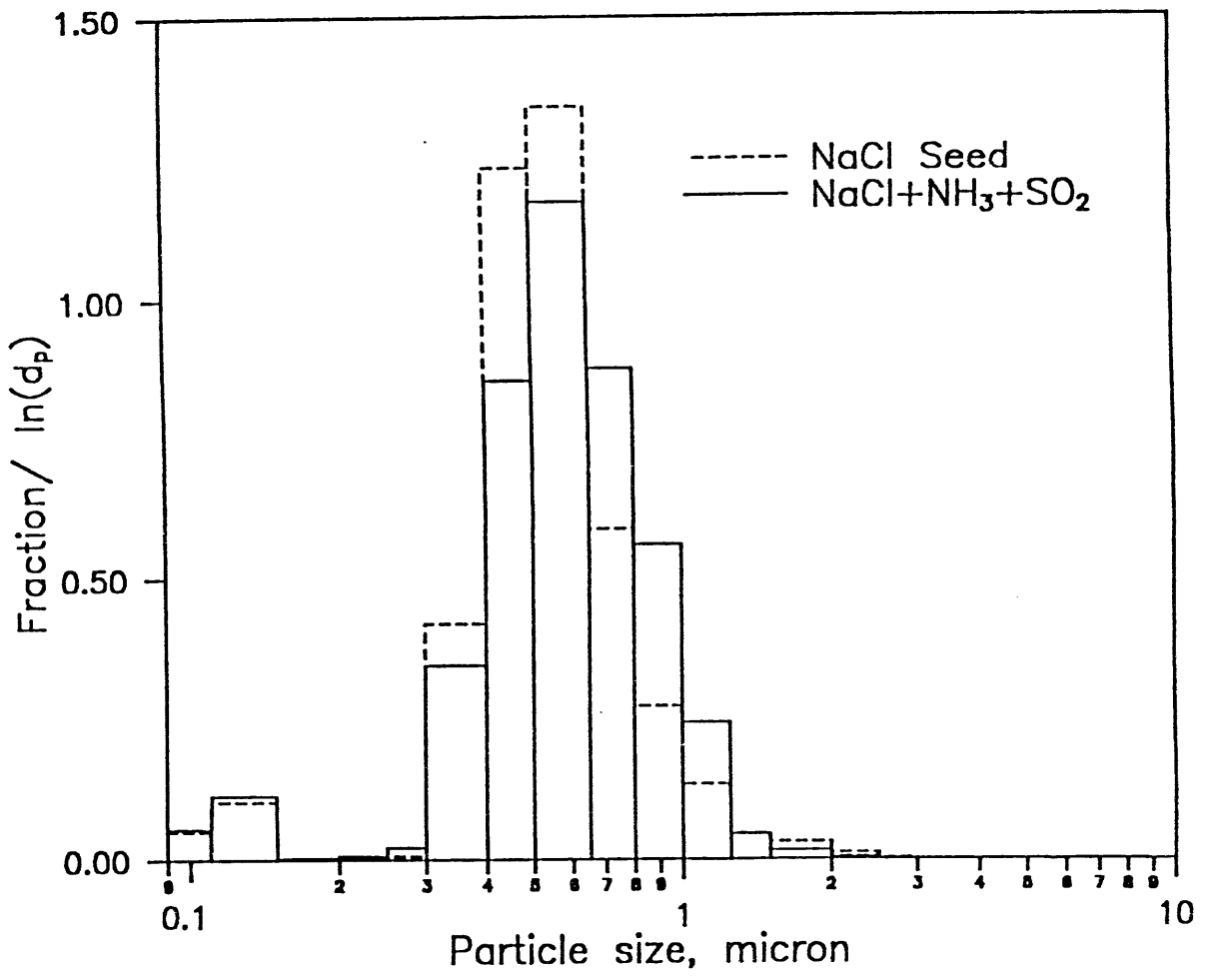

Figure 7b The size distribution histograms of Run 2 measured from OPC.

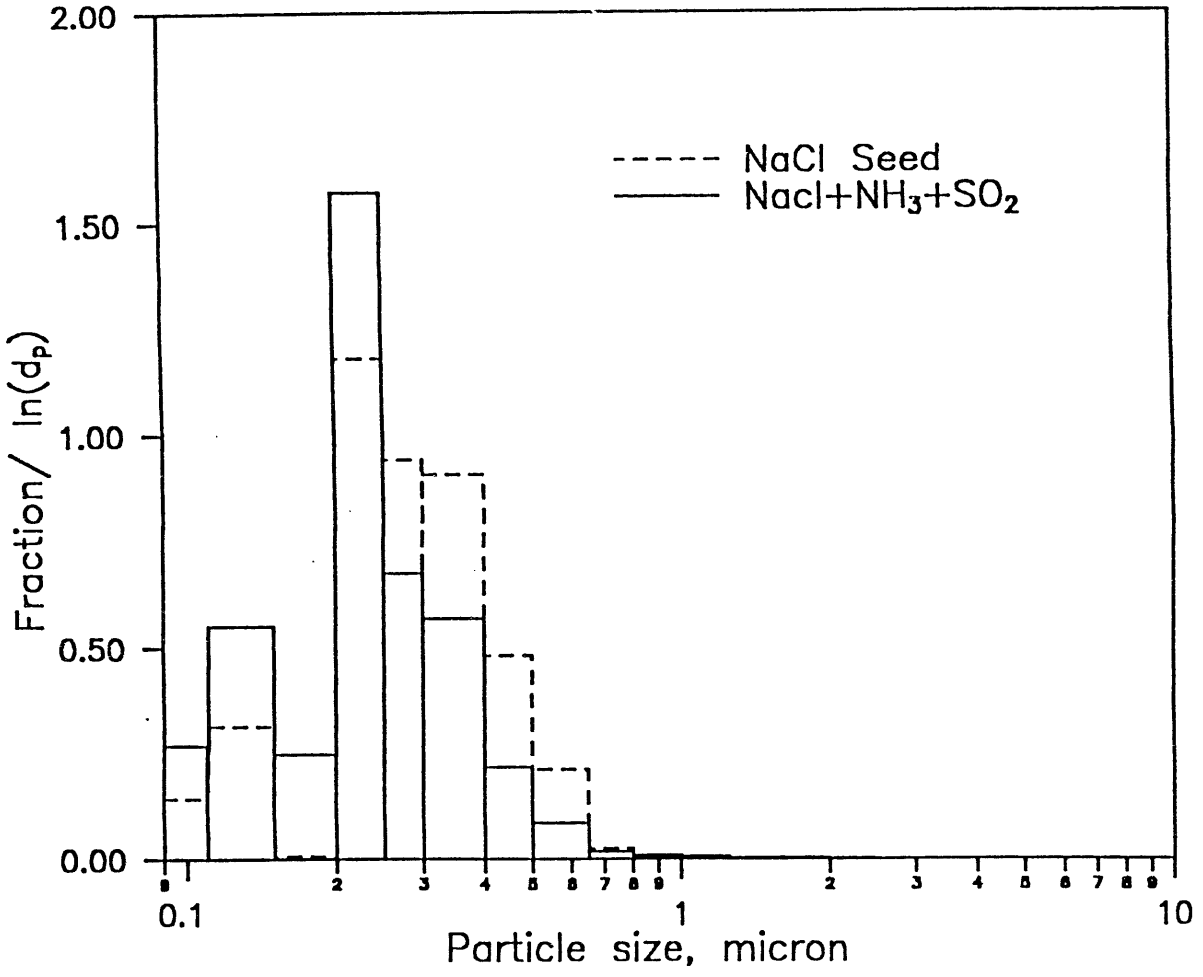

Figure 7c The size distribution histograms of Run 3 measured from OPC.

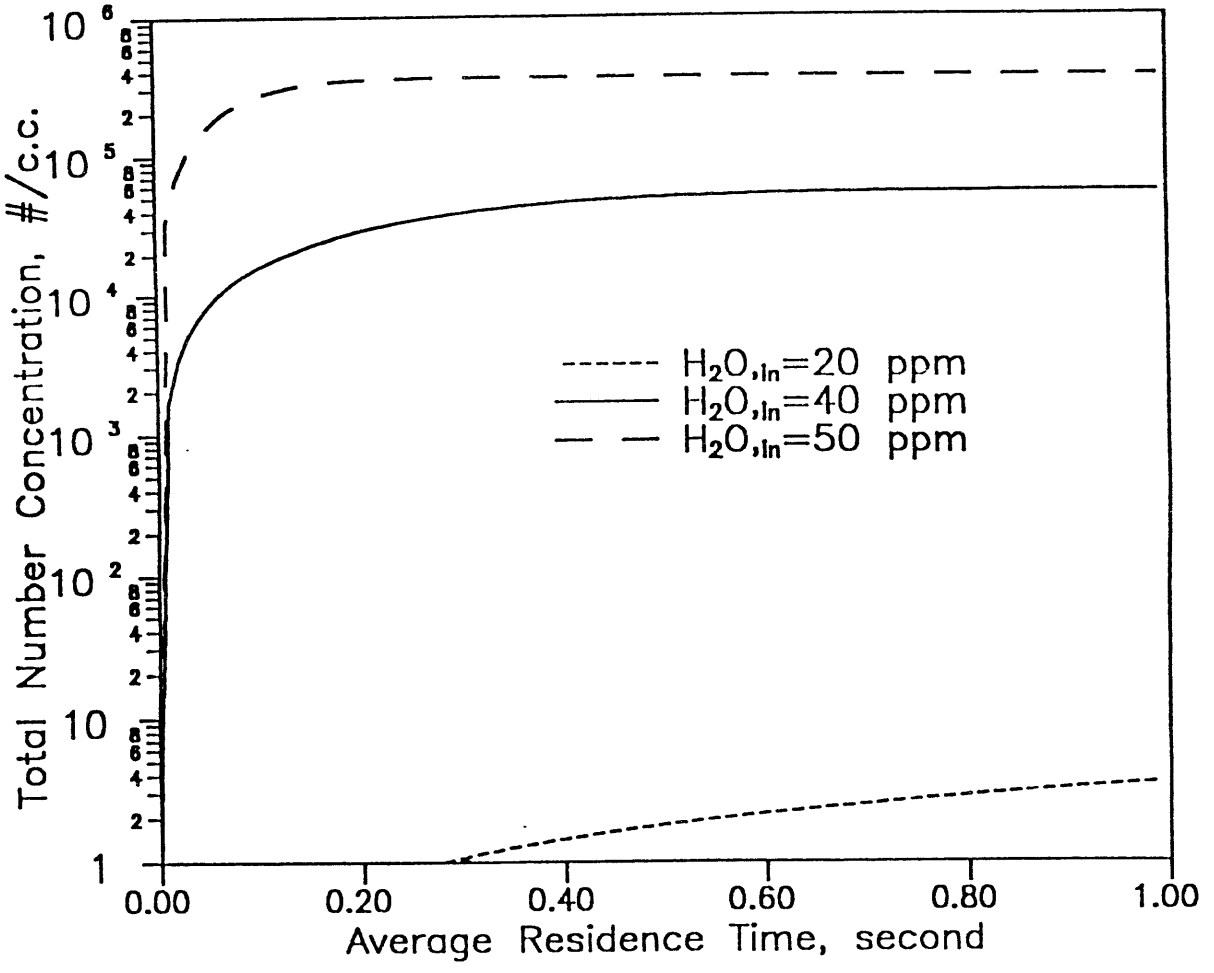

Figure 8 The effect of moisture content on the total particle number concentration without the introduction of seed particles.

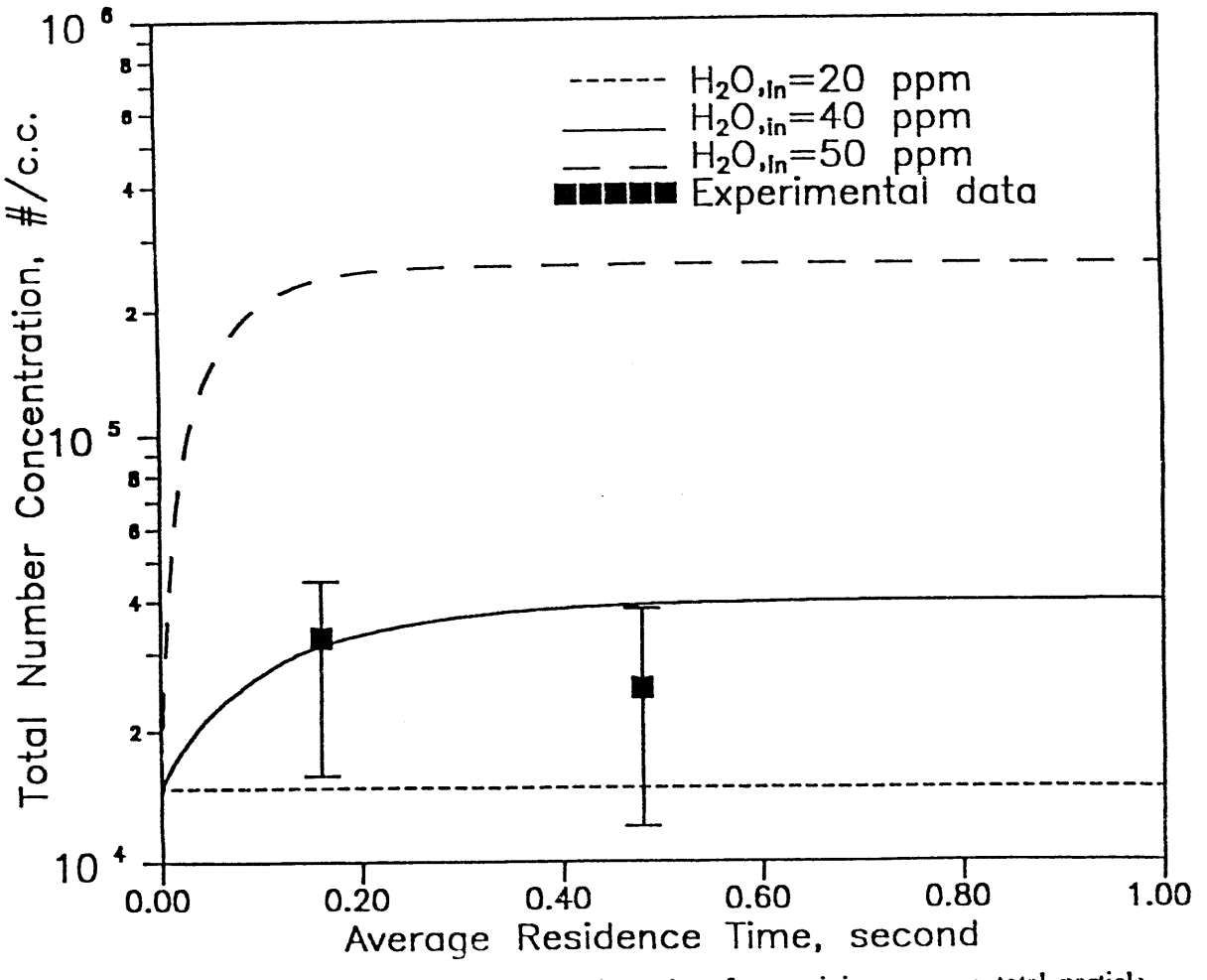

Figure 9a Measured and simulated results of cup-mixing average total particle number concentration as a function of average residence time with the presence of initial seed particles

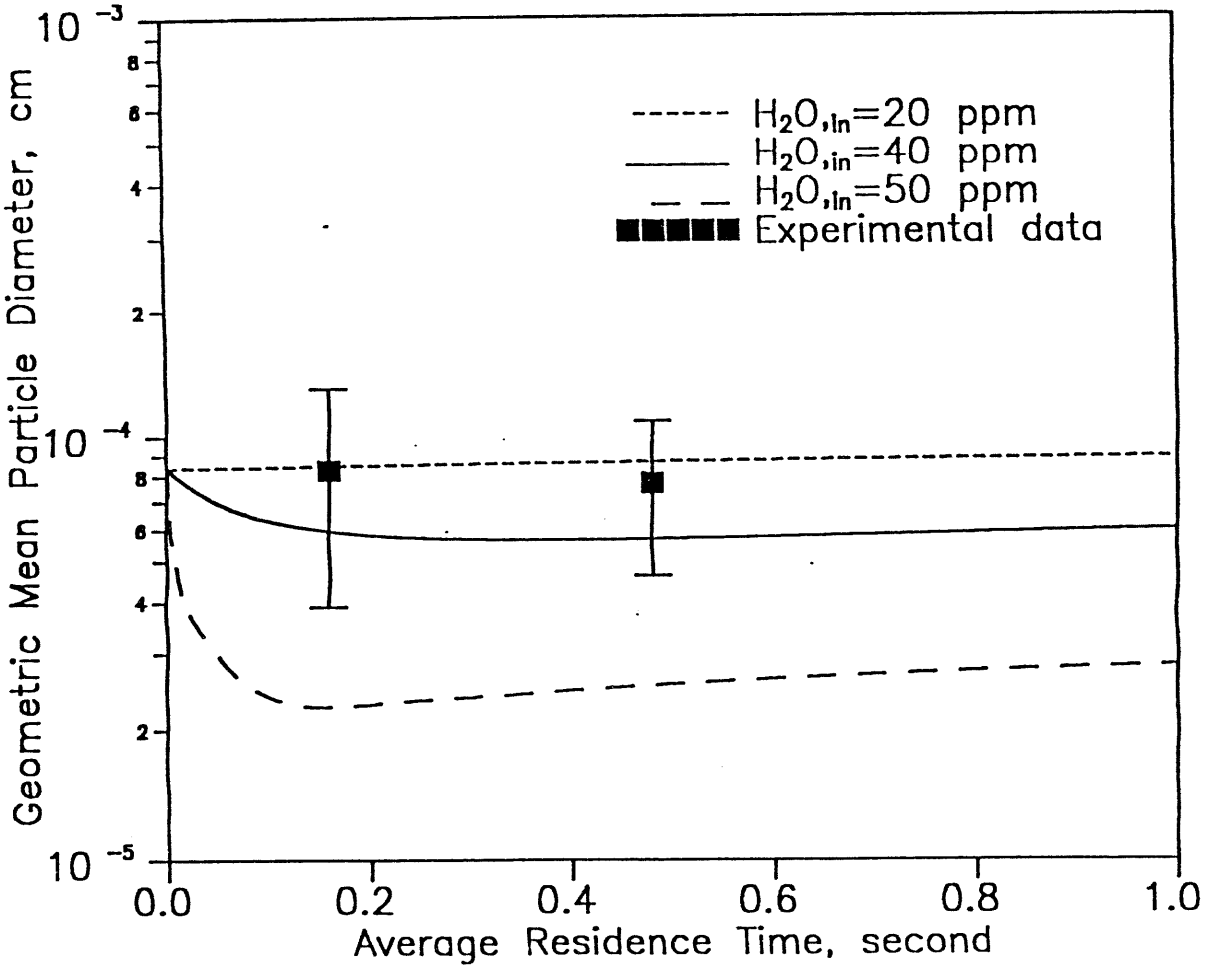

Figure 9b Measured and simulated results of cup-mixing average geometric mean particle diameter as a function of average residence time with the presence of initial seed particles

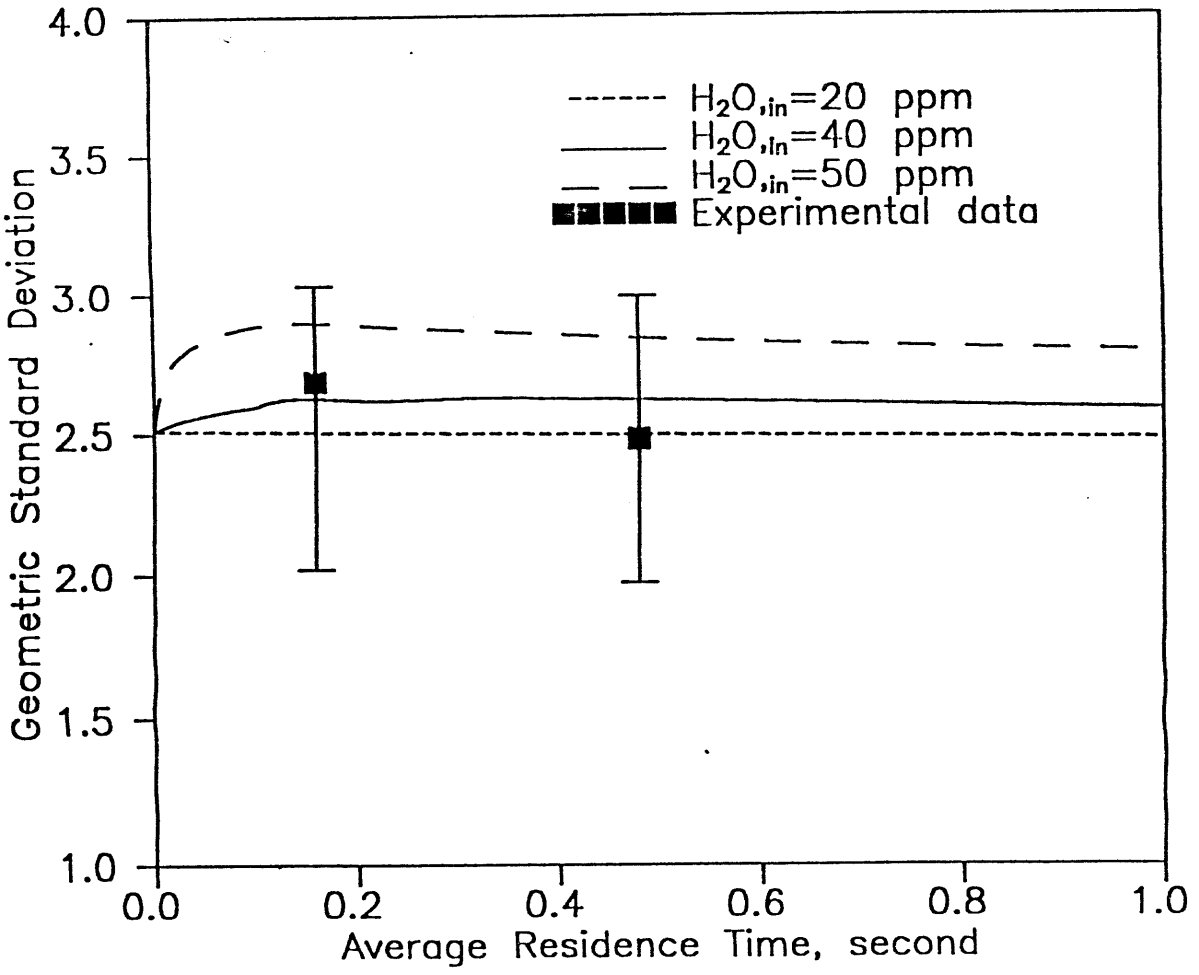

Figure 9c Measured and simulated results of cup-mixing average geometric standard deviation as a function of average residence time with the presence of initial seed particles

NH_3-SO_2 REACTIONS AT HUMID CONDITIONS D

Introduction

Sulfur dioxide removal by ammonia injection is favored at humid conditions (St. Clair, 1937; Scargill, 1971). However, the SO_2 removal decreases as the temperature is increased. The products of the NH_3-SO_2 reaction may vary by changing the moisture content and reaction temperature. The NH_3-SO_2 reactions at various temperatures and moisture contents encountered in a FGD system are studied in this section. Sulfur dioxide removal, ammonia utilization, product size distribution and composition are reported at different conditions. The experimental results are compared to the predictions of a thermodynamic equilibrium calculation for different reaction mechanisms.

Experimental Setup

Figure 10 shows the schematic diagram of the reactor system to study the NH_3-SO_2 reaction under humid conditions. The major equipment used in the experiments are listed in Table 10. Concentrations of the gases inlet to the reactor were controlled by using MKS mass flow controllers. Purified house air was passed through a Balston filter to remove CO_2, HCs and oil, and then dried and cleaned by passing it through a silica gel air dryer and a 0.2 μm Gelman air filter (AcroFlow II). The clean air was then saturated with water vapor in a temperature controlled humidifier to obtain the desired water vapor content. The system was designed to ensure that no water droplets were carried by the air flow. The relative humidity (RH) was measured by a Vaisala HMI31/HMP36

Relative Humidity/Temperature sensor system, with accuracies of $\pm 2\%$ RH and $\pm 0.3°C$ for humidity and temperature, respectively. The experimental conditions are listed in Table 11. 4.5% ammonia gas (in N_2) was introduced into the air stream and then mixed with 1.02% sulfur dioxide gas (in N_2) in a union tee junction. Immediately after mixing, the gases enter a 6.4 mm inside diameter stainless steel, laminar flow tube reactor. The reactor residence time is approximately 0.9 seconds, sufficient to reach a quasi-equilibrium state. Temperatures of the entire mixing-reacting system were controlled to be within $\pm 1°C$ by the use of temperature controllers and heating tapes. The gases reacted in the reactor and the particles were collected on a glass fiber filter where the temperature was maintained the same as the reactor temperature. The relative humidity and the temperature of the inner reactor tube were recorded and was stable for each experiment.

The total sulfur removal (in terms of $SO_4^=$), the total sulfite (in terms of $SO3^=$) and the ammonia utilization (in terms of NH_4^+) were determined by wet chemical analysis of the collected particles at different temperatures. The particles formed were extracted by washing the filter and the reactor walls with double distilled water. The sulfite ion ($SO_3^=$) concentration in the extracted solution was determined by iodide-iodate titration (Standard Methods, 1985). The $SO_3^=$ concentration measurement was completed within 10 minutes of the experimental run to minimize any oxidation by ambient air. The ammonium ion (NH_4^+) concentration was determined by titration with a hypochlorite solution followed by a back titration with a standard sodium thiosulfate solution (Kolthoff and Sandell, 1952). The sulfate ion ($SO_4^=$) concentration was determined gravimetrically

by precipitating as $BaSO_4$ (Standard Methods, 1985). All wet chemical analysis techniques used were calibrated using standard solutions. A mass balance was also performed for the ambient temperature tests to confirm the measurements. The sulfur dioxide measurements at the exit of the reactor using the Horiba PIR-2000 Infrared Gas Analyzer and the total sulfur determined by wet chemical analysis were in good agreement ($\pm 5\%$ standard deviation).

The experimental run was repeated at the same condition for product size measurements. Particles collected on the filter maintained at the reactor temperature were analyzed for size using a Micro-Image system (Analytical Imaging Concepts, Inc.). The Micro-Image system is an optical microscope which is connected to a computer system. Particles were transferred to a clean glass microscope slide and a drop of immersion oil was applied. The imaging system provided a size distribution of the particles. About 1000 particles were used for each size measurement. Since the particles were crystals and had irregular shapes, the projected area diameter was reported as the equivalent diameter (Hinds, 1982).

Equilibrium Chemistry

When gaseous NH_3, SO_2 and water vapor are mixed, a white crystallite material is formed. Shale (1973) postulated the following reactions:

$$2\,NH_{3\,(g)} + SO_{2\,(g)} + H_2O_{(g)} \rightleftharpoons (NH_4)_2SO_{3\,(s)} \qquad (29)$$

St. Clair (1937) conducted an equilibrium study and indicated that ammonium

$$NH_{3\,(g)} + SO_{2\,(g)} + H_2O_{(g)} \rightleftharpoons NH_4HSO_{3\,(s)} \tag{30}$$

pyrosulfite, $(NH_4)_2S_2O_5$, and hydrated ammonium sulfite, $(NH_4)_2SO_3 \cdot H_2O$, could also be the reaction products,

$$2\,NH_{3\,(g)} + 2SO_{2\,(g)} + H_2O_{(g)} \rightleftharpoons (NH_4)_2S_2O_{5\,(s)} \tag{31}$$

$$(NH_4)_2SO_{3\,(s)} + H_2O_{(g)} \rightleftharpoons (NH_4)_2SO_3 \cdot H_2O_{(s)} \tag{32}$$

The X-ray diffraction of NH_3-SO_2 reaction product performed by Hartley and Matteson (1975) and Stromberger (1984) indicated the possibility of ammonium sulfate as the major product. According to St. Clair (1937), ammonium sulfite and bisulfite are easily oxidized to the ammonium sulfate in comparison to the ammonium pyrosulfite. Therefore the following reaction scheme was proposed

$$(NH_4)_2SO_{3\,(s)} + \frac{1}{2}O_{2\,(s)} \rightleftharpoons (NH_4)_2SO_{4\,(s)} \tag{33}$$

$$NH_4HSO_{3\,(s)} + \frac{1}{2}O_{2\,(g)} + NH_{3\,(g)} \rightleftharpoons (NH_4)_2SO_{4\,(s)} \tag{34}$$

The equilibrium relationship of any of the above reactions, $aA_{(g)} + bB_{(g)} + cC_{(g)} + dD_{(s)} = eE_{(s)}$, is given by

$$K_p = (P_{A,in} - aX)^a (P_{B,in} - bX)^b (P_{C,in} - cX)^c \tag{35}$$

where K_p is the equilibrium constant of the reaction, X is the mole concentration of solid E formed from the gas phase reaction at equilibrium ; $P_{i,in}$ (i=A,B or C) is the inlet concentration of gaseous reactant A, B, or C. The equilibrium constants for the above

reactions are summarized in Table 12.

Results and Discussion

Room Temperature Experiments

Figure 11 shows the SO_2 removal efficiency at various moisture contents (0 to 57% RH) for an inlet SO_2 concentration of 3000 ppm and three different ammonia inlet concentrations. The temperature was held constant at $23.5 \pm 1°C$. The moisture content has a pronounced effect in all the tests in the range of 0 to 10% (0 to 3000 ppm), with practically no further increase in the SO_2 removal efficiency beyond 20% RH (6000 ppm). For moisture contents less than 3000 ppm, water vapor is the limiting reactant in determining SO_2 removal efficiencies. These are clearly indicated by equilibrium calculations performed previously. The maximum removal efficiency for an inlet NH_3 concentration of 3000 ppm is only around 57% even at the higher moisture content, and this is because ammonia and sulfur dioxide possibly react at approximately a 2:1 ratio. The products at low moisture content conditions are expected to be different than those formed in the high moisture content tests. The products at near anhydrous conditions were discussed previously, and were conjectured to be NH_3SO_2, $(NH_3)_2SO_2$, and $(NH_4)_2S_2O_5$. On the other hand, the products at humid conditions are mostly the 2:1 sulfites, $(NH_4)_2SO_3$ and $(NH_4)_2SO_3 \cdot H_2O$, as determined by wet chemical analysis. The microscope pictures were taken at two different moisture contents (20% and 57% RH) and are given in Appendix B.

The reaction products for inlet concentrations of NH_3 and SO_2 of 6000 and 3000

ppm, respectively and a moisture content of 20% RH was also analyzed by X-ray diffraction as shown in Figure 12. In comparison to standard patterns (Hanawalt Method Search Manual, 1977), the only identifiable product was $(NH_4)_2SO_4$ (peaks at $2\theta = 20.5$, 29.2 and 16.6). According to Stromberger (1984), the diffraction pattern of $(NH_4)_2SO_3 \cdot H_2O$ is similar to $(NH_4)_2SO_4$. Therefore it is also possible that $(NH_4)_2SO_3 \cdot H_2O$ is a product of the NH_3-SO_2-H_2O reaction. There are other undefined peaks which have intensities stronger than 10% (Figure 12). X-ray diffraction does not seem to be an appropriate method to identify all the reaction products until more identification files are available (no reference data in the literature for diffraction patterns of adducts).

High Temperature Experiments

Wet chemical analysis provides information on the total sulfur removal in terms of $SO_4^=$ concentration and the ammonia utilization in terms of NH_4^+ concentration. In addition, the total sulfites ($SO_3^=$) concentration can also be determined. However, it is not possible to distinguish between the 1:1 products of $(NH_4)_2S_2O_5$ and NH_4HSO_3. On dissolving into water, ammonium pyrosulfite forms the bisulfite (Marks and Ambrose, 1937),

$$(NH_4)_2S_2O_5 + H_2O = 2NH_4HSO_3 \qquad (36)$$

The possible 2:1 products, $(NH_4)_2SO_3$ and $(NH_4)_2SO_3 \cdot H_2O$, are also not distinguished by our chemical analysis. But since the focus of this study is on the total sulfur removal and the ammonia utilization, distinction of these products is not of major concern. Figure

13 shows the $NH_4^+/SO_4^=$ and a $SO_3^=/SO_4^=$ ratios from the wet chemical analysis as a function of the reactor temperature at water vapor content of 2.7% by volume. It is seen from the plot of $NH_4^+/SO_4^=$ ratio that a mixture of 1:1 and 2:1 products tends to form at lower temperatures. As the temperature increases, the 2:1 products become dominant. The ratio of $SO_3^=/SO_4^=$, however, does not show a clear trend as temperature varies. The average $SO_3^=/SO_4^=$ ratio of from all the experiments is 0.74. This means the sulfites are dominant before carrying out the wet chemical analysis. The oxidation of sulfites to sulfates is believed to occur after the particles have been collected on the filter, especially after dissolution in the distilled water.

Figure 14 illustrates the temperature effect on total sulfur removals at 2.7% of water vapor by volume. The symbols are experimental data and the lines are theoretical predictions assuming products to be either the ammonium bisulfite, the ammonium sulfite, or the ideal mixture of the two 2:1 products. It is seen that both the theoretical predictions of 1:1 and 2:1 products agree well with the experimental data at lower temperatures. However at higher temperatures, assuming the bisulfite as the product tends to underestimate the total sulfate removal. The ammonium sulfite, or the ideal mixture of the two 2:1 products appear to be the main products at higher temperatures. This observation is supported with the results of $NH_4^+/SO_4^=$ ratio plot as seen from Figure 13. An attempt has also been made by assuming an ideal mixture (Scott and Lamb, 1970) of all the four possible sulfites (NH_4HSO_3, $(NH_4)_2S_2O_5$, $(NH_4)_2SO_3$, and $(NH_4)_2SO_3$ $-H_2O$) as the products. The attempt did not yield good agreement with the experimental data. It seems that an ideal mixture of the four vapor products are not

possible. Instead, the reaction should involve the decomposition of one product completely to form another product (that is, an univariant system) unless the system is in equilibrium. One of the examples is the decomposition of ammonium pyrosulfite to form ammonium bisulfite as the moisture content is in excess of stoichiometric requirements (St. Clair, 1937). The only exception could be the 2:1 ammonium sulfites where the difference in their chemical structure is the water bond. In addition, pH values were also measured at those conditions, and no trend is observed as moisture content varies, with an average value of 7.54 and a standard deviation of ± 0.3. Scott and McCarthy (1967) measured the pH of ammonium bisulfite to be approximately 4.0, and the pH of ammonium sulfite to be approximately 8.0. These indicate that more 2:1 products were formed during the experiments at 51°C. Therefore it seems more possible to form the ideal mixture of the 2:1 products. Figures 15a and 15b show the experimental results and theoretical predictions of the effect of moisture content on the total sulfur removal and the ammonia utilization, respectively, at a temperature of 51°C. The ratios of the ammonia utilization and total sulfur removal do not show a clear trend as moisture content varies, with an average value of 1.8 and a standard deviation of ± 0.15. Therefore the theoretical predictions in Figures 15a and 15b were made by assuming that the 2:1 sulfites were the major product. It appears from the experimental data that the sulfur dioxide removal increases by about 30% and the ammonia utilization increases by about 25% for an increase of the moisture content from 1.6% to 6.4% (by volume). The assumption of the ideal mixture of 2:1 sulfites as products seems to fit the experimental data fairly well.

The effect of various moisture contents (2.7% and 6.4% by volume) on the size distributions of the NH_3-SO_2 reaction products at a temperature of 51°C is shown in Figure 16a. As can be seen, varying the moisture content does not yield a significant difference on the size distribution. Figure 16b examines the effect of various reaction temperatures (37, 42 and 51°C) on the size distributions of NH_3-SO_2 reaction products at a moisture content of 2.7%. The particle size distributions do not show any trends as reaction temperature varies. The microscope pictures of reaction products under humid and high temperature conditions are shown in Appendix B. It is seen that particles were crystallized and particles larger than those of under dry conditions were formed.

Summary

The NH_3-SO_2 reactions at humid conditions were studied experimentally. The experimental results were analyzed and compared by a thermodynamic analysis of possible reaction mechanisms. The effects of water vapor content and reaction temperature on the SO_2 removal and the product particle size have been determined. The amount of water vapor in the system is a very important parameter. Increasing the water vapor content from 1.6% to 6.4% by volume yields a 30% increase in the SO_2 removal efficiency at a reaction temperature of 51°C. This has been confirmed by the experimental data and the thermodynamic analysis. The NH_3-SO_2 reaction is favored at low temperatures. Increasing the reaction temperature results in a significant decrease of the SO_2 removal. The SO_2 removal drops to zero at temperatures of around 55°C at a moisture content of 2.7% by volume. Results of wet chemical analysis indicated that

the NH_3-SO_2 reaction products are primary the sulfite, which may oxidize later on to form sulfate particles after being collected on the filter. Ratios of $NH_4^+/SO_4^=$ by wet chemical analysis also show that more 2:1 sulfites were form at high reaction temperatures. The reaction products appear to be crystallized with a maximum size of around 1000 μm.

Table 10

Equipment used in humid experiments

Equipment		Precision/Range
Particle Measurement		
Scanning Electron Microscope	:	> 0.01 µm
Micro-Image System	:	> 0.3 µm
Humidity Sensor		
Vaisala HMP36/HMI31	:	±2% RH (0-90% RH)
		±3% RH (90-100% RH)
Temperature Controller		
Eurotherm Model 91	:	±1°C (0-400°C)

Table 11

Experimental conditions for the NH_3-SO_2-H_2O system.

Room Temperature Experiments:

Inlet SO_2 : 3000 ppm

Inlet NH_3 : 3000, 6000, 9000 ppm

Inlet H_2O : 0 - 57% RH (50 -15500 ppm)

Temperature : 23.5 ± 1°C

Elevated Temperature Experiments:

Inlet SO_2 : 3000 ppm

Inlet NH_3 : 3000 ppm

Inlet H_2O : 1.6 - 6.4% by volume

Temperature : 29 - 61°C

Table 12
Possible NH_3-SO_2 reactions and their equilibrium constants.

Possible Reactions	Equilibrium Expressions	Temp. Range	Sources
$(NH_4)_2S_2O_{5(s)}=2NH_3+2SO_2+H_2O$	$K_p=exp(94.6-39144/T)$	60~110□C	1
	$K_p=exp(96.5-40767/T)$	0~23□C	2
$(NH_4)_2SO_{3(s)}=2NH_3+SO_2+H_2O$	$K_p=exp(73.8-30601/T)$	60~110□C	1,3
	$K_p=exp(76.6-32630/T)$	0~23□C	2
$(NH_4)_2SO_3H_2O_{(s)}=2NH_3+SO_2+2H_2O$	$K_p=exp(93.8-38062/T)$	60~110□C	1,3
	$K_p=exp(96.7-40090/T)$	0~23□C	2,3
$NH_4HSO_{3(s)}=NH_3+SO_2+H_2O$	$K_p=exp(53.8-22116/T)$	60~110□C	1,3
	$K_p=exp(54.7-22928/T)$	0~23□C	2,3

1. St. Clair (1937)
2. Scargill (1971)
3. Tock, et al (1979)

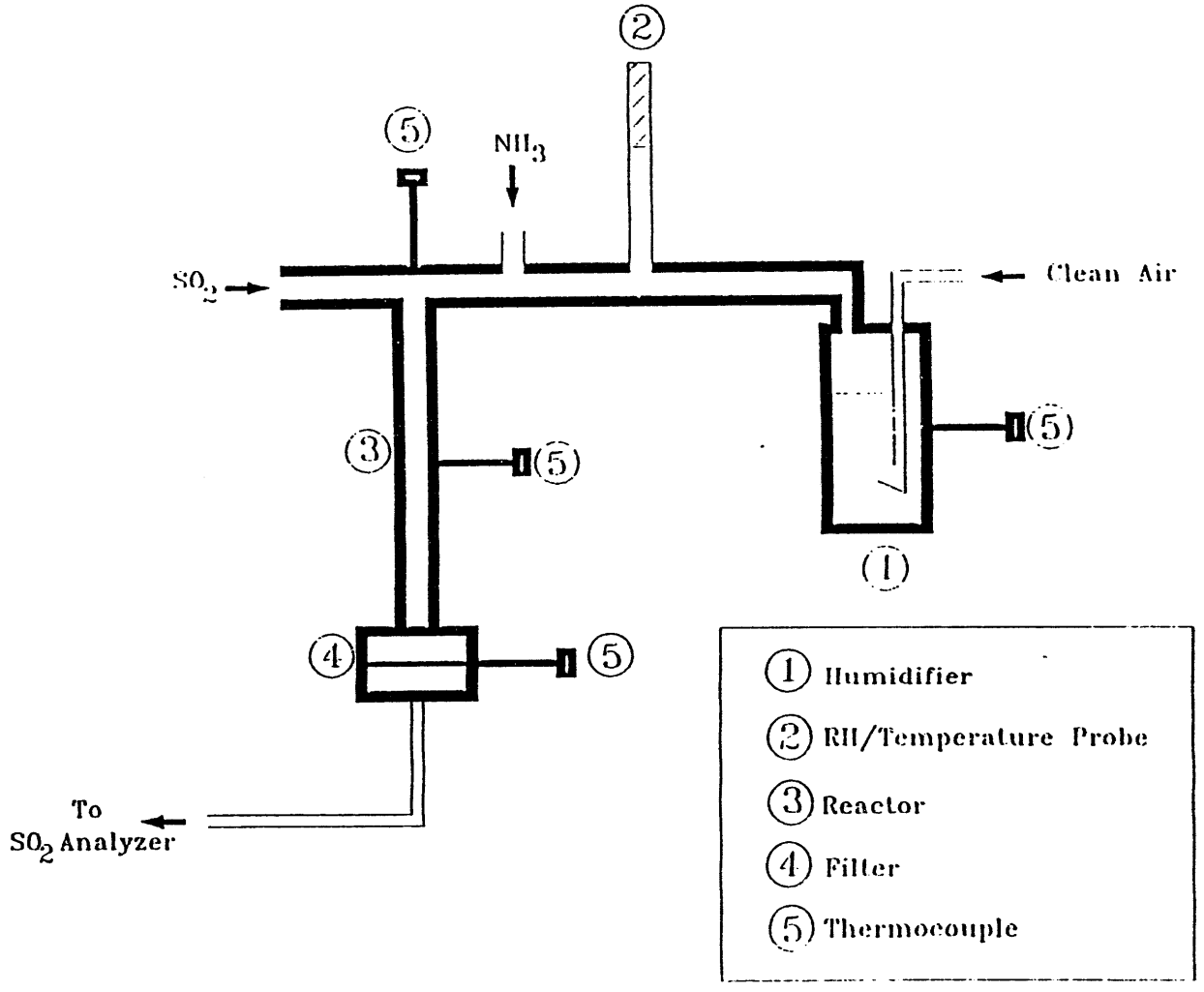

Figure 10 Schematic diagram of the NH_3-SO_2 main reactor system at humid and high temperature conditions.

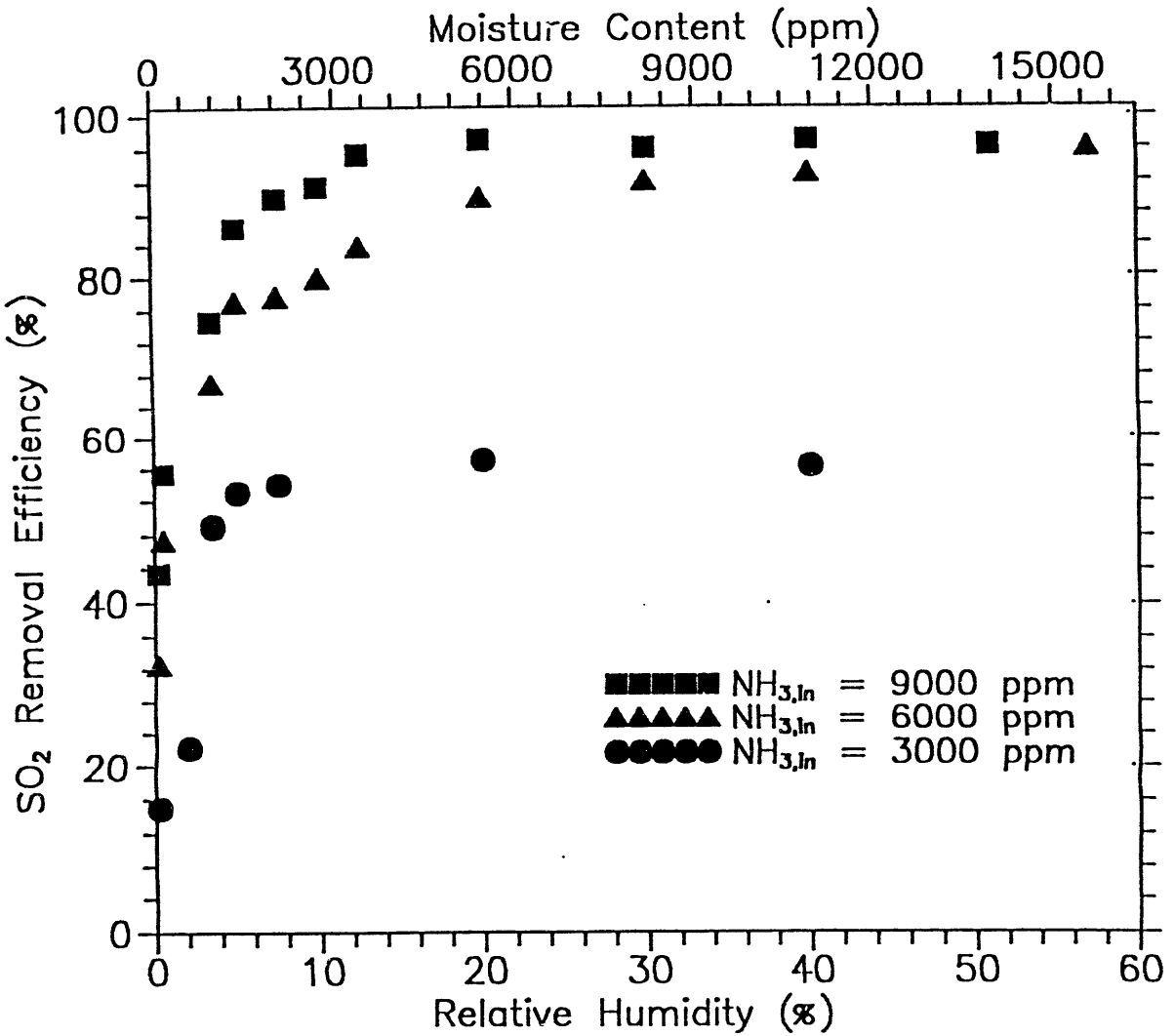

Figure 11 Effect of relative humidity on SO_2 removal at room temperature and inlet SO_2 concentration of 3000 ppm.

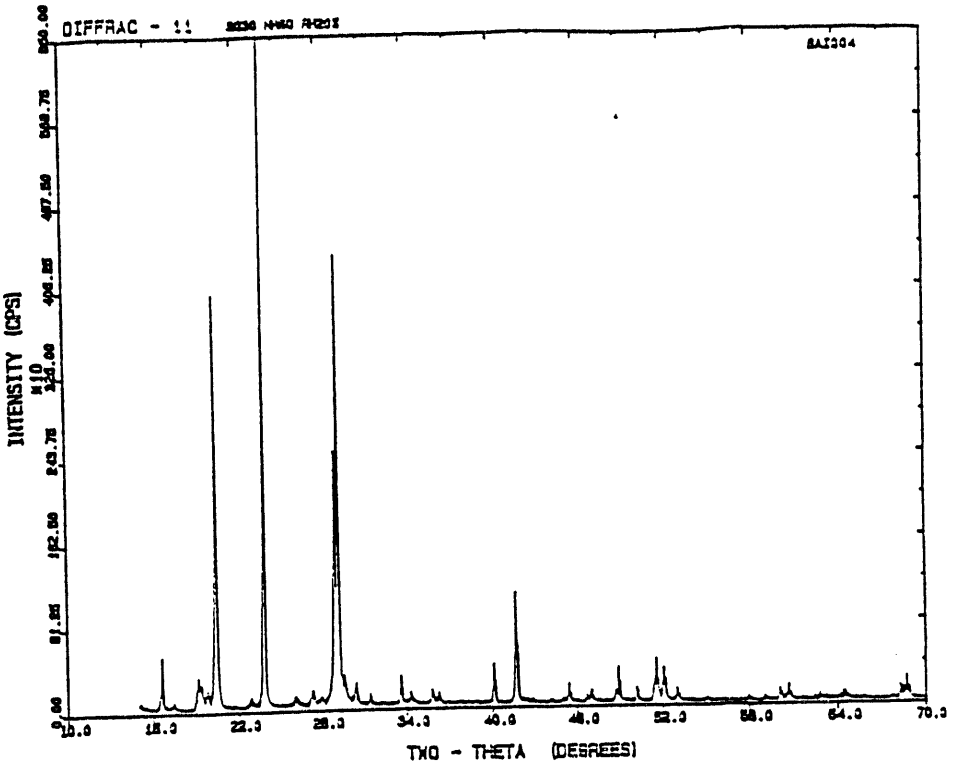

PEAK SEARCH PARAMETER:
SENSITIVITY FACTOR = 1.00
THE SMALLEST PEAK RELATIVE TO THE STRONGEST = 1.0

NO	2THETA	D	INTEG.I (%)	INTEG.I	MAX.I	FWHM
1	16.614	5.3313	10.3	2935.	323.	0.179
2	17.232	5.1034	1.6	445.	41.	0.219
3	19.114	4.6392	8.5	2406.	202.	0.238
4	19.342	4.5852	8.8	2497.	179.	0.279
5	19.777	4.4847	3.9	922.	80.	0.206
6	20.463	4.3364	82.5	23502.	2630.	0.179
7	22.331	3.9833	2.5	707.	52.	0.270
8	23.923	3.7156	100.0	28449.	4274.	0.133
9	26.123	3.4083	1.5	435.	44.	0.199
10	27.314	3.2623	3.6	1032.	97.	0.214
11	28.091	3.0773	22.1	6360.	1342.	0.080
12	29.228	3.0522	47.6	13663.	3536.	0.106
13	29.559	3.0124	5.8	1603.	146.	0.220
14	30.434	2.9346	4.6	1307.	121.	0.217
15	31.446	2.8424	1.7	479.	57.	0.167
16	33.313	2.6843	5.2	1514.	171.	0.173
17	34.235	2.6147	2.3	633.	67.	0.197
18	35.725	2.5092	3.2	905.	82.	0.222
19	36.213	2.4782	1.8	501.	50.	0.202
20	40.091	2.2477	7.5	2143.	245.	0.175
21	41.460	2.1761	21.0	5971.	691.	0.173
22	42.404	1.9953	2.2	619.	100.	0.124
23	47.037	1.9302	1.8	505.	62.	0.162
24	48.773	1.8655	2.5	722.	75.	0.192
25	49.361	1.8438	3.2	924.	179.	0.104
26	50.224	1.8150	2.2	717.	[illegible]	[illegible]
27	51.335	1.7788	0.5	148.	92.	0.032
28	51.727	1.7666	10.7	3041.	250.	0.243
29	52.353	1.7463	7.3	2063.	189.	0.218
30	52.725	1.7346	3.4	963.	82.	0.234
31	60.391	1.5246	1.3	379.	68.	0.111
32	63.214	1.4726	2.1	609.	97.	0.125
33	68.240	1.3662	2.7	757.	149.	0.101

Figure 12 The X-ray diffraction result of NH_3-SO_2 reaction products at room temperature and relative humidity of 20%.

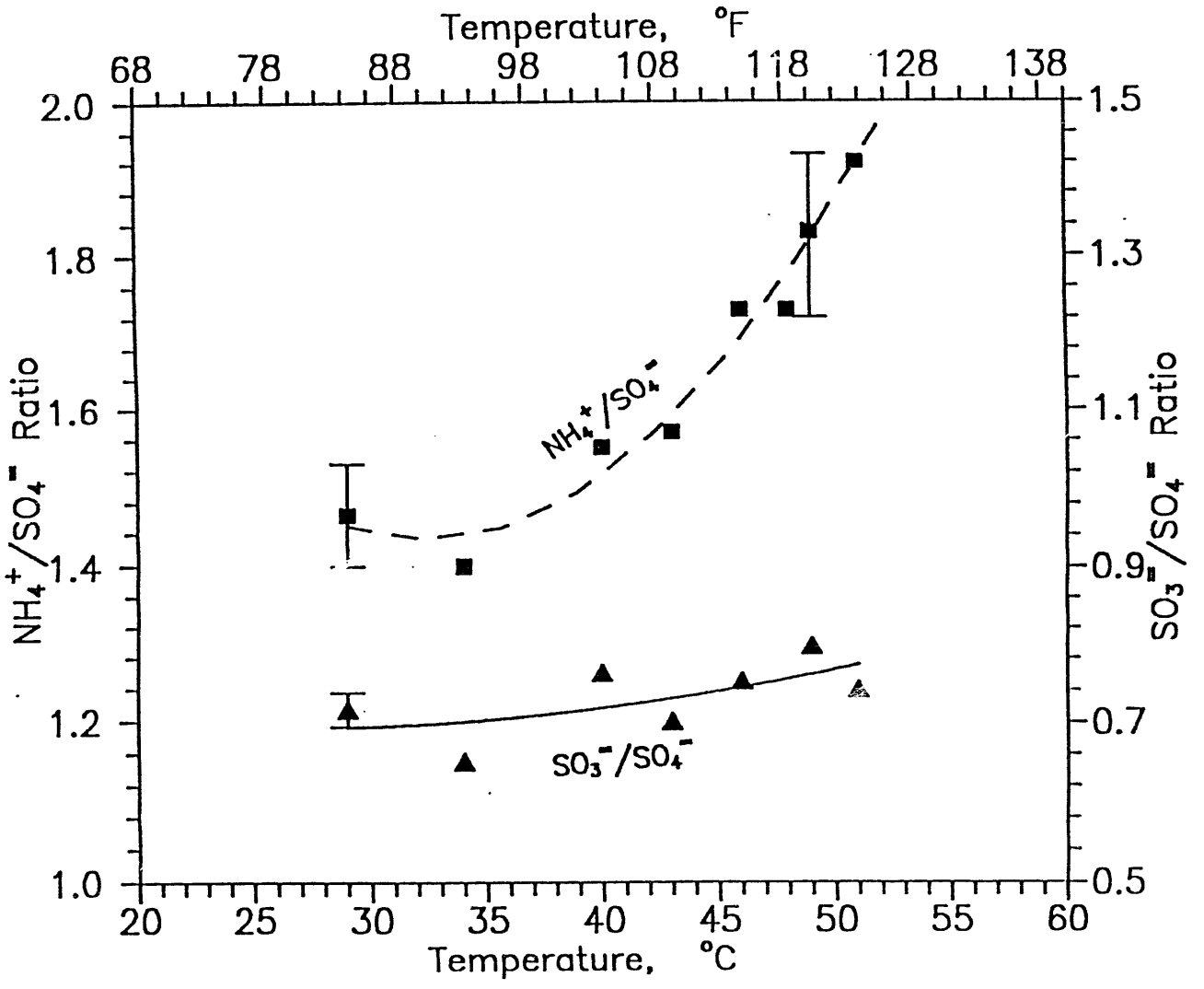

Figure 13 $NH_4^+/SO_4^=$ and $SO_3^=/SO_4^=$ ratios from the wet chemical analysis as a function of reaction temperature at H_2O = 2.7% by volume.

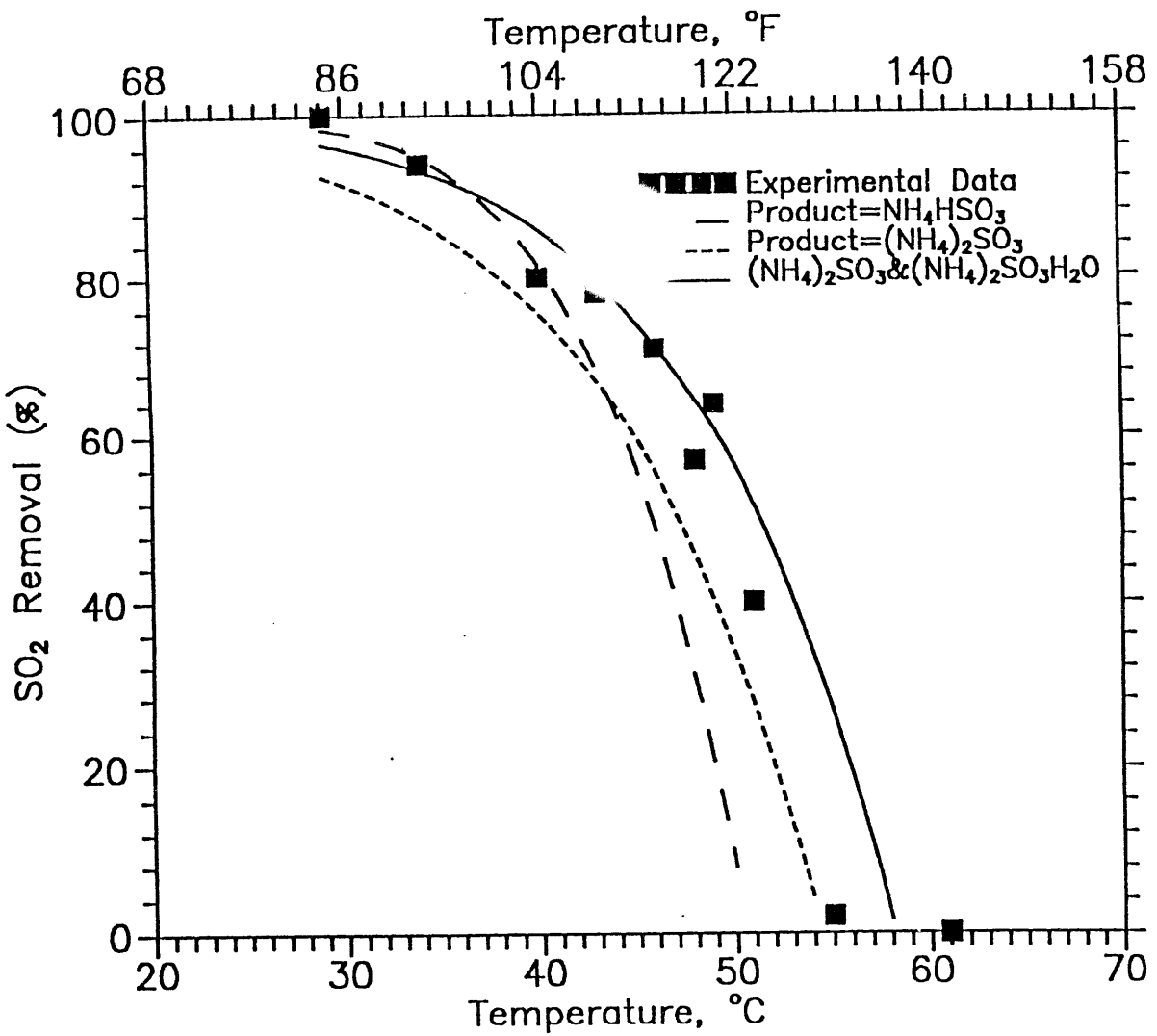

Figure 14 Effect of reaction temperature on the sulfur dioxide removal under a moisture content of 2.7% by volume (0.017 lb H_2O/lb dry air).

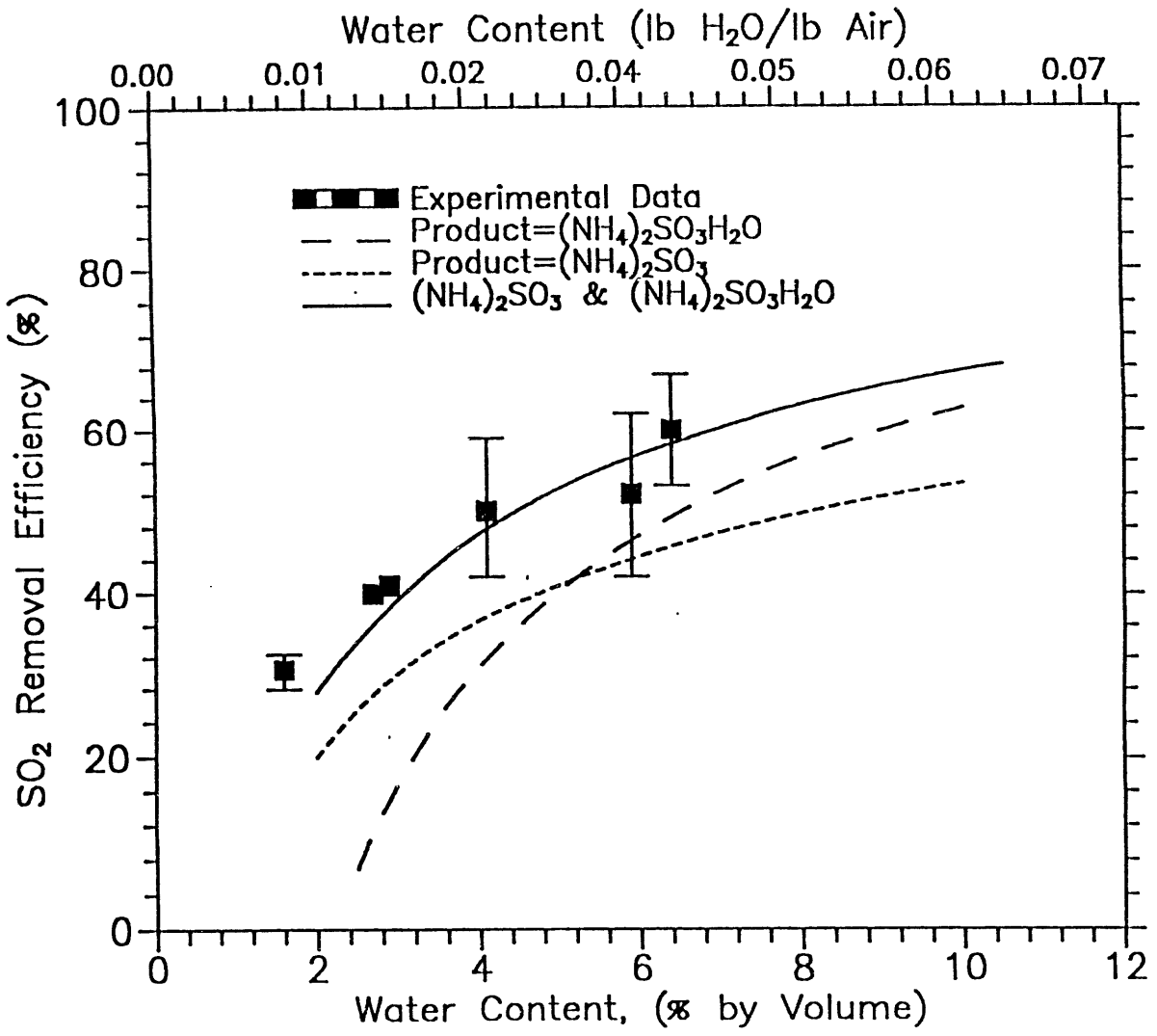

Figure 15a Effect of moisture content on the sulfur dioxide removal under a temperature of 51°C (124°F).

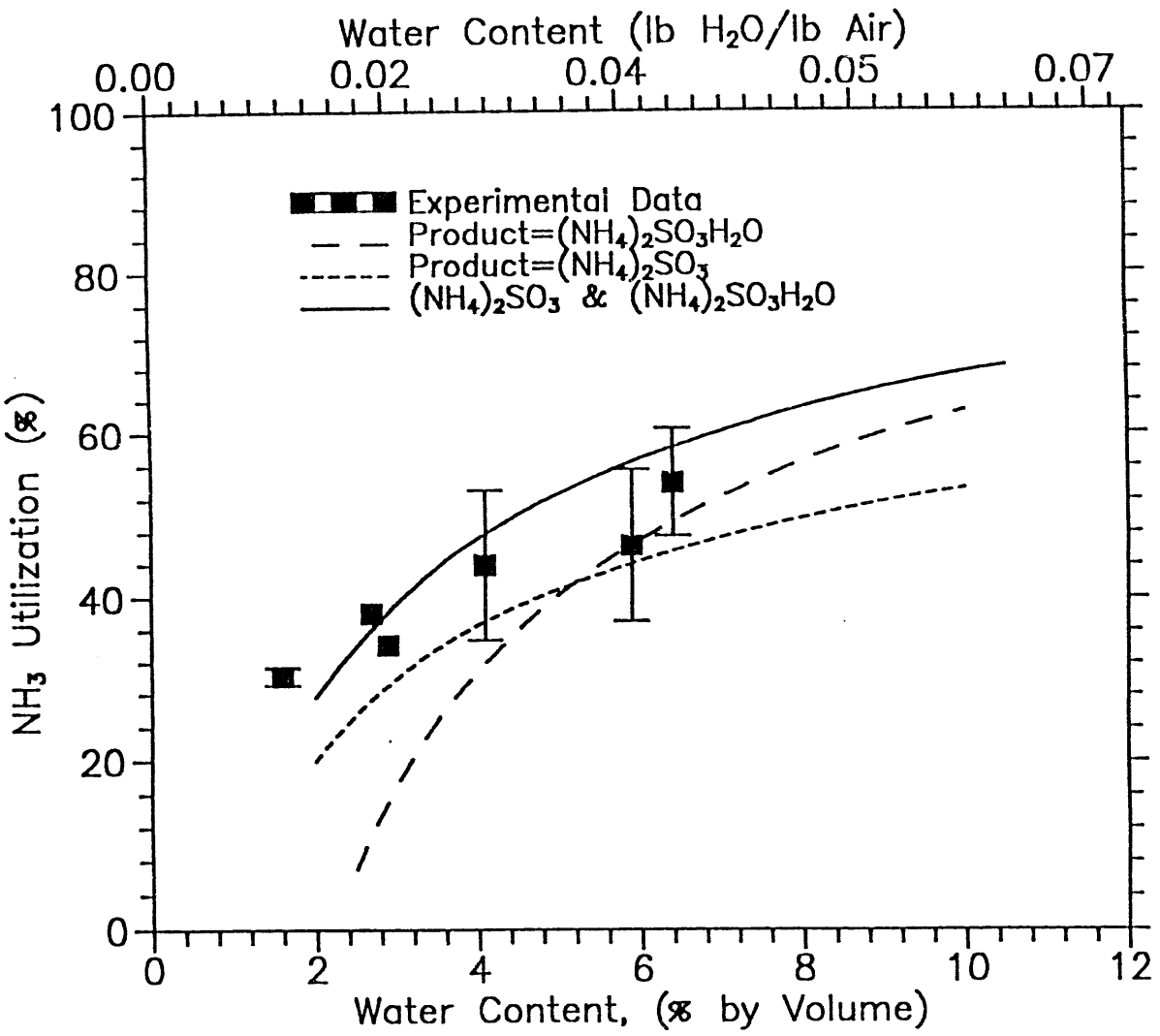

Figure 15b Ammonia utilization as a function of moisture content under a temperature of 51°C (124°F).

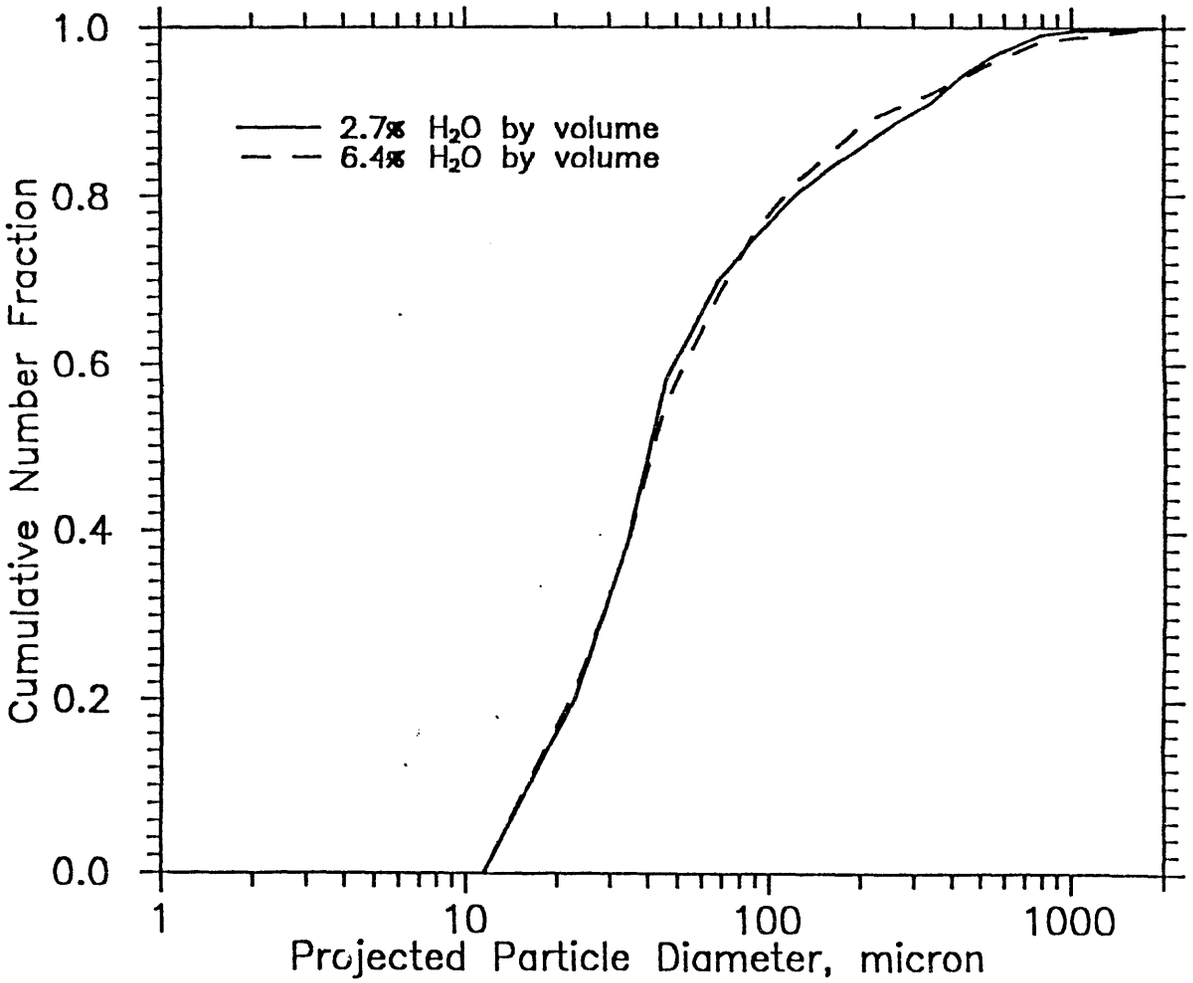

Figure 16a Size distributions of NH_3-SO_2 reaction product at a reaction temperature of 51 °C under different moisture content conditions.

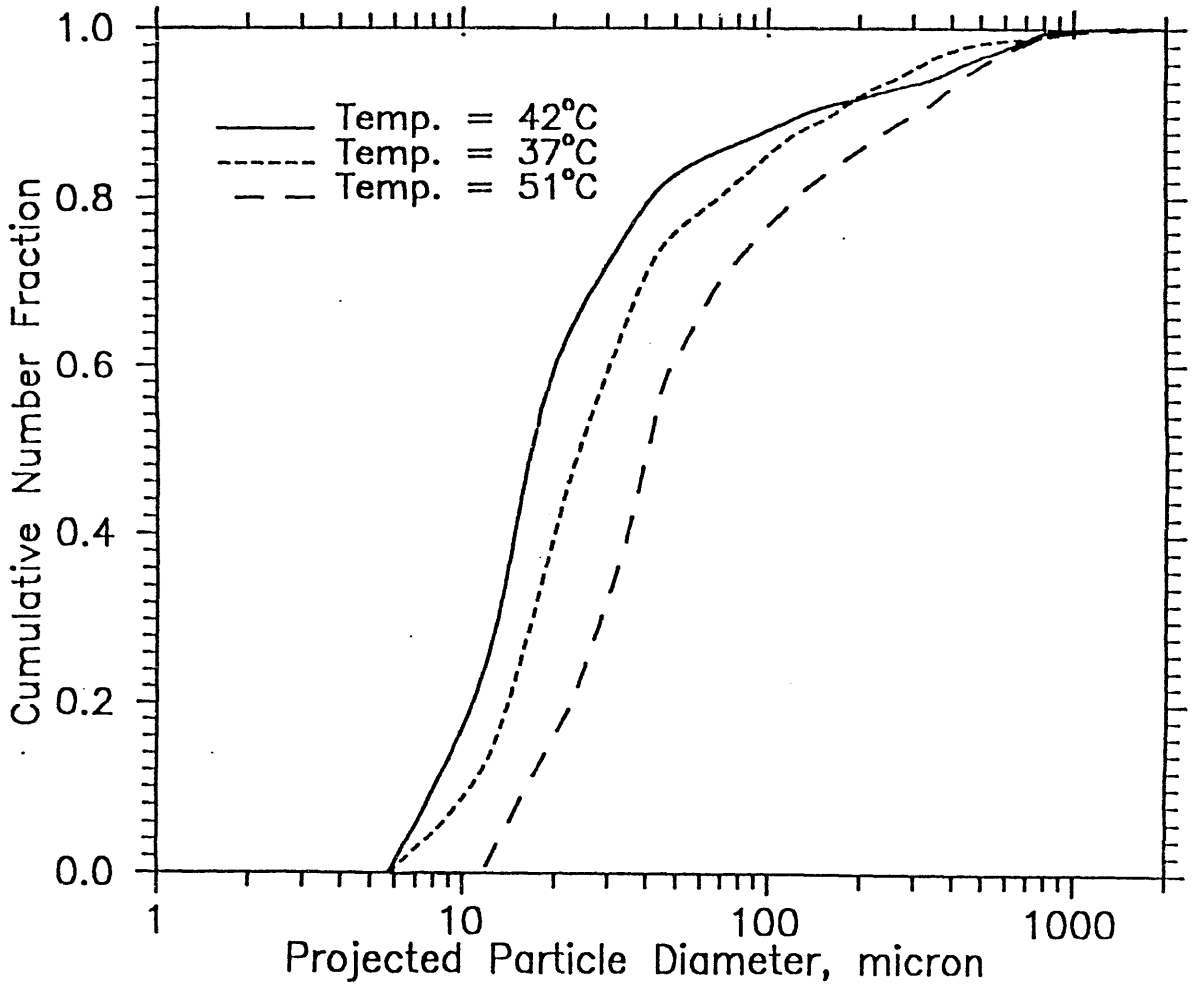

Figure 16b Size distributions of NH_3-SO_2 reaction product at a moisture content of 2.7% by volume under different reaction temperatures.

APPLICABILITY TO A FULL SCALE SYSTEM

Introduction

This section presents a discussion of applying ammonia injection to a coal-burning power plant which utilizes high sulfur coal as the fuel. Figure 17 is the sketch of a typical coal-burning power plant. Temperatures after the air preheater are appropriate for the ammonia injection method to be applied. The temperature after the air preheater is usually around 300°F. Since there is minimum heat loss in the dust collector and stack, the gas leaving the top of the stack will be about this temperature (Slack, 1967). Pollution control equipments must be inserted into the power plant at a proper temperature location to ensure sufficient sulfur dioxide removal to meet existing regulations. Also, because regulations change, and sometimes these changes have been applied to existing units, extra capacity for SO_2 removal is desirable.

Thermodynamic Analysis

As indicated in the previous section, the thermodynamic analysis of assuming products as $(NH_4)_2SO_3$ and $(NH_4)_2SO_3$ -H_2O fits the experimental data well at a moisture content of 0.017 lb H_2O /lb dry air. Therefore Figure 18 shows SO_2 removal as a function of reaction temperature and moisture content based on assuming these two sulfites as products. The typical moisture content in a flue gas system is usually between 0.05 to 0.08 lb H_2O/lb dry air. The 1:1 sulfites, $(NH_4)_2S_2O_5$ and NH_4HSO_3, could also be products at such a high moisture content. Therefore the amount of sulfur dioxide

removal is calculated by assuming all the four sulfites, $(NH_4)_2SO_3$, $(NH_4)_2SO_3 \cdot H_2O$, $(NH_4)_2S_2O_5$ and NH_4HSO_3, as products and is shown in Figure 19. It is seen that assuming four products to occur simultaneously yields a higher SO_2 removal efficiency than assuming only two products. Table 13 lists the approach to saturation temperatures at various operating temperatures and moisture content conditions. A higher SO_2 removal is expected as seen in Figure 18 if the moisture content can be kept higher. However, the approach to saturation temperature must be maintained at a certain value in order to obtain a dry removal scheme. Figure 18 is based on results of the thermodynamic analysis without considering enhanced removal of product by means of vapor condensation onto fly ash particles.

Applicability of NH_3 Injection

Previous research has shown that the sublimation temperature for the NH_3-SO_2 reaction in flue gas to be 180°F (Keener et al., 1988). This temperature is higher than the sublimation temperature (130 to 140°F) reported in this study. Figure 19 shows the experimental data from this study and those from a pilot scale study (Keener et al., 1988). The results from equilibrium calculations of assuming two and four products are also shown in Figure 19. Two sets of thermodynamic data were used in the calculation, with one from St. Clair (1937) and the other from Scargill (1971). It appears that the SO_2 removal efficiency is higher when using thermodynamic data of Scargill (1971) than that of St. Clair (1937). However, even using the Scargill's data, the predicted SO_2 removal is lower than the pilot scale observation. This is because the thermodynamic

analysis accounts for the reaction between ammonia, sulfur dioxide and water vapor only without considering the effects of existing fly ash particles, or other constituents in the flu gas. For instance, it is estimated from the previous results of this project and other references (Hurst and Bielawski, 1980; Martinez et al., 1975) that ash particles can contribute from 5-30% SO_2 removal depending on the chemical and physical properties of the ash (e.g., alkalinity, metals content, etc.). As can be seen from results of the pilot scale study, the baseline SO_2 removal is about 30%, which could be from the contribution of fly ash particles. Also, the effects of the other constituents in the flu gas stream (e.g., the oxidation of SO_2 to SO_3 in the presence of ammonia and flyash with subsequent reaction) cannot be discounted. If subtracting out the baseline SO_2 removal as shown by the error bars in Figure 19, a better agreement is obtain between the thermodynamic prediction and the pilot scale observation. Therefore it is possible to utilize NH_3 injection method in conjunction with other removal techniques and achieving over 90% SO_2 removal from utility plants burning high sulfur coal.

One of the best methods is combining ammonia injection with a spray dryer system (Keener et al., 1988). The simplified sketch of combined $NH_3/Ca(OH)_2$ injection technique to a flue gas system is depicted in Figure 20. The outlet temperature of a typical spray dryer is about 140 to 150°F (60 to 65°C). Under this temperature, the SO_2 removal is about 50% at the approach to saturation temperature of 10 to 30°F when only ammonia injection is applied. On the other hand, the removal efficiency of SO_2 is about 60 to 65% when only $Ca(OH)_2$ slurry is injected (Keener et al., 1988). The utilization of lime is quite low at high SO_2 concentration and deteriorates with higher and higher

concentration. While the utilization of ammonia is higher at high SO_2 concentration. Therefore ammonia is injected before entering the spray dryer to obtain the best utilization of both reagents.

In order to increase the total surface area of fly ash and $Ca(OH)_2$, Martinez et al. (1991) conducted a study where mixtures of fly ash and $Ca(OH)_2$ were hydrated which resulted in a high surface area sorbent. The average SO_2 removal was about 60% at temperatures between 55 to 85°C. This provides another possibility for an NH_3 injection method to be applied. The primary product of NH_3-SO_2 reaction is in the form of vapor, which is easier to condense onto the existing fly ash/$Ca(OH)_2$ than the SO_2 which is in the form of gas. Therefore when injecting ammonia gas into a hydrated fly ash/$Ca(OH)_2$ mixture, the SO_2 removal is expected to be higher than the NH_3/$Ca(OH)_2$ method and the hydrated fly ash/$Ca(OH)_2$ method in spray dryer systems as described earlier.

Table 13 **Approach to saturation temperatures (°F) at various operating temperatures and moisture contents.**

lb H_2O/lb dry air	0.03	0.05	0.06	0.07	0.08	0.1	0.12
Operating temp. °F(°C)							
95 (35)	5	-	-	-	-	-	-
104 (40)	14	-	-	-	-	-	-
113 (45)	23	6	-	-	-	-	-
122 (50)	32	15	8	3	-	-	-
131 (55)	41	24	17	12	7	-	-
140 (60)	50	33	26	21	16	8	1
149 (65)	59	42	35	30	25	17	10
158 (70)	68	51	44	39	34	26	19
167 (75)	77	60	53	48	43	35	28
176 (80)	86	69	62	57	52	44	37

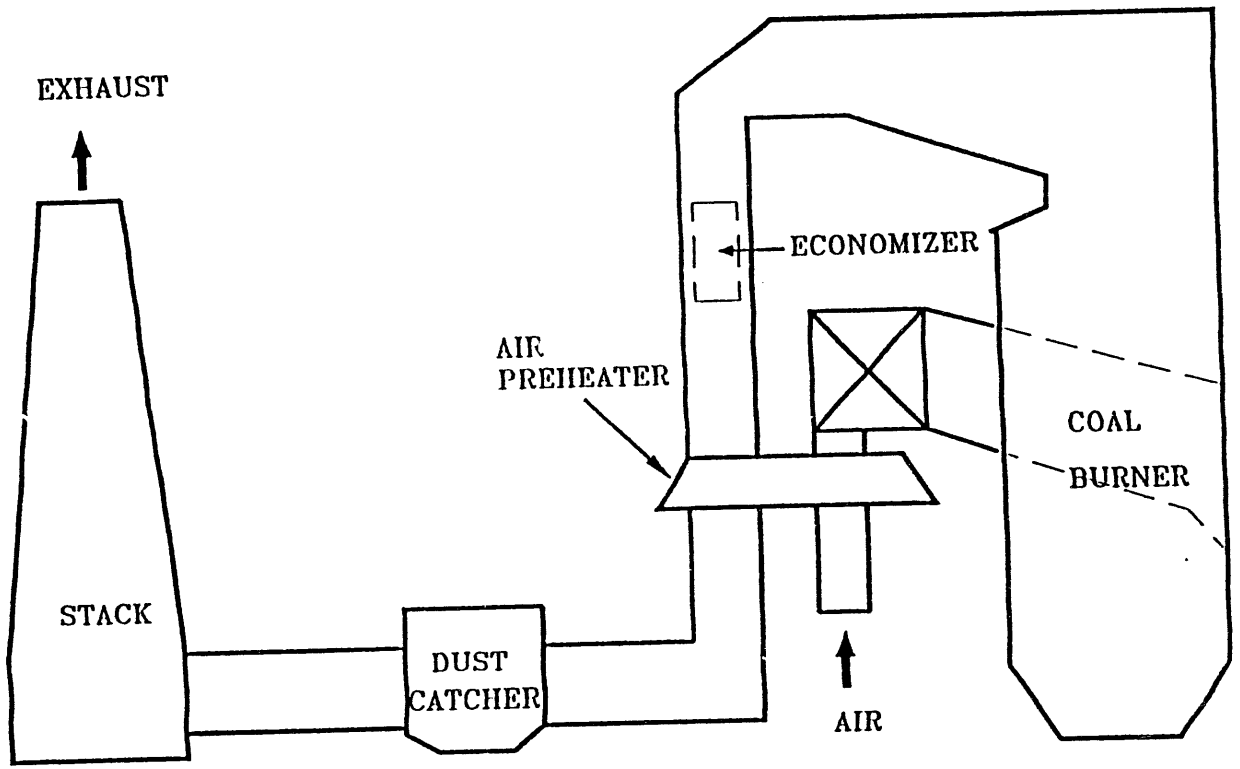

Figure 17 Simplified sketch of a typical power plant.

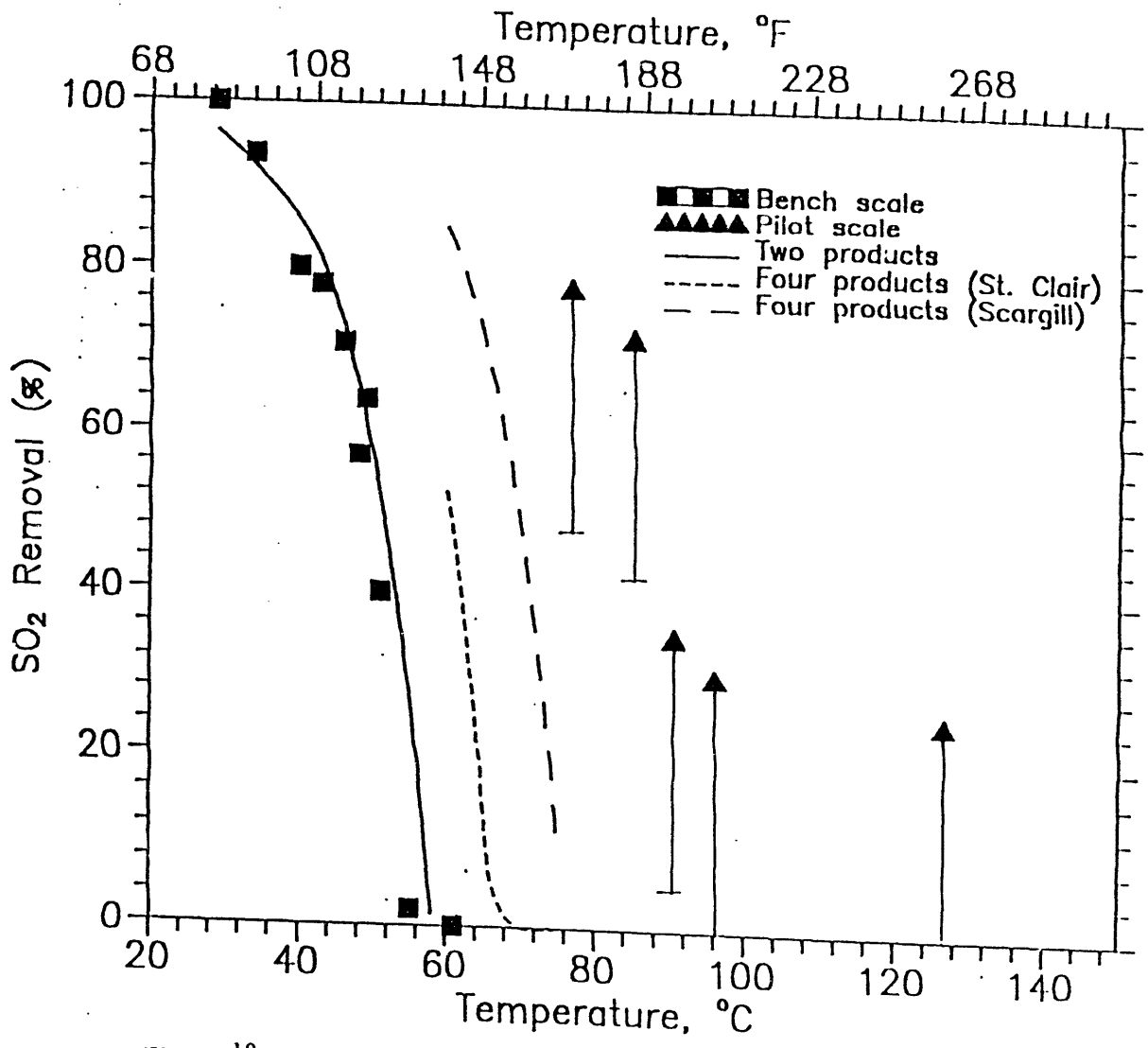

Figure 19 Bench scale and pilot scale results of SO_2 removal efficiencies as a function of temperature. Symbols are experimental data and lines are theoretical predictions from thermodynamic analysis.

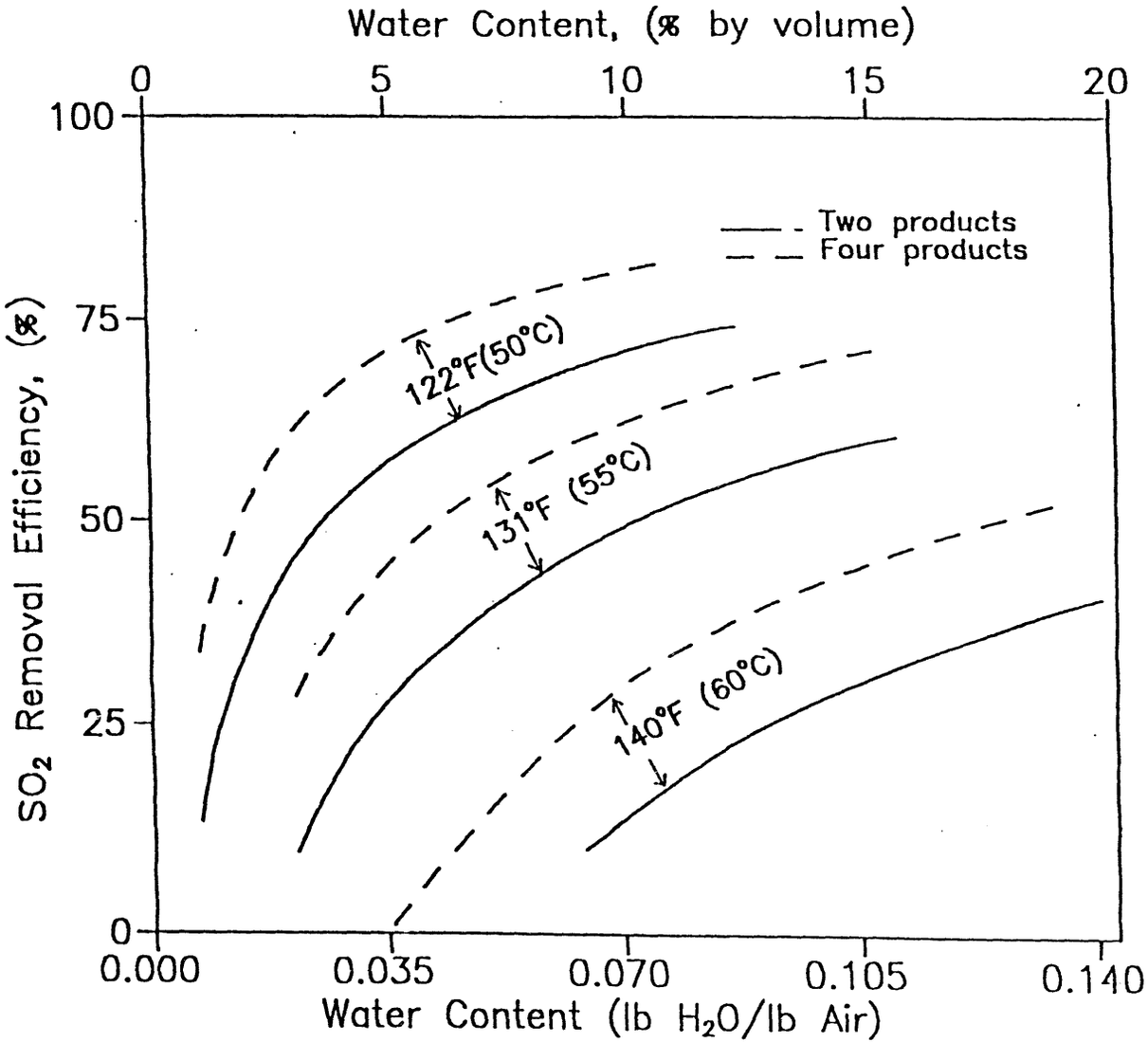

Figure 18 SO_2 removal as functions of moisture content and reaction temperature.

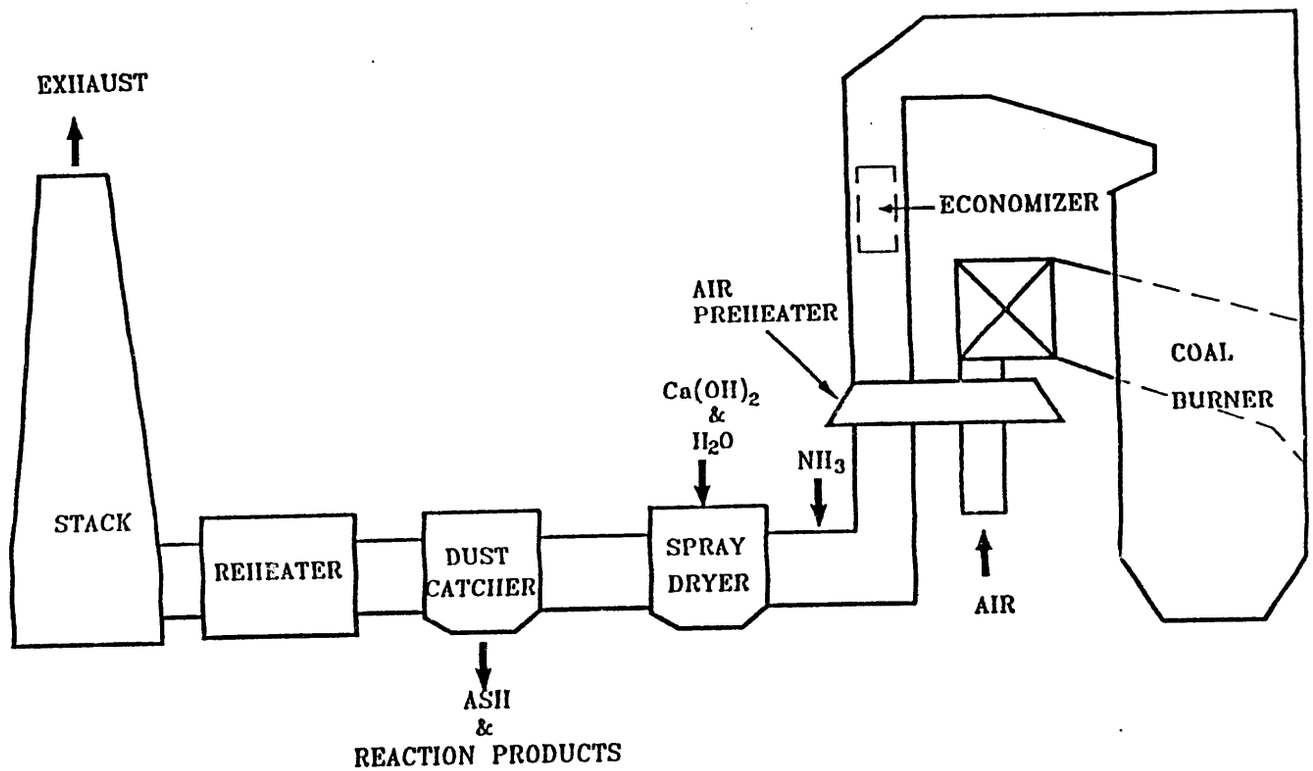

Figure 20 Design of a power plant utilizing $NH_3/Ca(OH)_2$ injection as SO_2 removal technique.

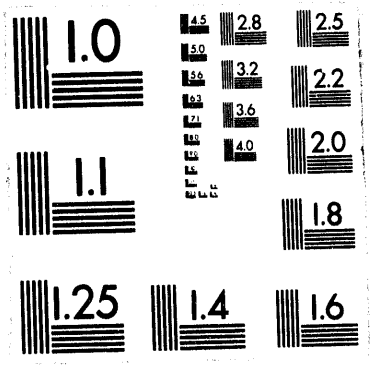
1.0
2.8
2.5
3.2
2.2
3.6
4.0
2.0
1.1
1.8
1.25
1.4
1.6

2 of 2

CONCLUSIONS

A fundamental study of chemical reactions between ammonia, sulfur dioxide and water vapor has been conducted experimentally and theoretically . The results of the study have been applied to NH_3 injection techniques for the removal of SO_2 in a flue gas desulfurization (FGD) system. The results of this study could also be applied to atmospheric chemistry in the stratosphere where an aerosol layer of the products of these reactions is expected to form.

The effects of reaction residence time, presence of inert particles and moisture content on the SO_2 removal and the product particle size distributions have been determined. Results indicated that both gas phase and particle phase reach equilibria in a very short time. The presence of inert particles increases the SO_2 removal efficiency slightly, with a greater increase in removal efficiency at higher surface areas. Moisture content is the most important parameter affecting SO_2 removal. Increasing the moisture content from 1.6% to 6.4% by volume results in a 30% increase of the SO_2 removal at a reaction temperature of 51°C.

Size distributions of the NH_3-SO_2 reaction products were found to vary from submicron sizes to larger than 1000 μm depending on the moisture content. The measured particle size at trace water conditions appeared to be lognormally distributed with a mean size in the submicron ranges. The product particles under humid conditions crystallize to form much larger particles. Varying the reaction temperature and moisture content under humid conditions ($>$ 2.7% H_2O by volume) does not show a trend on the

change of particle size.

The products at near anhydrous conditions were concluded to be NH_3SO_2, $(NH_3)_2SO_2$ and $(NH_4)_2S_2O_5$. While the products at humid conditions could be either the 1:1 sulfites, NH_4HSO_3 and $(NH_4)_2S_2O_5$, or the 2:1 sulfites, $(NH_4)_2SO_3$ and $(NH_4)_2SO_3$ $-H_2O$, or a mixture of the 1:1 and 2:1 sulfite. Those sulfite particles could subsequently oxidize to form the more stable sulfate particles.

A gas-to-particle formation model has been developed to simulate the NH_3-SO_2 system in the presence and absence of seed aerosols at trace water conditions. This model accounts for simultaneous nucleation, coagulation, condensation and chemical reaction. Two sets of surface tension and particle density (σ = 70 ergs cm^{-2} and ρ_p = 1.8 g cm^{-3}; and σ = 93 ergs cm^{-2}, ρ_p = 2.0 g cm^{-3}) fit the experimental data well at trace water conditions. SO_2 removal was predicted theoretically by a thermodynamic analysis at humid conditions. Both experimental and theoretical results indicated that the SO_2 removal decreased as reaction temperature increased. The SO_2 removal efficiency reduces to zero at a temperature of around 55°C and a moisture content of 2.7% by volume (RH=17%).

The applicability of utilizing ammonia injection to a flue gas system has been discussed in terms of two possible removal schemes. One utilizes ammonia injection alone and the other is in conjunction with the injection of $Ca(OH)_2$ slurry in a spray dryer system. Both schemes have the potential of achieving over 90% SO_2 removal from power plants burning high-sulfur coals.

RECOMMENDATIONS FOR FUTURE WORK

This study provides fundamental information of the effects of reaction residence time, moisture content and effect of inert seed particles on the NH_3-SO_2 reactions. Chemical reactions between NH_3-SO_2 reaction products and fly ash at the surface of fly ash could also contribute to the SO_2 removal. Further information of chemical properties of the fly ash in the NH_3-SO_2 system is needed. An ash feeder such as a Wright dust feeder or a fluidized-bed aerosol generator should be used to introduce fly ash at typical sizes and concentrations. Various fly ashes with different chemical compositions (for example, various alkalinities) should be examined to obtain information on the chemical effect of fly ash particles.

The ammonia injection method requires minimal installation space, produces a dry product thus resulting in reduced requirement for process equipment. The product can also be sold as a fertilizer if the fertilizing market is available. On the other hand, reheating of the flue gas may also be necessary which is quite expensive. Therefore, further information on the economical analysis of the ammonia injection system is necessary to obtain an optimal control strategy and apply to a real flue gas desulfurization system.

LITERATURE CITED

1. Badar-ud-Din; Aslam, M. "Ammonia-Sulfur Dioxide Reaction". *Pakistan J. Sci. Res.* 1953, 5, 6-10.

2. Bai, H.; Biswas, P. "Reaction of Sulfur Dioxide with Ammonia to Form Aerosols: Applications in Flue Gas Desulfurization". Abstracts of Papers, Annual Meeting of the AAAR, Philadelphia, 1990; P1F-2, 265.

3. Bai, H.; Biswas, P; Keener, T.C. "Sulfur Dioxide Removal By Reaction with Ammonia Gas to Form Solid Products". Paper 91-103.24, 84th Annual Meeting of Air and Waste Management Association, June, 1991.

4. Bai, H.; Biswas, P; Keener, T.C. "Particle Formation by NH_3-SO_2 Reactions at Trace Water Conditions," *Industrial and Engineering Chemistry Research*, vol. 31, no. 1, 88-94, 1992.

5. Bower, J. H. "Comparative Efficiencies of Various Dehydrating Agents Used for Drying Gases". *Bur. Standards J. Research.* 1934, 12, 241-248.

6. Carabine, M.D.; Maddock, J.E.L.; Moore, A.P. "Particle Size Distributions in Aerosols Form from Gaseous Reactants". *Nature Phys. Sci.* 1971, 231,18.

7. Cussler, E.L. Diffusion, Mass transfer in fluid system. Cambridge University Press, Chapter 5, 1984.

8. Davis, W.T.; Keener, T.C.; Means, C.S.; Dooley, R.P. "Research on the Simultaneous Removal of SO_2 and Particulates from Stoker-Fired Boilers", Paper 77-26.3. 70th Annual Meeting of the Air Pollution Control Association, June, 1977.

9. Divers, E.; Ogawa, M. "Ammonium Amidosulphite". *J. Chem. Society, Trans.*, 1900, 77, 327-335.

10. EPA, Environmental Progress and Challenges: EPA's Update, EPA-230-07-88-

033, August, 1988.

11. Friedlander, S.K. "Dynamics of Aerosol Formation by Chemical Reaction". *Annals New York Academy of Sciences* 1983, 404, 354-364.

12. Friedlander, S.K. *"The General Dynamic Equation for the Continuous Distribution Function". in Smoke, Dust and Haze*; Wiley: New York, 1977, 263-265.

13. Hanawalt Method Search Manual, 1977 Powder Diffraction File, International Center for Diffraction Data, Swarthmore, PA.

14. Hartley E.M.; Matteson M.J. "Sulfur Dioxide Reactions with Ammonia in Humid Air". *Ind. Eng. Chem. Fundam.* 1975, 14, 67-72.

15. Hinds W.C. Aerosol Technology, John Wiley & SONS, Chapter 19, 1982

16. Hurst, T.B.; Bielawski, G.T. EPA Symposium on Flue Gas Desulfurization, Houston, TX, 1980. From references of Reed et al., 1984.

17. IMSL Contents Document, Vol. 2, Version 1.0, International Mathematical and Statistical Libraries, Houston, 1987.

18. Johnstone, H.F. "Recovery of Sulfur Dioxide from Waste Gases Equilibrium Partial Pressures over Solutions of Ammonia-Sulfur Dioxide-Water System". *Ind. Eng. Chem.*, 1935, 27, 587-593.

19. Johnstone, H.F. "Recovery of Sulfur Dioxide from Waste Gases Effect of Solvent Concentration on Capacity and Steam Requirements of Ammonia Sulfite-Bisulfite Solutions". *Ind. Eng. Chem.*, 1937, 29, 1396-1398.

20. Keener, T.C.; Davis W.T. "Demonstration of a $Ca(OH)_2/NH_3$ Based System for Removal of SO_2 on High Sulfur Coals". Final Report to the Ohio Coal Development Office, Columbus, Ohio, August, 1988.

21. Kodas, T.T.; S.K. Friedlander; S.E. Pratsinis. "Effect or Reactant Mixing on Fine Particle Production in a Tubular Flow Reactor". *Ind. & Eng. Chem. Res.*

1987, 26, 1999-2007.

22. Kolthoff, I.M. and Sandell, E.B. "Textbook of Quantitative Inorganic Analysis", 3rd Ed., 1952, Macmillan Co., New York.

23. Landreth, R.; de Pena, R.G.; Heicklen, J. "Thermodynamics of the Reactions $(NH_3)_n \cdot SO_{2(s)} = nNH_{3(g)} + SO_2$". *J. Phys. Chem.* 1974, 78, 1378-1380.

24. Landreth, R.; de Pena, R.G.; and Heicklen, J. "Redetermination of the Thermodynamics of the Reactions $(NH_3)_n \cdot SO_{2(s)} = nNH_{3(g)} + SO_2$-. *J. Phys. Chem.* 1985, 89, 1690-1692.

25. Lee, B., J. Air & Waste Management Assoc., 1990, 40, 1464.

26. Liu, B.Y.H.; Levi, J. "Generation of Submicron Sulfuric Acid Aerosol by Vaporization and Condensation". in *Generation of Aerosols*; K. Willeke, ed., Ann Arbor Science, 1980, Chapter 15.

27. Marks, G.W.; Ambrose, P.M. "Recovery of Sulphur in Solid Compounds by the Addition of Ammonia and Water Vapor to Smelter Gas". *U.S. Bu: Mines Rept. Inv. No. 3339*, 1937, 31-40.

28. Marten, J.C. "A History of Flue Gas Desulfurization System Since 1850: Research, Development and Demonstration". *J. Air Poll. Control Assoc.*, 1977, 27, 948.

29. Martinez, J.C.; Izquierdo, J.F.; Cunill, F.; Tejero, J; Querol, J. "Reactivation of Fly Ash and $Ca(OH)_2$ Mixtures for SO_2 Removal of Flue Gas". *Ind. Eng. Chem. Res.*, 1991, 30, 2143-2147.

30. McCain, J.; Gooch, J.P.; Smith, W.B. "Results of Field Measurements of Industrial Particulate Sources and Electrostatic Precipitator Performance". *J. Air Poll. Control Assoc.* 1975, 25, 117-121.

31. Pratsinis, S.E. "Simultaneous Aerosol Nucleation, Condensation and Coagulation in Aerosol Reactors". *J. Colloid Int. Sci.* 1988, 124, 2, 416-427.

32. Raes, F.; Kodas, T.T.; Friedlander, S.K. "Aerosol Formation by a Reversible Chemical Reaction: Laser-induced NH_4NO_3 Aerosol Formation in a Tubular Reactor". *Aerosol Science and Technology* 1990, 12, 856-868.

33. Ramsey, Brit. Patent 1427, (1883). From references of Marten, J.C., 1977.

34. Reed, G.D.; Davis, W.T.; Pudelek R.E. "Analysis of Coal Fly Ash Properties of Importance to Sulfur Dioxide Reactivity Potential". *Environ. Sci. Technol.* 1984, 18, 548-552.

35. Scargill, D. "Dissociation Constants of Anhydrous Ammonium Sulphite and Ammonium pyrosulphite Prepared by Gas-phase Reactions". *J. Chem. Soc.(A): Inorg. Phys. Theor.* 1971, 2461-2466.

36. Scott,W.D.; Lamb, D.; Duffy, D. "The Stratospheric Aerosol Layer and Anhydrous Reactions Between Ammonia and Sulfur Dioxide". *J. Atmos. Sci.* 1969, 26, 727-733.

37. Scott, W.D.; Lamb, D. "Two Solid Compounds which Decompose into a Common Vapor. Anhydrous Reactions of Ammonia and Sulfur Dioxide". *J. Am. Chem. Soci.* 1970, 92, 13, 3943-3946.

38. Scott, W.D.; McCarthy, J.L. "The System Sulfur Dioxide-Ammonia-Water at 25°C" *Ind. & Eng. Chem. Fund.* 1967, **6**, 40-48.

39. Shale, C.C.; Simpson, D.G.; Lewis, P.S. "Removal of Sulfur and Nitrogen Oxides from Stack Gases by Ammonia". Important Chemical Reactions in Air Pollution Control, Chemical Engineering Progress Symposium Series, 115, 1971, 67, 52-57.

40. Shale, C.C. "Ammonia Injection: A Route to Clean Stack". Pollution Control and Energy Needs, Advances in Chemistry Series 127, American Chemical Society, Washington D.C., 1973, 195-205.

41. Simpson, L.L. Industrial Turbulent Mixing. In Turbulent in Mixing Operations: theory and application to mixing and reaction (Edited by Brodkey R.S.), Academic Press, New, 1975.

42. St. Clair, H.W. "Vapor Pressure and Thermodynamic Properties of Ammonium Sulphites". *U.S. Bur. Mines Rept. Inv. No. 3339*, 1937, 19-29.

43. Standard Methods for the Examination of Water and Wastewater, 16th. Ed., American Public Health Association, Washington, DC, 1985.

44. Stromberger, M.J. The Removal of Sulfur Dioxide From Coal-Fired Boiler Flue Gas By Ammonia Injection. MS Thesis, University of Cincinnati, December, 1984.

45. Tock, R.W.; Hoover, K.C.; Faust G.J. "SO_2 Removal by Transformation to Solid Crystals of Ammonia Complexes". AIChE Symposium series. No. 188, 1979, 75, 62-82.

46. Trusell, F.; Diehl, H. "Efficiency of Chemical Desiccants". *Anal. Chem.* 1963, 35, 674-677.

47. Vance, J.L.; Peters, L.K. "Aerosol Formation Resulting from the Reaction of Ammonia and Sulfur Dioxide". *Ind. Eng. Chem. Fundam.* 1976a, 15, 202-206.

48. Vance, J.L.; Peters, L.K. "Comments on the Direct Aerosol Formation by Reaction of Ammonia and Sulfur Dioxide". *J. Atmos. Sci.* 1976b, 33, 1824-1825.

APPENDIX A: LIST OF DIMENSIONLESS PARAMETERS IN PARTICLE FORMATION MODEL

$$1 / \varepsilon = 1 / \varepsilon_{FM} + 1 / \varepsilon_C$$

$$\varepsilon_{FM} = v_g'^{2/3} \exp (8 \ln^2\sigma_g)$$

$$\varepsilon_C = 4Kn / 3 \, v_g'^{1/3} \exp (3.5\ln^2\sigma_g)$$

$$1/\zeta = 1 / \zeta_{FM} + 1 / \zeta_C$$

$$\zeta_{FM} = r_g'^{1/2} b_0 [\exp(8/25 \ln^2\sigma_g) + 2\exp(5/8 \ln^2\sigma_g) + \exp(1/8 \ln^2\sigma_g)]$$

$$\zeta_C = K[1 + \exp(\ln^2\sigma_g) + B_5(Kn/r_g')\exp(0.5\ln^2\sigma_g)(1 + \exp(2\ln^2\sigma_g))]$$

$$1/\eta = 1/\eta_{FM} + 1/\eta_C$$

$$\eta_{FM} = v_g'^{2/3} \exp(2\ln^2\sigma_g)$$

$$\eta_C = 4/3 \, Kn \, v_g'^{1/3} \exp(0.5\ln^2\sigma_g)$$

$$1/\psi = 1/\psi_{FM} + 1/\psi_C$$

$$\psi_{FM} = r_g'^{1/2} b_2 \exp(1.5\ln^2\sigma_g) \, [\exp(25/8 \ln^2\sigma_g) + 2 \exp(5/8 \ln^2\sigma_g) + \exp(1/8 \ln^2\sigma_g)]$$

$$\psi_C = K[1 + \exp(\ln^2\sigma_g) + B_5(Kn/r_g')\exp(-0.5\ln^2\sigma_g)(1 + \exp(-2\ln^2\sigma_g))]$$

$$\tau = [n_s s_1 (k_B T/2\pi m_1)^{1/2}]^{-1}$$

APPENDIX B: MICROSCOPIC PICTURES OF THE NH_3-SO_2 REACTIONS

(1) Room Temperature; RH = 57%

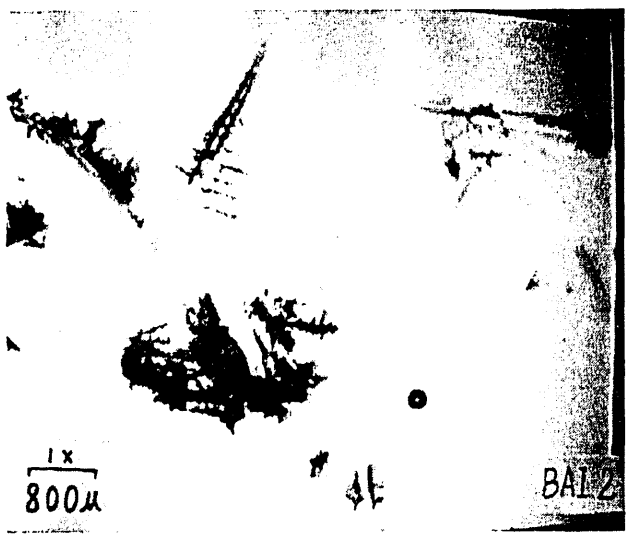

(2) Room Temperature; RH = 20%

(3) Temperature = 51°C; H_2O = 2.7% by volume

(4) Temperature = 51°C; RH = 6.4% by volume

(2) Temperature = 51°C, RH=6.4% by volum

APPENDIX C : SAMPLE COMPUTER PROGRAM "SO2NH3.F"

```
C*****************************************************************
C PROGRAM NOSEED1.F
C THIS PROGRAM PREDICTS AEROSOL DYNAMICS USING
C THE LOGNORMALLY PRESERVING SIZE DISTRIBUTION
C
C PROGRAMMER: HSUNLING BAI
C PROGRAM INITIATE DATE: August, 1988
C LAST MODIFIED DATE: SEP. 23, 1991
C*****************************************************************
C  THIS PROGRAM CONSIDERS FOR THIS REACTION:
C
C                                Kp
C  (2-x1)NH3+(2-x1-x2)SO2+(1-x1-x2)H2O <--> x1 NH3SO2 +
C      x2 (NH3)2SO2 + (1-x1-x2) (NH4)2S2O5
C
C WHERE NUCLEATION IS DOMINATED BY THE FORMATION OF (NH4)2S2O5
C  NUCLEI, THEN OTHER MONOMERS CONDENSE ON THE (NH4)2S2O5
NUCLEI.
C*****************************************************************
C
C
C MOST OF THE VARIABLES USED ARE EITHER SELF EXPLANATORY
C OR DEFINED BELOW (IN ALPHABETICAL ORDER)
C
C    D1 - DIAMETER OF 1 MOLECULE
C    DPV - VOLUME AVERAGE DIAMETER
```

```
C   EKP1 - EQUILIBRIUM CONSTANT OF (NH3)SO2 FORMATION
C   EKP2 - EQUILIBRIUM CONSTANT OF (NH3)2SO2 FORMATION
C   ICOAG - FLAG FOR COAGULATION (T OR F)
C   ICOND - FLAG FOR CONDENSATION
C   INUC  - FLAG FOR NUCLEATION (T OR F)
C   IRXN  - FLAG FOR REACTION (T OR F)
C   PI - COSTANT (3.1415926)
C   PNH3 - VAPOR PRESSURE OF NH3 AT A SPECIFIED TEMP.
C   PS1 - VAPOR PRESSURE OF (NH3)SO2  AT SATURATION
C   PS2 - VAPOR PRESSURE OF (NH3)2SO2  AT SATURATION
C   PS - AVERAGE VAPOR PRESSURE OF THE TWO SLOID COMPOUNDS
C   PSO2 - VAPOR PRESSURE OF SO2 AT A SPECIFIED TEMP.
C   RHO - CONDENSIBLE GAS DENSITY
C   RG - GEOMETRIC MEAN PARTICLE RADIUS
C   S1 - SURFACE AREA OF 1 MOLECULE
C   SIG - SURFACE TENSION
C   SR - SATURATION RATIO
C   TAU - CHARACTERISTIC TIME FOR PARTICLE GROWTH
C   V1 - VOLUME OF 1 MOLECULE
C   VG - GEOMETRIC MEAN VOLUME OF A PARTICLE
C   XISD - SEED CONCENTRATION
C   XII - NUCLEATION RATE
C   XK - BOLTZMANN'S CONSTANT
C   XKN - KNUDSEN NUMBER
C   XKSTAR - CRITICAL CLUSTER CONCENTRATION
C   XLAM - MEAN FREE PATH
C   XMW1 - MASS OF 1 MOLECULE
C   XMU - CARRIER GAS VISCOSITY
C   XM1 - MOLECULAR WEIGHT OF NH3SO2
C   XM2 - MOLECULAR WEIGHT OF (NH3)2SO2
C   XMW - CONDENSIBLE SPECIES MOLECULAR WEIGHT
C   XM0 - PARTICLE CONCENTRATION
C   XM1 - TOTAL PARTICLE CONCENTRATION
C   XM2 - SECOND VOLUME MOMENT
C   XNAV - AVOGADROS NUMBER
C   XNS - MONOMER CONCENTRATION AT SATURATION
C   XSIG - GEOMETRIC STANDARD DEVIRATION
C   YSO2 - MOLE FRACTION OF SO2
C   YNH3 - MOLE FRACTION OF NH3
C
C   Y(1) - Y(20) -  SATURATION RATIO        ! DIMENSIONLESS
C   Y(21) - Y(40) - PARTICLE CONCENTRATION  ! DIMENSIONLESS
C   Y(41) - Y(60) - TOTAL PARTICLE VOLUME   ! DIMENSIONLESS
C   Y(61) - Y(80) - SECOND VOLUME MOMENT    ! DIMENSIONLESS
```

```
C*****************************************************************
      IMPLICIT REAL*8 (A-H,O-Z)

      LOGICAL  INUC,ICOND,ICOAG,ITHRM,IDPAR,IRXN,INIT

      DIMENSION Y(1000),A(1,1),PARAM(50)
      DIMENSION Y1(100),Y2(100),Y3(100),Y4(100)

      CHARACTER *15 OUTPUT,INPUT,GRAPH,GRA,TEST

      COMMON /VAPOR/ PNH3,PSO2,PH2O,EKP1
      COMMON /MONOMER/ V1,XMW1,S1,RHO,XNS,SIG,D1
      COMMON /MONOMER1/ V3,XMW3,S3,TAU3
      COMMON /GAS/ XMU,T,P,XLAM,TAU
      COMMON /CONSTANT/ PI,XK,HP
      COMMON /SCALE/ SCALE
      COMMON /RXN/ RD,REACTIME
      COMMON /VELOCITY/ NEQ,RF(100),R(100)
      COMMON /LOG/ INUC,ICOND,ICOAG,NFLAG,IRXN

      EXTERNAL FCN,FCNJ,DIVPAG,DZREAL,F

      INTRINSIC DLOG,DEXP

      DATA XXM1,XXM2,XXM3,XNAV /81.D0,98.D0,180.d0,6.023D23/
C     DATA YNH3,YSO2 /.1D0,1.D-3/

      PI=3.1415926D0
      XK=1.38D-16
      HP=6.62D-27
      XMU=1.8D-4
      XLAM=6.5D-6
C     RHO=1.25D0
C     SIG=100

C10   WRITE(*,*) ' ENTER THE INPUT FILE NAME '
C     READ(*,15) INPUT
C15   FORMAT(A15)
10    OPEN(1,FILE='dat1.dat',STATUS='OLD')

C     WRITE(*,'(A)') ' ICOND'
C     READ(*,*) ICOND
C     WRITE(*,'(A)') ' ICOAG'
```

```
C     READ(1,20) ICOAG
C20    FORMAT(A15)

C     WRITE(*,'(A)') ' INUC'
C     READ(*,*) INUC

      TOL=1.D-5
      PARAM(1)=1.D-10
      PARAM(4)=50000000
      PARAM(10)=2
      PARAM(12)=2

      ICOND=.TRUE.
C      IRXN=.TRUE.
      ICOAG=.TRUE.
      INUC=.TRUE.

      READ(1,25) OUTPUT
25     FORMAT(A15)

      READ(1,30) GRAPH
30     FORMAT(A15)

      READ(1,35) GRA
35     FORMAT(A15)

      OPEN(7,FILE=OUTPUT,STATUS='NEW')
      OPEN(8,FILE=GRAPH,STATUS='NEW')
      OPEN(9,FILE=GRA,STATUS='NEW')

      NEQ=20
      NEQ1=80
      NEQ2=21
      DR=1.D0/NEQ

      DO 40 I=1,NEQ2
        R(I)=DR*(I-1)
        RF(I)=2.D0*(1.D0-R(I)**2.D0)
40     CONTINUE

C      WRITE(*,*) 'Reaction rate? (True/False)'
      READ(1,*) IRXN
C      WRITE(*,*) 'LOTHE-POUND (1)/CLASSICAL (2) NUC.RATE ?'
      READ(1,*) NFLAG
```

```
C     WRITE(*,*) ' SURFACE TENSION=?,PARTICLE DENSITY=?'
      READ(1,*) SIG,RHO

C     WRITE(*,*) 'YNH3=? YSO2=? YH2O=? MOLE FRAC.OF  NH3SO2
C     +   &(NH3)2SO2=?'
      READ(1,*) YNH3,YSO2,YH2O,x1,x2
C     WRITE(*,*) 'ENTER SOURCE OF EQUIL. CONS., 1=St.Clair,
C     +   2=Scargill'
      READ(1,*) NAUTHOR
C     WRITE(*,*) 'ENTER SOURCE OF EQUIL. CONS., 1=Landreth,2=Scott'
      READ(1,*) NAUTH1

C     WRITE(*,*) 'TEMP=?, PRESSURE(UNIT=TOR)=?'
      READ(1,*) T,TOR
      P=TOR/760.D0

C     WRITE(*,*) 'enter scaling factor?'
      READ(1,*) SCALE

      XMW=XXM1*x1+XXM2*x2+XXM3*(1-X1-x2)

      IF(NAUTHOR.EQ.1) THEN
       EKP1=DEXP(94.6-39144./T)
      ELSE
       EKP1=DEXP(96.5-40767./T)
      ENDIF

      IF (NAUTH1.EQ.1) THEN
       EKd1=DEXP(22.7-9259./T)
       EKd2=DEXP(43.8-16606./T)
      ELSE
       EKd1=DEXP(42.7-16205./T)
       EKd2=DEXP(88.0-31306./T)
      ENDIF

      XMW1=XMW/XNAV
      XMW3=XXM3/XNAV
      V1=XMW/XNAV/RHO
      V3=XXM3/XNAV/RHO
      D1=(6.D0/PI*V1)**(1.D0/3.D0)
      D3=(6.D0/PI*V3)**(1.D0/3.D0)
      S1=PI*D1*D1
      S3=PI*D3*D3
```

```
      PNH3=YNH3*P
      PSO2=YSO2*P
      PH2O=YH2O*P
      SR=PNH3**2.D0*PSO2**2.D0*PH2O/EKP1
C
C     CALCULATE THE SATURATION VAPOR PRESSURE!!

      CALL SATVAP(PX)
C     PX=4.9995743D-5
C
      IF(PX.LE.0.D0) THEN
        WRITE(7,*) 'No equil. vapor available! Temp. probably too high'
        GO TO 150
      ENDIF

      WRITE(7,*) 'Ptotal=',PX
      PS=PX/SR*1.01325D6
      XNS=PS/T/XK
      TAU=(XNS*S1*(XK*T/(2*PI*XMW1))**0.5D0)**(-1.D0)
      TAU3=(XNS*S3*(XK*T/(2*PI*XMW3))**0.5D0)**(-1.D0)

      WRITE(7,41) SCALE
41    FORMAT(1X,'SCALE FACTOR OF NUCLEATION RATE=',1X,E10.2)
      WRITE(7,42) PSO2,PNH3,PH2O,x1,x2
42    FORMAT(1X,'The inlet SO2,NH3 &H2O (atm)=',1X,F10.6,2X,F10.6,2X,
     +F10.6/1X,'mole frac. of NH3SO2 & (NH3)2SO2=',F8.4,2X,F8.4)
      WRITE(7,45) XMW,TAU3,TAU,XNS

45    FORMAT(1X, 'THE AVE. MOLECULAR WEIGHT OF THE TWO SOLID
     +  COMPOUND IS:',F10.3,/1X,'CHARACTERISTIC TIMES are
     +  (Nuc.& Cond.):',E12.4,2X,E12.4,/1X,'THE MONOMER
     +  CONCENTRATION AT SATURATION IS:',E12.4)

C     WRITE(*,*) 'ENTER THE INTERVAL TO BE PRINTED (SEC)'
      READ(1,*) W1

      IF (IRXN) THEN
C       WRITE(*,*) ' ENTER THE REACTION RATE, sat. ratio & Reac. Time?'
        READ(1,*) REAC,SR,REACTIME
        RD=REAC/XNS*TAU
      ELSE
        RD=0.D0
      ENDIF
```

```
      WRITE(7,50) SIG,RHO,RD,REACTIME
50     FORMAT(/1X,'THE SURFACE TENSION IS:',F12.3,/1X,'THE PARTICLE '
     +,'DENSITY IS:',F12.3,/1X,'THE REACTION RATE IS(NORMALIZED):',E12.3
     +,/1X,'THE REACTION TIME IS (sec):',E12.4)

C     WRITE(*,*) ' INITIAL SEED (.TRUE./.FALSE.)?'
      READ(1,*) INIT

      IF (INIT) THEN
        WRITE(*,*) ' STD. DEVIATION ',' VOL. AVE. DIAM. ',' SEED CONC.'
        READ(1,*) SD,DPV,XISD

        WRITE(7,55) SD,XISD,DPV,SR
55       FORMAT(1X,'STD. DEVIRATION =' ,F12.6, / 1X 'SEED CONC. '
     + ,E12.6, / 1X ' VOL. AVE. DIAMETER = ' , E12.6, / 1X, 'SATURATION
     +  RATIO = ',F12.4)

        XNSD=XISD
        XILNS=(DLOG(SD))**2.D0
      ELSE
        DPV=0.D0
        SD=0.D0
        XM0=0.D0
        XM1=0.D0
        XM2=0.D0
        RG=0.D0
        GO TO 60
      ENDIF

      XM0=XNSD
      XM1=PI/6.D0*DPV**3.D0*XM0
      VG=XM1/XM0/(DEXP(9.D0/2.D0*XILNS))
      RG=(VG*3.D0/4.D0/PI)**(1.D0/3.D0)
      DPG=2.D0*RG
      XM2=XM0*VG*VG*DEXP(9.D0/2.D0*2.D0*2.D0*XILNS)
C
      CUP1=0.D0
      CUP2=0.D0
      CUP3=0.D0
      CUP4=0.D0
C
60     DO 65 I=1,NEQ
        Y(I)=SR
        Y(NEQ+I)=XM0/XNS
```

```
      Y(2*NEQ+I)=XM1/XNS/V1
      Y(3*NEQ+I)=XM2/XNS/V1/V1
      CUP1=CUP1+Y(I)*RF(I)*DR*3.d0/4.D0
      CUP2=CUP2+Y(I+NEQ)*RF(I)*DR*3.D0/4.D0
      CUP3=CUP3+Y(I+2*NEQ)*RF(I)*DR*3.D0/4.D0
      CUP4=CUP4+Y(I+3*NEQ)*RF(I)*DR*3.D0/4.D0
65    CONTINUE

      SR=CUP1
      XM0=CUP2*XNS
      XM1=CUP3*XNS*V1
      XM2=CUP4*XNS*V1*V1

      K=1
      T0=0.D0
      WRITE(7,70) T,YSO2
70    FORMAT(1X,'TEMP.=',F12.1,2X,'INITIAL MOLE FRACTION =',F12.5)

      WRITE(7,75)
75    FORMAT(/4X,'T(SEC)',4X,'SR',6X,'M0',7X,'M1',7X,'M2',
     +7X,'SD',8X,'DPG(cm)',4X,'DPV')

      WRITE(7,80)
80    FORMAT(1X,'-----------------------------------------',
     +'-------------------------------')

      WRITE(7,85) T0,SR,XM0,XM1,XM2,SD,DPG,DPV
85    FORMAT(1X,F8.4,1X,E8.3,1X,3(E8.3,1X),3(E9.4,1X))

      WRITE(8,90) T0,SR,XM0,XM1,XM2
90    FORMAT(1X,F8.4,2X,E8.3,2X,3(E8.3,2X))

      WRITE(9,95) T0,SD,DPG,DPV
95    FORMAT( 1X,F8.4,2X,F9.4,2X,2(E9.4,2X))

C     WRITE(*,*) ' ENTER THE STOP TIME AND TIME INTERVAL'
      READ(1,*) TSTOP,DT

      IDO=1
      TE=DT
100   TEND=TE/TAU

      CALL DIVPAG (IDO,NEQ1,FCN,FCNJ,A,T0,TEND,TOL,PARAM,Y)
C
```

```
      CUP1=0.D0
      CUP2=0.D0
      CUP3=0.D0
      CUP4=0.D0

      DO 110 I=1,NEQ
        CUP1=CUP1+Y(I)*RF(I)*DR*3.d0/4.D0
        CUP2=CUP2+Y(I+NEQ)*RF(I)*DR*3.D0/4.D0
        CUP3=CUP3+Y(I+2*NEQ)*RF(I)*DR*3.D0/4.D0
        CUP4=CUP4+Y(I+3*NEQ)*RF(I)*DR*3.D0/4.D0
110   CONTINUE

      SR=CUP1
      XM0=CUP2*XNS
      XM1=CUP3*XNS*V1
      XM2=CUP4*XNS*V1*V1

      IF(XM1.GT.1.D-150.AND.XM2.GT.1.D-150.AND.XM0.GT.
     +  1.D-150) THEN
        G=CUP3/CUP2/DSQRT(CUP4)*CUP3/DSQRT(CUP2)
        VG=G*V1
        IF(G.GT.0.D0) THEN
          RG1=G**(1.D0/3.D0)
          RG=RG1*D1/2.D0
          DPG=2.D0*RG
          DPV1=(CUP3/CUP2)**(1.D0/3.D0)
          DPV=DPV1*D1
          XKN=XLAM/RG
          XLNS=1.D0/9.D0*DLOG(CUP2/CUP3*CUP4/CUP3)
          IF(XLNS.GT.0.D0) THEN
            SD=DEXP(XLNS**0.5D0)
          ENDIF
        ENDIF
      ENDIF

      W=(K-1.D-8)*W1
      IF(TE.LT.W) GO TO 115
      WRITE(7,120) TE,SR,XM0,XM1,XM2,SD,DPG,DPV
120   FORMAT(1X,F8.4,1X,E8.3,1X,3(E8.3,1X),3(E9.4,1X))
      WRITE(8,125) TE,SR,XM0,XM1,XM2
125   FORMAT(1X,F8.4,2X,E8.3,2X,3(E8.3,2X))
C     WRITE(*,*) TE,SR,XM0,SD,DPG
      WRITE(9,130) TE,SD,DPG,DPV
130   FORMAT(1X,F8.4,2X,F9.4,2X,2(E9.4,2X))
```

```
      K=K+1
115   TE=TE+DT
      IF (TE.GT.TSTOP) GO TO 135
      GO TO 100

C     WRITE(*,*) 'DO YOU WANT TO SOLVE ANOTHER SET?(Y/N)'

135   CALL DIVPAG (3,NEQ1,FCN,FCNJ,A,T0,TEND,PARAM,Y)
      READ(1,140) TEST
140   FORMAT(A15)

      IF(TEST.EQ.'Y') THEN
        GO TO 10
      ENDIF

150   STOP
      END

C*********************************************************
C                    FCN
C*********************************************************

C     SUBROUTINE FCN IS REQUIRED BY THE  SUBROUTINE  DGEAR  TO
C     CALCULATE THE DERIVATIVES OF THE DIFFERENTIAL EQUATIONS.

C     THIS PROGRAM IS WRITTEN BY HSUN-LING BAI,
C     NOVEMBER 6. 1990, UNIVERSITY OF CINCINNATI.

      SUBROUTINE FCN (N,X,Y,YPRIME)

      IMPLICIT REAL*8 (A-H,O-Z)

      LOGICAL  ICOAG,IRXN,INUC,ICOND,ITHRM,IDPAR

      DIMENSION Y(N),YPRIME(N)
      DIMENSION DXNS(20),DXNN(20),DXNV(20),DXNW(20),DXCS(20)
     + ,DXCV(20),DXCW(20),DXCON(20),DXCOW(20)

      COMMON /MONOMER/ V1,XMW1,S1,RHO,XNS,SIG,D1
      COMMON /MONOMER1/ V3,XMW3,S3,TAU3
      COMMON /GAS/ XMU,T,P,XLAM,TAU
      COMMON /CONSTANT/ PI,XK,HP
      COMMON /SCALE/ SCALE
      COMMON /RXN/ RD,REACTIME
```

```
      COMMON /VELOCITY/ NEQ,RF(100),R(100)
      COMMON /LOG/ INUC,ICOND,ICOAG,NFLAG,IRXN

      DO 10 I=1,NEQ
        IF(Y(3*NEQ+I).GT.1.D-150.AND.Y(NEQ+I).GT.1.D-150.AND.Y(2*NEQ+I)
     +    .GT.1.D-150) THEN
          G=Y(2*NEQ+I)/Y(NEQ+I)/DSQRT(Y(3*NEQ+I))*Y(2*NEQ+I)/
     +    DSQRT(Y(NEQ+I))
          VG=G*V1
          IF(G.GT.0.D0) THEN
            RG1=G**(1.D0/3.D0)
            RG=RG1*D1/2.D0
            XKN=XLAM/RG
            XLNS=1.D0/9.D0*DLOG(Y(NEQ+I)/Y(2*NEQ+I)*Y(3*NEQ+I)/
     +        Y(2*NEQ+I))
            IF (XLNS.GT.0.D0) THEN
              SD=DEXP(XLNS**0.5D0)
            ENDIF
          ENDIF
        ENDIF

C     NUCLEATION-----------------------------------

      IF (INUC) THEN
        CALL NUC (Y(I),RG,NFLAG,XKSTAR,XI)
        XII=XI*SCALE
        DXNS(I) = XII/XNS*XKSTAR*TAU
        DXNN(I) = XII/XNS*TAU
        DXNV(I) = XII/XNS*XKSTAR*TAU
        DXNW(I) = XII/XNS*XKSTAR*XKSTAR*TAU
      ELSE
        DXNS(I) = 0.D0
        DXNN(I) = 0.D0
        DXNV(I) = 0.D0
        DXNW(I) = 0.D0
      ENDIF

C     REACTION-------------------------------------

      IF (IRXN) THEN
        XT=X*TAU
        IF (XT.LE.REACTIME) THEN
          DXRS = RD
        ELSE
```

```
        DXRS = 0.D0
      ENDIF
    ENDIF

C     CONDENSATION--------------------------------

    IF (ICOND) THEN
      IF(Y(2*NEQ+I).GT.1.D-150.AND.Y(NEQ+I).GT.1.D-150) THEN
        CALL CON (VG,XLNS,COEFM1,COEFSX,COEFM2)
        DXCS(I) = COEFSX*Y(NEQ+I)*(Y(I)-1.D0)*TAU/V1
        DXCV(I) = COEFM1*Y(NEQ+I)*(Y(I)-1.D0)*TAU/V1
        DXCW(I) = COEFM2*Y(2*NEQ+I)*(Y(I)-1.D0)*TAU/V1
      ELSE
        DXCS(I) = 0.D0
        DXCV(I) = 0.D0
        DXCW(I) = 0.D0
      ENDIF
    ELSE
        DXCS(I)=0.D0
        DXCV(I)=0.D0
        DXCW(I)=0.D0
    ENDIF

C     COAGULATION--------------------------------

    IF (ICOAG) THEN
      IF(Y(2*NEQ+I).GT.1.D-150.AND.Y(NEQ+I).GT.1.D-150.AND.Y(3*NEQ+I)
     +    .GT.1.D-150) THEN
        CALL COAG (SD,RG,XKN,COM0,COM2)
        DXCON(I) = COM0*Y(NEQ+I)**2.D0*XNS*TAU
        DXCOW(I) = COM2*Y(2*NEQ+I)**2.D0*XNS*TAU
      ELSE
        DXCON(I) = 0.D0
        DXCOW(I) = 0.D0
      ENDIF
    ELSE
      DXCON(I)=0.D0
        DXCOW(I)=0.D0
    ENDIF

C*************************************************************

    YPRIME(I)=(DXRS-DXNS(I)-DXCS(I))/RF(I)
    YPRIME(NEQ+I)=(DXNN(I)-DXCON(I))/RF(I)
```

```
      YPRIME(2*NEQ+I)=(DXNV(I)+DXCV(I))/RF(I)
      YPRIME(3*NEQ+I)=(DXNW(I)+DXCW(I)+DXCOW(I))/RF(I)

C*********************************************************

10    CONTINUE

      RETURN
      END

C*********************************************************

      SUBROUTINE FCNJ (NEQ,X,Y,DYPDY)
      IMPLICIT REAL*8 (A-H,O-Z)
      DIMENSION Y(NEQ),DYPDY(*)

      RETURN
      END
C
C
C*********************************************************************
C
C    SUBROUTINE FOR CALCULATING THE CONDENSATION COEFFICIENTS
C
*********************************************************************
C
C                        NUC
C
C  ********************************************************************
C
        SUBROUTINE NUC (SR,RG,NFLAG,XKSTAR,XII)
C
C       SUBROUTINE NUC CALCULATES THE NUCLEATION RATE. NFLAG =
1
C    IMPLIES THE LOTHE-POUND THEORY. NFLAG = 2 IMPLIES THE
C    CLASSICAL BECKER-DOERING NUCLEATION THEORY.
C
C       DP - CRITICAL CLUSTER DIAMETER (CMS)
C       HP - PLANCKS CONSTANT (6.62D-27 ERGS)
C       PI - CONSTANT (3.1415927D0)
C       RHO - DENSITY (GM/CC)
C       SIG - SURFACE ENERGY (DYNE/CM)
C       SIGMAD-SURFACE TENSION GROUP
C       SR - SATURATION RATIO (DIMENSIONLESS)
```

```
C       T - TEMPERATURE (INPUT DEGREES K)
C       V1 - VOLUME OF ONE MOLECULE (CC)
C       XII - NUCLEATION RATE (#/CC/SEC)
C       XK - BOLTZMAN CONSTANT (1.38D-16 ERGS/K)
C       XMW - MOLECULAR WEIGHT (GM)
C       XNAV - AVOGADRO NUMBER  (6.023D23)
C       XNS - SATURATION NUMBER CONCENTRATION
C       XS - MOLE FRACTION AT SATURATION
C
C       ******* XNAV  HAS BEEN REPLACED WITH XNS **********
C
      IMPLICIT REAL*8 (A-H,O-Z)
C
      COMMON /MONOMER/ V1,XMW1,S1,RHO,XNS,SIG,D1
      COMMON /MONOMER1/ V3,XMW3,S3,TAU3
      COMMON /GAS/ XMU,T,P,XLAM,TAU
      COMMON /CONSTANT/ PI,XK,HP
C
C     USE (NH4)2S2O5 AS THE ONLY NUCLEATION PRODUCT!!

      V1=V3
      XMW1=XMW3
      S1=S3
      TAU=TAU3
C
      IF (SR .LE. 1.D0 ) GO TO 199
C
      IF (NFLAG .EQ. 2) GO TO 13
C
C     LOTHE AND POUND NUCLEATION THEORY
C     ITERATIVE PROCEDURE TO CALCULATE CRITICAL DIAMETER
C
      DOLD = 4.D0*SIG*V1/XK/T/DLOG(SR)
5     DNEW=4.D0*SIG*V1/XK/T/DLOG(SR)*(1.D0-6.D0*XK*T/PI/SIG
     +       /DOLD/DOLD)
       IF (DABS (DNEW-DOLD) .LT. 1.D-9) THEN
         DP = DNEW
         GOTO 10
       ENDIF
         DOLD = DNEW
         GOTO 5

C       NUCLEATION RATE IS CALCULATED FROM
```

```
10    XII = (1.D0-18.D0*XK*T/PI/SIG/DP/DP)**0.5D0*DEXP(DLOG(PI*XNS)
     +        + 0.5D0*DLOG(SIG/2.D0/PI/XMW1) + DLOG(2.D0*V1/PI)
     +        - PI*SIG*DP*DP/3.D0/XK/T + 12.D0*DLOG(DP) - 6.D0*DLOG(HP)
     +        + 3.D0*DLOG(RHO*XK*T) + DLOG(1.1D-5))

      SIGMAD = SIG*V1**(2.D0/3.D0)/XK/T
      XKS = PI/6.D0*(4.D0*SIGMAD)**3.D0
      XKSTAR = XKS/(DLOG(SR))**3.D0
C
      GOTO 199
C
C     CLASSICAL NUCLEATION THEORY
C
13    SIGMAD = SIG*V1**(2.D0/3.D0)/XK/T
      XKS = PI/6.D0*(4.D0*SIGMAD)**3.D0
      XKSTAR = XKS/(DLOG(SR))**3.D0
      COEF1 = (2.D0/9.D0/PI)**(1.D0/3.D0)
      PEP=XKSTAR*(DLOG(SR)/2.D0)

      IF (PEP.LT.600.D0) THEN
        COEF2 = DEXP(-PEP)
        XII = XNS/TAU*SR**2.D0*COEF1*SIGMAD**(.5D0)*COEF2
      ELSE
        COEF2=0.D0
        XII=0.D0
      ENDIF
C
199   RETURN
      END

C*****************************************************************
C
C  SUBROUTINE FOR CALCULATING THE CONDENSATION COEFFICIENTS
C
      SUBROUTINE CON (VG,XLNS,COEFM1,COEFSX,COEFM2)

C     LIST OF VARIABLES

C     COEFM1 : CONDENSATION COEFF IN dM1/dt (SEC*#/CM^3)
C     COEFSX : CONDENSATION COEFF IN dSX/dt (SEC*#/CM^3)
C     COEFM2 : CONDENSATION COEFF IN dM2/dt (SEC*#/CM^3)
C     VG : GEOMETRIC AVERAGE VOLUME (CC)
C     PI : CONSTANT 3.1415927D0
C     SD : STANDARD DEVIATION
```

```
C     T : TEMPERATURE (KELVIN)
C     V1 : VOLUME OF MONOMER MOLECULE (CC)
C     XK : BOLTZMAN CONSTANT (1.38D-16 ergs/K)
C     XLAM : MEAN FREE PATH (CM)
C     XNS : NUMBER OF MOLECULES AT SATURATION(NO./CC)
C     XMW1 : MONOMER MOLECULE MASS(g)
C

      IMPLICIT REAL*8 (A-H,O-Z)

      COMMON /MONOMER/ V1,XMW1,S1,RHO,XNS,SIG,D1
      COMMON /GAS/ XMU,T,P,XLAM,TAU
      COMMON /CONSTANT/ PI,XK,HP

C ***************************************************************
      A = 1.D0/3.D0
C     F1 = (36.D0*PI)**A*V1*XNS*DSQRT(XK*T/2.D0/PI/XMW1)
C     F2 = DSQRT(8.D0*XK*T/PI/XMW1)
C     C1 = (48.D0*PI*PI)**A*XNS*V1*XLAM/3.D0
C ***************************************************************

      IF (VG .GT. 0.D0 ) THEN
C       XLNS  = (DLOG(SD))**2.D0
        ETAC1 = V1**A/TAU*VG**(2.D0*A)*DEXP(2.D0*XLNS)
        DELC1 = ETAC1
        PSIC1 = 2.D0*V1**A/TAU*VG**(2.D0*A)*DEXP(8.D0*XLNS)
        ETAC2 = 8.D0/3.D0/TAU/D1*XLAM*V1**(2.D0*A)*
     +          VG**A*DEXP(XLNS/2.D0)
        DELC2 = ETAC2
        PSIC2 = 16.D0/3.D0/TAU/D1*XLAM*V1**(2.D0*A)*
     +          VG**A*DEXP(3.5D0*XLNS)
        COEFM1 = ETAC1*ETAC2/(ETAC1+ETAC2)
        COEFSX = DELC1*DELC2/(DELC1+DELC2)
        COEFM2 = PSIC1*PSIC2/(PSIC1+PSIC2)
      ELSE
        COEFM1 = 0.D0
        COEFSX = 0.D0
        COEFM2 = 0.D0
      ENDIF

      RETURN
      END

C
```

```
C*****************************************************************
C SUBROUTINE COAG.F
C
C COMPUTE COAGULATION COEFFICIENTS, ASSUMING SIZE
C DISTRIBUTION TO BE LOGNORMAL.
C
C LIST OF VARIABLES :
C *****************************************************************
C COM0 - COAGULATION COEFFICIENCT OF ZEROTH MOMENT (CM^3/SEC)
C COM2 - COAGULATION COEFFICIENCT OF SECOND MOMENT (CM^3/SEC)
C  RHO  - CONDENSIBLE GAS DENSITY (G/CC)
C  RG - MEAN GEOMETRIC PARTICLE RADIUS (UM)
C  SD - STANDARD DEVIATION
C  T - TEMPERETURE(K)
C  XK   - BOLTZMANN'S CONSTANT
C  XKN - KNUDSEN NUMBER(=mean free path/RG)
C  XLAM - MEAN FREE PATH
C  XMU - CARRIER GAS VISCOSITY
C *****************************************************************
C
C                    LISTING OF COAG.F
C
C *****************************************************************

      SUBROUTINE COAG (SD,RG,XKN,COM0,COM2)
C
      IMPLICIT REAL*8 (A-H,O-Z)
C
      COMMON /MONOMER/ V1,XMW1,S1,RHO,XNS,SIG
      COMMON /GAS/ XMU,T,P,XLAM,TAU
      COMMON /CONSTANT/ PI,XK,HP
C
      IF(SD.LT.1.D0) THEN
        COM0=0.D0
        COM2=0.D0
      ELSE
        XLNS=DLOG(SD)*DLOG(SD)
        B0 = 0.633D0 + 0.092D0*SD**2.D0 - 0.022D0*SD**3.D0
        B2 = 0.39D0 + 0.5D0*SD - 0.214D0*SD**2
     +       + 0.029D0*SD**3.D0
        C1=(6*XK*T*RG/RHO)**.5D0
        C2 = 2.D0*XK*T/(3.D0*XMU)
C
        GAM1 = DEXP(25.D0/8.D0*XLNS) + 2.D0*DEXP
```

```
     +      (5.D0/8.D0*XLNS) + DEXP(XLNS/8.D0)
      PSI1 = DEXP(25.D0/8.D0*XLNS) + DEXP(5.D0/8.D0*XLNS)
     +       + DEXP(XLNS/8.D0)
C
      GAMFM = C1*B0*GAM1
      PSIFM = 2*C1*B2*DEXP(1.5D0*XLNS)*PSI1
C
      GAM2 = 1.D0 + DEXP(XLNS) + 1.257*XKN*DEXP(XLNS
     +       /2.D0)*(1.D0 + DEXP(2.D0*XLNS))
      PSI2 = 1.D0 + DEXP(XLNS) + 1.257*XKN*DEXP(-XLNS
     +       /2.D0)*(1.D0 + DEXP(-2.D0*XLNS))
C
      GAMC = C2*GAM2
      PSIC = 2*C2*PSI2
C
      COM0 = GAMFM*GAMC/(GAMFM + GAMC)
      COM2 = PSIFM*PSIC/(PSIFM + PSIC)
C
     ENDIF

     RETURN
     END

C
C*****************************************************
C THIS SUBROUTINE SOLVE A NONLINEAR EQUATION.
C THIS PROGRAM IS USED TO SOLVE THE EQUILIBRIUM
C CONCENTRATION OF EACH GAS.
C
C THIS PROGRAM WAS WRITTEN BY HSUNLING BAI, 4/18/90
C*****************************************************
C
     SUBROUTINE SATVAP (PS)
C
     IMPLICIT REAL*8 (A-H,O-Z)
     DIMENSION INFO(5),X(5),XGUESS(5)
     COMMON /VAPOR/ PNH3,PSO2,PH2O,EKP1
     EXTERNAL F,DZREAL

C
C    ! SET INITIAL GUESS

     DATA XGUESS/1.999D-5,2.999D-5,3.99D-5,4.99D-5,6.999D-5/
```

```
      NROOT=5

C     WRITE(*,*) 'ENTER THE OUTPUT FILE NAME'
C     READ(*,10) OUTPUT
C10   FORMAT(A15)
C     OPEN(UNIT=9,FILE=OUTPUT,STATUS='NEW')
C
C NOTE * THE FOLLOWING PARAMETERS MUST BE SPECIFIED BASED ON
C        THE EQUATIONS TO BE SOLVED.

      EPS=1.D-20
      ERRABS=1.D-20
      ERRREL=1.D-20
      ETA=1.D-20
      ITMAX=100000
C
      CALL DZREAL(F,ERRABS,ERRREL,EPS.ETA,NROOT,ITMAX,
     +  XGUESS,X,INFO)

      PS=0.D0
      PSO=PSO2/2.D0
      PNH=PNH3/2.D0


      DO 30 I=1,5
        IF (X(I).GE.0.D0.AND.X(I).LE.PSO.AND.X(I).LE.PNH.AND
     +     .X(I).LE.PH2O.AND.INFO(I).LE.ITMAX) THEN
          PS=X(I)
        ENDIF
 30   CONTINUE

      RETURN
      END

C ***************************************************************

      FUNCTION F(X)
      IMPLICIT REAL*8 (A-H,O-Z)
      COMMON /VAPOR/ PNH3,PSO2,PH2O,EKP1
C
      F= (PNH3-2.*X)**2.D0*(PSO2-2.*X)**2.D0*(PH2O-X)-EKP1

      RETURN
      END
```

DATE
FILMED
5/10/94

END